2013

Amplifying Conjugated Polymers for Fluorescent Chemosensing

Deepa Pangeni
Louisiana State University and Agricultural and Mechanical College, dpange1@tigers.lsu.edu

AMPLIFYING CONJUGATED POLYMERS FOR FLUORESCENT CHEMOSENSING

A Dissertation

Submitted to the Graduate Faculty of the
Louisiana State University and
Agricultural and Mechanical College
in partial fulfillment of the
requirements for the degree of
Doctor of Philosophy

in

The Department of Chemistry

by
Deepa Pangeni
B.S., Hanover College, 2007
December 2013

Bal Prasad Pangeni (1954 - 2011)

Acknowledgments

First of all, I would like to thank Dr. Evgueni E. Nesterov for his continuous guidance and support all these years of my life as a graduate student. He has given me valuable suggestions in both academic and personal life. I have learnt a lot and truly respect and admire him for his passion and dedication to chemistry. Due to his support, guidance and motivation, I am in this position to finish my PhD and begin the new chapter of my life. I would also like to thank my committee members, past and current group members for all their guidance and support they have given in these many years.

More importantly, I would like to dedicate this work to my parents “buwa” and “ama” who taught me to work diligently and make me believe that outcome would eventually fall in my hands. Along the same line, I would like to thank my siblings for their unconditional love and support.

My acknowledgments will not be complete without thanking my husband who has loved and cared in good and in rough times. He has been always there for me with a big smile and hug whenever I needed.

Table of Contents

Acknowledgments……..iii

List of Tables……vi

List of Figures……....vii

List of Schemes…….....xi

List of Abbreviations……xii

Abstract…….xiv

Chapter 1. Amplifying Fluorescent Polymers……..1
1.1 Conjugated Polymers……...1
1.2 Signal Amplification……4
1.3 Signal Amplification via Turn-Off Mechanism……...5
1.4 Signal Amplification via FRET……..…9
1.5 Turn-On Amplification: Biosensing…….....11
1.6 Energy Transfer……14
1.7 Research Focus of This Dissertation……15
1.8 References……18

Chapter 2. "Higher Energy Gap" Control in Fluorescent Conjugated Polymers: Turn-On Amplified Detection of Organophosphorous Agents……....21
2.1 Introduction……....21
2.2 Synthesis……27
2.3 Spectroscopic Properties……29
2.4 DCP Sensing Studies……..……...31
2.5 Conclusions……....40
2.6 References……..41

Chapter 3. "Higher Energy Gap" Control Principle in the Design of an Amplifying Fluorescent Sensory Polymer for H_2S Detection …….……...…….....45
3.1 Introduction……....45
3.2 Synthesis……....49
3.3 Spectroscopic Characterizations……....54
3.4 Future Work……...56
3.5 References……..57

Chapter 4. Polycyanines – Near-Infrared Fluorescent Conjugated Polymers……....59
4.1 Introduction……....59
4.2 Design and Synthesis……63
4.3 Spectral Properties……67
4.4 ^{1}H-NMR Studies……....70
4.5 Conclusions……...…72
4.6 References……..73

Chapter 5. Experimental Details……....75
5.1 General Procedures……...……...……..75
5.2 Synthetic Details……....76
5.3 References……..94

Appendix A. NMR of Selected Compounds…….……95

Appendix B. Permission to Reuse Contents from Publications ……...……...126

The Vita……...147

List of Tables

Table 4.1. Spectroscopic Properties of cyanine oligomer and polymer **P9** in DMSO……...68

Table 4.2. Diffusion coefficient of different oligomers and polymer **P9** in DMSO solution……72

List of Figures

Figure 1.1. Examples of conjugated polymers for various applications…….....1

Figure 1.2. Illustration of the mechanism of the exciton migration to the analyte binding site on the conjugated backbone, resulting in photonic signal amplification…..……..……..2

Figure 1.3. Bold traces show the absorption and the dashed traces are the emission spectra of the polymers. Red shifted emission of the polymer **P-II** was observed with introduction of an anthracene end group…….....3

Figure 1.4. Schematic representation of a ladder type polymer **P-III**…….……4

Figure 1.5. Demonstration of an amplified quenching in a CP (**P-IV)** by paraquat (PQ^{2+}). Emission spectra of **small molecule (top)** and the **P- IV (bottom)** as a function of added PQ^{2+}……6

Figure 1.6. Decrease in fluorescence intensity of iptycene functionalized polymer PPE (**P-V**) after exposure of the polymer toTNT vapours……7

Figure 1.7. Polymer is fluorescent before binding with analyte (TNT) and then subsequently quenched after interacting with TNT vapor……..……..….7

Figure 1.8. K^{+}-induced aggregation of a crown ether-functionalized polymer (**P-VI**)…….…...8

Figure 1.9. Thymine functionalized polythiophene Polymer (left) and sugar functionalized PPE polymer (right) showed strong fluorescent quenching upon interaction with analyte due to the analyte-induced polymer aggregation…….…..……...……...…9

Figure 1.10. Schematic description of amplified fluorescent detection of a complimentary ssDNA strand (blue) by using FRET from CP (**P-IX)** (black) to fluorescein chromophore linked to a PNA reporter (red). Adding complementary DNA results in formation of triplex where efficient FRET from CP to fluorescein produces an amplified fluorescent response, adding non-complementary DNA (green) produces no response…….10

Figure 1.11**.** Strong FRET upon addition of a complimentary target ssDNA verse weak FRET when noncomplimentary ssDNA is used……..…….……...11

Figure 1.12. Whitten's quencher-tether-ligand-based strategy to biosensing. Addition of avidin to a solution of conjugated polyelectrolyte and biotin-functionalized quencher resulted in a turn-on (fluorescence recovery) response……..12

Figure 1.13. Wang's polymer **P-X** which showed increase in fluorescent intensity after addition of fluoride……..……13

Figure 1.14. Fluoride-induced lactonization of side chains on the polymer backbone producing emissive sites with a smaller band gap that gave a new amplified emission, increasing with time…….…….…13

Figure 1.15. Illustration of decreasing exciton diffusion length due to a higher energy gap roadblock site……..……..…….16

Figure 2.1. A) Schematic energy diagram illustrating the concept of amplified turn-on fluorescent sensing through the formation of a lower energy gap fluorophore and an example of CP turn-on sensor for fluoride detection developed by Kim and Swager.[12] B) Schematic diagram of the "higher energy gap" control of CP fluorescence: an analyte (red circle) binding creates a higher energy gap unit in the CP backbone which decreases the length of exciton migration in the polymer, therefore causing increase of the intensity of fluorescent emission…….…….23

Figure 2.2. Absorption (solid traces) and fluorescence (dashed traces) spectra of 9.5 μM solutions of CP **P1** and small-molecule counterpart **M1** in DMF (concentration of **P1** is based on repeating unit). Dashed green trace corresponds to an excitation spectrum of **M1**. For **P1** ε = 33900 M^{-1} cm^{-1} at λ_{max} 426 nm; emission λ_{max} 524 nm, quantum yield $\Phi = 0.11$; for **M1** ε = 47000 M^{-1} cm^{-1} at λ_{max} 331 nm; emission λ_{max} 444 nm, quantum yield $\Phi = 0.02$……...…...30

Figure 2.3. ^{1}H NMR spectra (in acetone-D6, 400 MHz)) of **M1** (bottom) and the product after treatment of DMF solution of **M1** with DCP in CH_2Cl_2 followed by pouring in aqueous $NaHCO_3$ and extraction with CH_2Cl_2 (top)……...…...32

Figure 2.4. Absorption (top) and fluorescence (bottom) spectra of 9.5 μM solutions of **M1** and **P1** in DMF (concentration of **P1** is based on repeating unit) upon addition of the increasing concentration DCP solutions in CH_2Cl_2. For fluorescence spectra, excitation wavelength was 310 nm for **M1** and 400 nm for **P1**. The spectra were acquired in 30 min after addition of DCP……..33

Figure 2.5. Normalized fluorescence intensity (F/F_0) vs. time in reaction of DCP with polymer **P1** and small-molecule sensor **M1** in DMF (100 μl of a 0.2 mM stock solution of DCP in CH_2Cl_2 was added to 2 ml of 10 μM solution of **P1** or **M1** in DMF). The lines show exponential fit to the experimental data using first-order kinetic treatment (R^2 0.93 for both **M1** and **P1**, first-order rate constant for **M1** k_{obs} = 0.66 min^{-1})……..……34

Figure 2.6. A) Fluorescence spectra of 9.5 μM solution of **M1** in DMF acquired at 400 nm excitation upon addition of the increasing concentration DCP solutions in CH_2Cl_2. The spectra were acquired in 30 min after addition of DCP. B) Dependence of fluorescent response of small-molecule sensor **M1** on excitation wavelength (310 nm *vs.* 400 nm). The traces show change in integrated fluorescence intensity of 9.50 μM solution of **M1** upon addition of increasing concentrations of DCP. The intensity is expressed as a ratio of integrated area of a fluorescent band at each DCP concentration divided by the area of the fluorescent band in the absence of DCP (F/F_0). The plot uses logarithmic scale for DCP concentration axis……...…...35

Figure 2.7. Change in integrated fluorescence intensity of 9.50 μM solutions of polymers **P1** and **P3**, and small-molecule sensor **M1** upon addition of increasing concentrations of DCP. The intensity is expressed as a ratio of integrated area of a fluorescent band at each DCP concentration divided by the area of the fluorescent band in the absence of DCP (F/F_0). The plot uses logarithmic scale for the DCP concentration axis……...36

Figure 2.8. Fluorescence spectra of 9.5 μM solutions of **P3** in DMF (concentration based on repeating unit) upon addition of the increasing concentration DCP solutions in CH_2Cl_2. The spectra were acquired in 30 min after addition of DCP……....37

Figure 2.9. Absorption (dashed traces) and fluorescence (solid traces) spectra of a thin film of **P1** before and after exposure for 1 min to saturated vapor of DCP at room temperature……..…...39

Figure 3.1. Fluorescent H_2S probes based on reduction of azide to amino group by H_2S…….46

Figure 3.2. An example of Nucleophilic addition of H_2S to a non-fluorescent to generate a fluorescent species……..……47

Figure 3.3. Proposed H_2S sensing reaction mechanism of CouMS probe and ratiometric fluorescence (left) and absorbance (right) response upon addition of H_2S……..…48

Figure 3.4. Proposed reaction mechanism for the detection of H_2S using fluorescent CP……...49

Figure 3.5. Absorption and Emission spectra of different CPs to be used in H_2S Sensing……..55

Figure 3.6. Change in Fluorescence intensity of polymer after addition of NaSH in DMSO. The left graph corresponds to polymer **P7** and the right graph corresponds to polymer **P8**……56

Figure 4.1. Representation of NIR- conjugated polymers used for potential use in fabricating OLED and photovoltaic cells…….60

Figure 4.2. Incorporation of red-fluorescent dyes in constructing NIR conjugated polymers.....61

Figure 4.3. Generic structure and examples of the most common heterocyclic components found in cyanine dyes……...61

Figure 4.4. Chemical structures of Benzindocyanine and Indocyanine dye and their spectroscopic characterization in methanol……..……...63

Figure 4.5. TGA and DSC measurements for polymer **P9** prepared as outline in scheme 4.1. Data were acquired at the heating rate of 10 $^oC.\ Min^{-1}$ in N_2 atmosphere……..64

Figure 4.6. Normalized absorption and emission spectra of the monomer **30**, dimer **31**, tetramer **34** and **P9** in DMSO……...68

Figure 4.7. Normalized Absorbance of Monomer, Dimer, Tetramer and polymer **P9** in DMSO at concentrations ranging from 100uM to 0.1uM……..…..69

Figure 4.8. Variable- temperature ^{1}H-NMR spectra of cyanine polymer **P9**…….....70

Figure 4.9. Comparison of NMR spectra of monomer **30** and cyanine polymer **P9**…….....71

List of Schemes

Scheme 2.1. Reaction of DCP with hydroxy- oxime **1** produces isoxazole **2**. Chemical structures of small molecule **M1** and polymer **P1**……....…26

Scheme 2.2. Preparation of monomers **6** and **8**……..27

Scheme 2.3. Preparation of small molecule sensor **M1** and polymers **P1** and **P3**…….28

Scheme 3.1**.** Synthesis of the monomer **15**……....50

Scheme 3.2. Attempted synthesis of polymer **P4** using pre-functionalized monomer……..51

Scheme 3.3. Attempted synthesis of polymer **P4** using post-functionalization method……...52

Scheme 3.4. Synthesis of the Polymer **P7**…….54

Scheme 3.5. Synthesis of the Polymer **P8**……54

Scheme 4.1. Earlier reaction scheme for the synthesis of the poly (cyanine) polymer……63

Scheme 4.2. Synthesis of the intermediates……..65

Scheme 4.3. Synthesis of Monomer, Dimer and Tetramer……...66

Scheme 4.4. Synthesis of polymer **P9**……...67

List of Abbreviations

AFP- amplifying fluorescent polymer

Ac_2O- acetic anhydride

AcOH- acetic acid

CO- carbon monoxide

CPs- conjugated polymers

Cy5- cyanines dye

d- deuterium

DCM- dichloromethane

DCP- diethylchlorophoshate

DMF- N,N-dimethylformamide

DMSO- dimethylsulfoxide

FTIR- Fourier transform infrared spectroscopy

GPC- gel permeation chromatography

HOMO- Highest Occupied Molecular Orbital

H_2S- Hydrogen Sulfide

LUMO- Lowest Occupied Molecular Orbital

MIP- Molecularly Imprinted Polymer

mp- melting point

NaSH- Sodium hydrosulfide

NMR- Nuclear Magnetic Resonance

NIR- Near infrared

NO- Nitric Oxide

Py- Pyridine

PPV-poly-(*p*-phenylene vinylene)

PPE- poly-(*p*-phenylene ethynylene)

SDS- sodium dodecylsulfate

TBAF- tetrabutylammonium fluoride

TEA- triethylamine

TNT- Trinitrotoluene

TsCl- *p*- toluenesulfonyl chloride

TMS- tetramethylsilane or trimethylsilyl

UV/Vis- ultraviolet/visible

λ- lamda (wavelength)

Abstract

Chemo- and biosensors based on fluorescent conjugated polymers benefit from greater detection sensitivity due to amplification of the electronic perturbations produced by analyte binding. This amplification stems from the exciton-transporting properties of conjugated polymers. In the conventional sensor design paradigm, excitons migrate from the bulk of the polymer to the analyte binding sites which can be either fluorescence quenching sites (turn-off sensors) or lower energy fluorophores (turn-on sensors). In this dissertation, we proposed an alternative design paradigm when analyte binding creates a higher energy gap site in the polymer backbone. In the case of isolated polymer chains in dilute solution, these higher energy gap sites act as "roadblocks" for migrating excitons, effectively limiting the exciton migration length. This is responsible for an amplified enhancement of fluorescence of conjugated polymer sensors. As a proof of concept, we utilized this design principle to develop an amplifying turn-on sensor for organophosphorous warfare agents mimics, and demonstrated substantial signal gain and much broader analyte detection range relative to the corresponding small-molecule analogue. In addition, we utilized this novel "higher energy gap" control concept to develop an amplifying fluorescent conjugated polymer sensor for the detection of hydrogen sulfide. This new paradigm expands the generality and universality of the signal amplification concept in conjugated polymers, and can be used to design amplifying turn-on fluorescent sensors for various practically useful analytes. The last part of this dissertation focuses on the conceptual design of near infrared (NIR) conjugated polymers based on cyanine building blocks. We developed a synthetic approach to this class of fluorescent materials which can eventually become useful in biomedical and bioimaging applications.

Chapter 1. Amplifying Fluorescent Polymers

1.1 Conjugated Polymers

Conjugated Polymers (CPs) have received wide interest in the field of optoelectronic devices and chemical and biological sensors after the discovery by Shirakawa, Heeger and MacDiarmid in 1970 that polyacetylene (PA) dramatically increased the conductivity when subjected to oxidative doping via exposure to halogens.[1,2] The main characteristics of CPs is the array of alternating single and double (or triple) bonds along the conjugated backbone. The extended over the large number of monomer units π-conjugation is responsible for their unique optical and electronic properties.[3] The CPs are used in the photovoltaic cells[4], light emitting diodes (OLED's)[3], bio- and chemical sensors[5] (Figure 1.1).

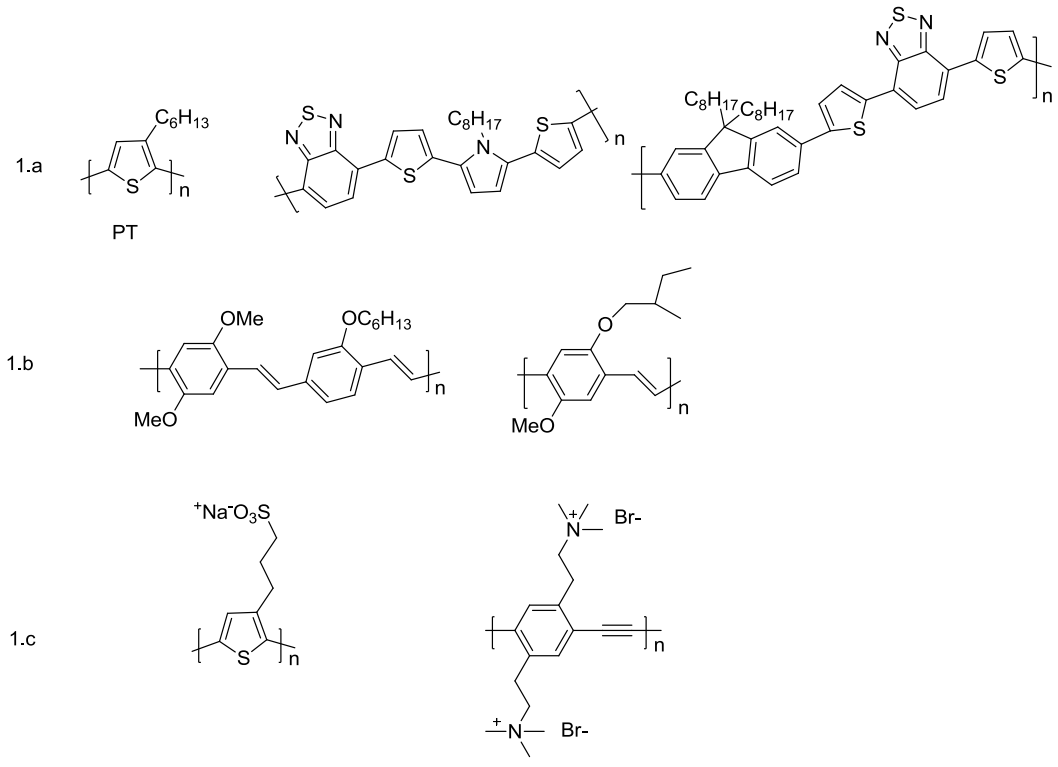

Figure 1.1. Examples of conjugated polymers for various practical applications. a) photovolatics,[4] b) OLEd's[3] c) Biosensors.[5]

Conjugated Polymers provide an effective medium for the transport of excitons and charges (electrons and holes). Design of CP- based fluorescent chemo- and biosensors is a rapidly growing field, due to the unparalleled sensitivity and selectivity provided by CPs. The use of CPs in the sensory field is advantageous over using small molecule sensors due to the efficient energy migration from the bulk of CP to the analyte binding site. Analyte interaction at one binding site can affect the electronic and optical properties of the entire CP chain, which leads to the generation of a measurable amplified optical or electrochemical response.[6] Conjugated polymers are used in the detection of various analytes ranging from explosives and biomolecules to toxic transition metal ions.

In pristine (neutral sate) CPs have a direct band gap or energy gap between the valence band and conduction band which can be altered by chemical modification of the repeating unit of CP.[7] Typically, after binding of an analyte with a receptor, a low energy gap is created at the binding site which is also known as a local minimum or defective site (Figure 1.2).

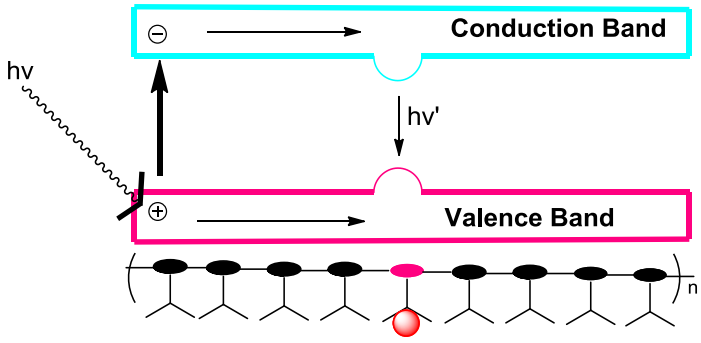

Figure 1.2. Illustration of the mechanism of the exciton migration to the analyte binding site on the conjugated backbone, resulting in photonic signal amplification.

Photoexcitation of CP results in the generation of excited states (excitons) that during their lifetime randomly migrate within the backbone of the polymer. These randomly walking excitons can sample around the backbone until they find a trapping or defective site. Eventually,

all these excitons end up at the local minimum, depopulating the conduction band and producing an amplified fluorescent signal (Figure 1.2).[8]

Therefore, emission of CP is dominated by the excitation energy (excitons) migration to the local minima within the polymer band structures. For example, in case of poly(*p*-phenylene ethynylene) (PPE) polymer with a terminal anthracene fluorophore, the dominating longer wavelength emission was due to the energy migration to the anthracene group with a lower energy gap relative to the CP backbone band gap (Figure 1.3). [9,10]

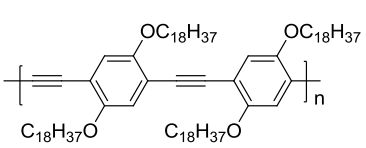

Polymer **P-I**

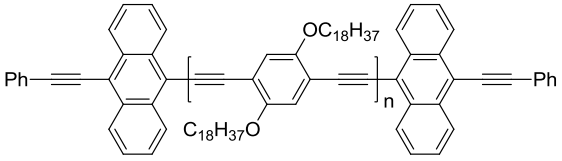

Anthracene Capped Polymer **P-II**

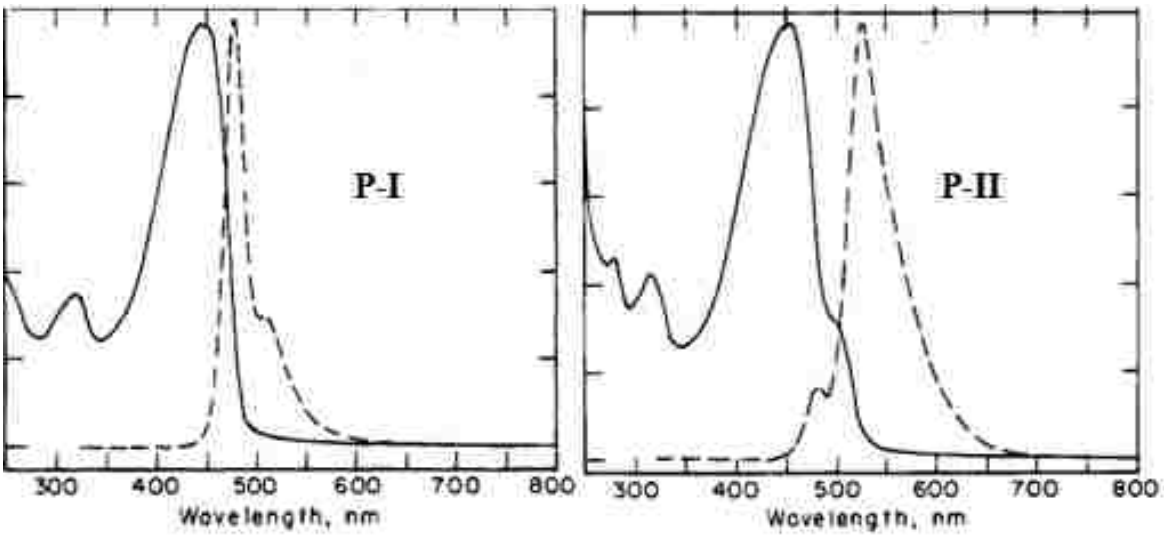

Figure 1.3. Bold traces show the absorption and the dashed traces are the emission spectra of the polymers. Red shifted emission of the polymer **P-II** was observed with introduction of an anthracene end group. (Reproduced with permission from ref. 10. Copyright © 1995, American Chemical Society.)

Similarly, for a complex ladder type polymer **P-III** the emission spectrum was found to be dominated by defective sites present in low concentrations (Figure 1.4). This kind of effect (red shifted emission) was likely due to the migration of excitons to the defective sites which were created due to the incomplete cyclization in the process of the polymer preparation.[11]

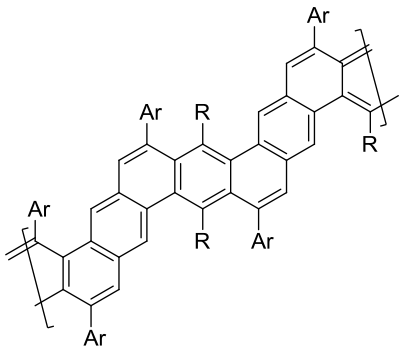

P-III

Figure 1.4. Schematic representation of a ladder type polymer **P-III**.

1.2 Signal Amplification

The ability of CPs to produce amplified fluorescent signal after interacting with an analyte makes them an ideal platform for sensory applications. The amplification stems from the efficient energy transfer from the higher energy polymer π-conjugated backbone to a lower energy gap analyte binding site. Due to their ability to amplify analyte binding event, CPs are also referred to as amplifying fluorescent polymers (AFP's).[12] The new amplified signal obtained can be attenuation, or enhancement, or change in wavelength relative to the initial fluorescence of the CP. The increase in fluorescence intensity is referred to as "turn-on", and decrease in the intensity as "turn-off" response whereas the new signal at different wavelength characterizes a ratiometric sensor.

Turn-off sensor functions by creating a fluorescence quenching site by analyte binding. For example, if initially CP is in the fluorescent state, an analyte interaction with one of many receptors that are wired in series results in fluorescence quenching.

1.3 Signal Amplification via Turn-Off Mechanism

The first example of signal amplification in CPs was demonstrated by Swager and co-workers for the detection of paraquat, a powerful electron acceptor and fluorescence quenching agent acting based on an electron transfer mechanism.[13]

They demonstrated the signal amplification by fluorescence quenching mechanism using PPE possessing cyclophane as a repeating unit directly integrated into the polymer backbone and paraquat as a quencher, which is well known to bind with cyclophane. In addition to the polymer, a model compound or a small molecule containing a single cyclophane receptor was also studied in order to evaluate the signal amplification of CP and to understand the mobility of excitons in the polymer chain. Upon binding of the analyte (quencher) with receptor (cyclophane) in the small molecule sensor, fluorescence was partially quenched producing a lower magnitude turn-off response. In contrast, in case of the CP, the excitons migration in the band gap upon encountering the quencher-bound receptor site produced fluorescence that was dramatically quenched relative to the response of the small molecule sensor (Figure 1.5).

In that study, they also investigated the exciton lifetime which was ~0.6 ns and therefore during its lifetime the exciton could sample around 65 receptors producing a 65- fold increase in signal compared to the small molecule.[14] Therefore, one binding of an analyte with receptor affected the energy distribution of the entire CP backbone via energy migration from the polymer backbone to the analyte bound site.

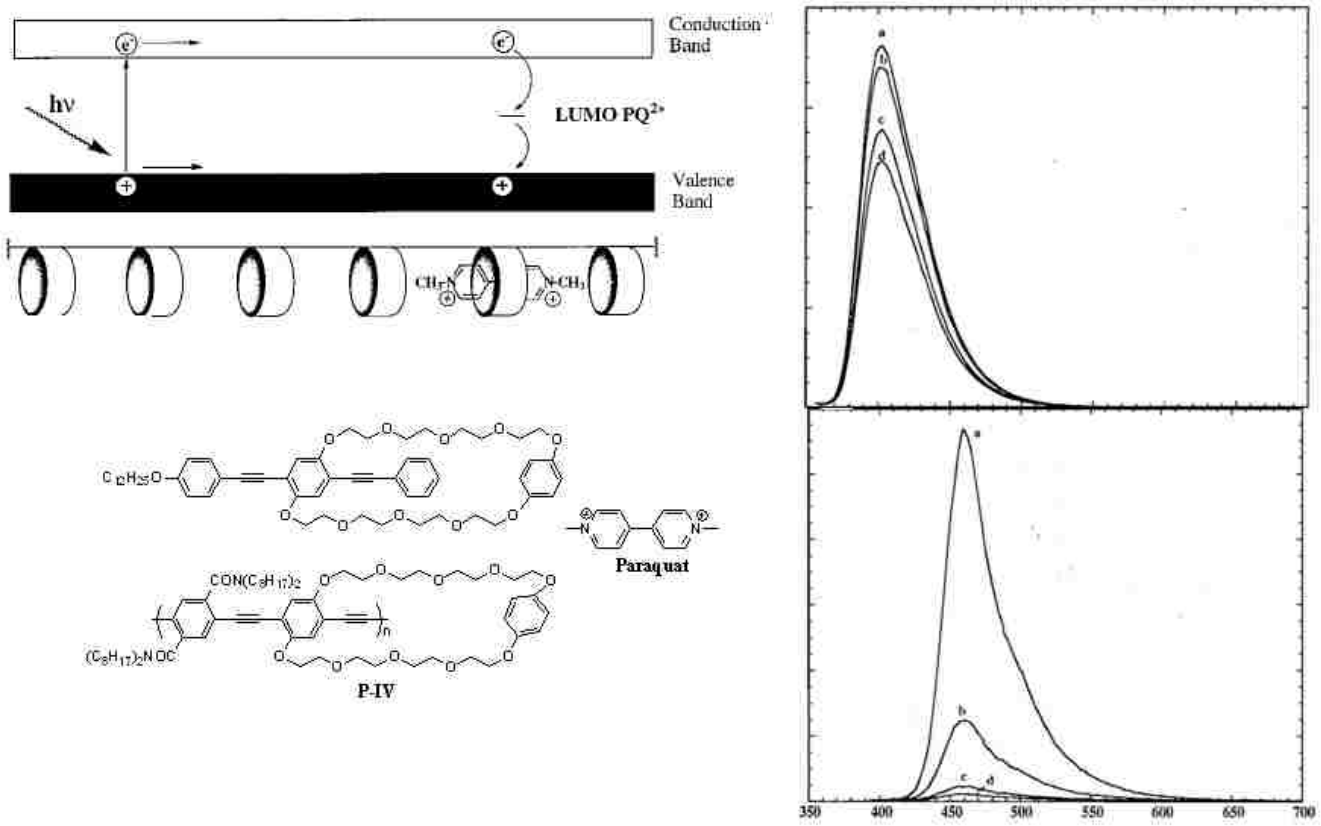

Figure 1.5. Demonstration of an amplified quenching in a CP (**P-IV)** by paraquat (PQ^{2+}). Emission spectra of **small molecule (top)** and the **P-IV (bottom)** as a function of added PQ^{2+}. (Reproduced with permission from ref. 1. Copyright © 2001, American Chemical Society.)

CP based materials showed excellent chemosensory efficiency for the detection of electron-deficient analytes such as nitroaromatic compounds, which cause fluorescence quenching via the electron-transfer mechanism. Swager and the group synthesized an iptycene functionalized PPE polymer (**P-V)** spin casted to a thin film. The bulky iptycene groups prevented the polymer chains from aggregating and created substantial cavities (large internal free volume) for an analyte (TNT) to enter and bind producing a large decrease in the fluorescent response (Figure 1.6).[15] Indeed, this polymer is now the best sensing material for TNT and other nitroaromatic explosives detection, and is a core of widely used commercially manufactured explosive detecting devices.

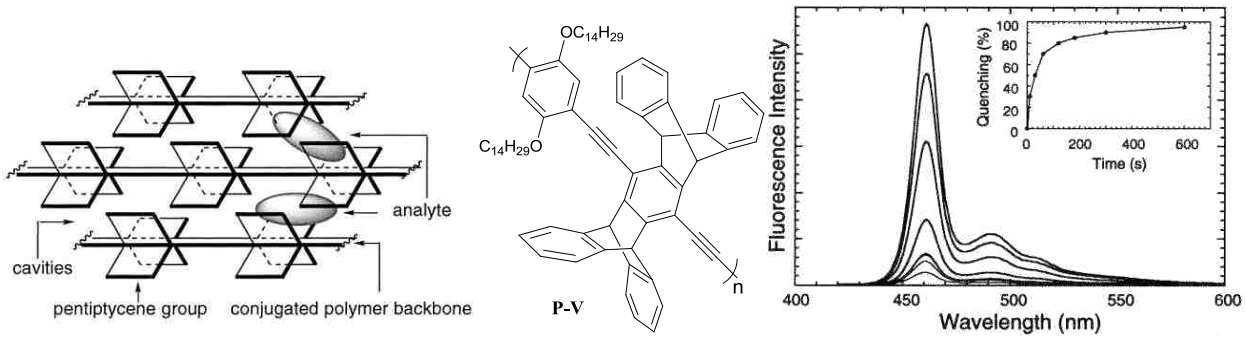

Figure 1.6. Decrease in fluorescence intensity of iptycene functionalized PPE polymer (**P-V**) after exposure of the polymer to TNT vapors. (Reproduced with permission from ref. 15. Copyright © 1998, American Chemical Society.)

Nesterov[16] and the group used molecular imprinting technique to create molecular shape specific cavities for analyte recognition and prepared a TNT-molecularly imprinted polymer (MIP) which upon exposure to TNT vapors showed significant decrease in the fluorescence intensity. The MIP polymers possess shape-selective cavities where TNT molecules can perfectly fit. As a result there was a decrease in the fluorescence intensity. In both cases, quenching behavior was observed due to the strong electron deficient nature of the nitroaromatic analytes (Figure 1.7).

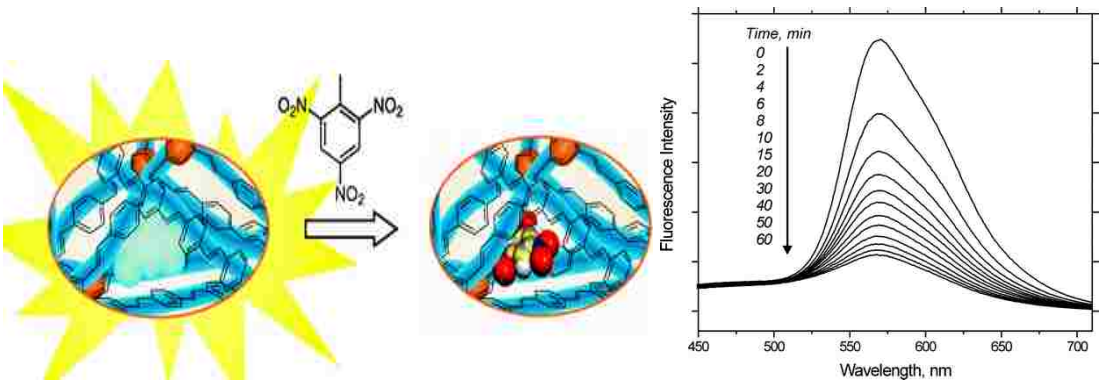

Figure 1.7. Polymer is fluorescent before binding with analyte (TNT) and then subsequently quenched after interacting with TNT vapor. (Reproduced with permission from ref. 16. Copyright © 2007, American Chemical Society.)

Swager[17], Leclerc[18], Xi[19] and others have designed crown ether based conjugated polymers for the detection of small ions such as K^+, Na^+, Li^+. Binding of these small ions with crown ethers results in the formation of π-stacked aggregates and consequent fluorescence quenching (Figure 1.8).

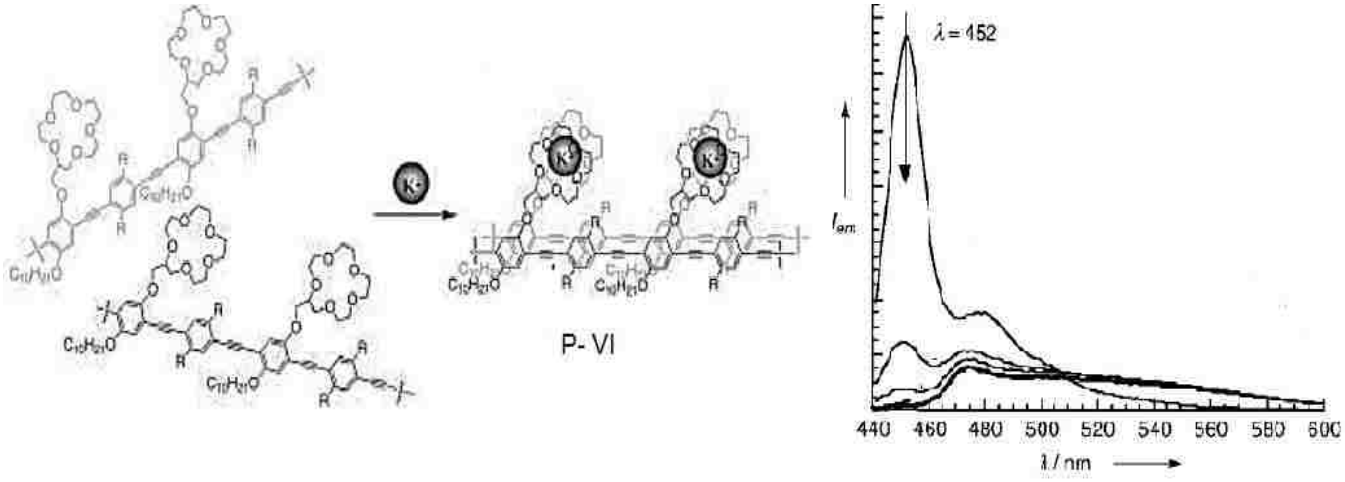

Figure 1.8. K^+-induced aggregation of a crown ether-functionalized polymer (**P-VI**). (Reproduced with permission from ref 17. Copyright © 2000, Wiley-VCH.)

Detection of the larger metal ions such as Hg^{2+} and Pb^{2+} was done by Bunz[20], Wang[21] and others. For example, Wang and co-workers used thymine-functionalized CP which upon exposure to Hg^{2+}, showed substantial fluorescence quenching. Similar to the case of smaller ions, the coordination of Hg^{2+} with thymine resulted in π- stacked polymer aggregates that lead to the quenching of the fluorescence of CP. Bunz and co-workers designed carbohydrate-functionalized water-soluble PPE polymer that upon coordination with Pb^{2+} also showed quenched fluorescence due to the similar analyte binding induced CP aggregation (Figure 1.9).[22]

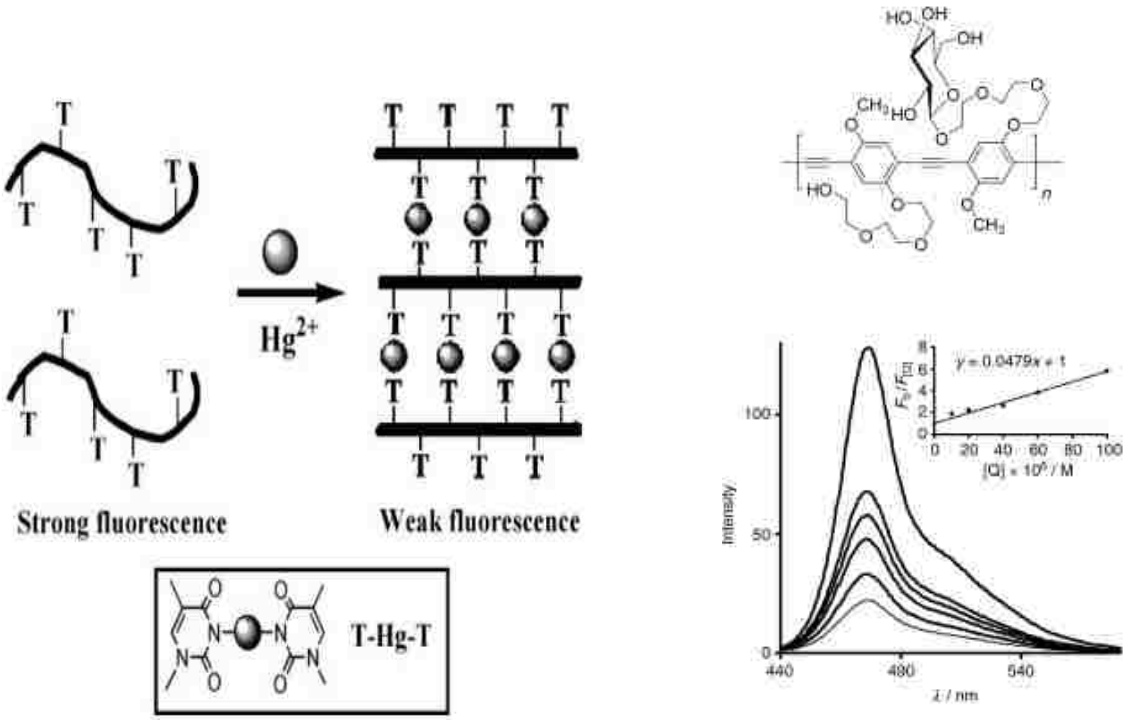

Figure 1.9. Thymine functionalized polythiophene polymer (left) and carbohydrate-functionalized PPE polymer (right) showed strong fluorescent quenching upon interaction with analyte due to the analyte-induced polymer aggregation.(Reproduced with permission from ref. 21, 22. Copyright © 2006, 2004, Wiley- VCH).

1.4. Signal Amplification via FRET

Fluorescence Resonance Energy Transfer (FRET) is a widely used technique in the detection of large biomolecules such as proteins, DNA, etc. CPs provide an excellent manifold for collecting and transport of excitons (an antenna effect). Therefore CPs act as excellent energy donors in the FRET-labeling biosensing. Due to electrostatic interaction between CP and chromophore labeled DNA, they form a dimer that leads to the efficient energy transfer from the CP to the chromophore-labeled DNA, producing a new signal.[23]

Gaylord, Bazan and Heeger developed a method for the detection of specific DNA by using FRET (Figure 1.10).[24] The system consists of three parts; a cationic conjugated poly(fluorene-cophenylene) polymer (**P-IX**), a probe peptide nucleic acid (PNA) strand labeled at the 5' end with fluorescein which shows strong spectral overlap with the polymer and the target DNA strand.

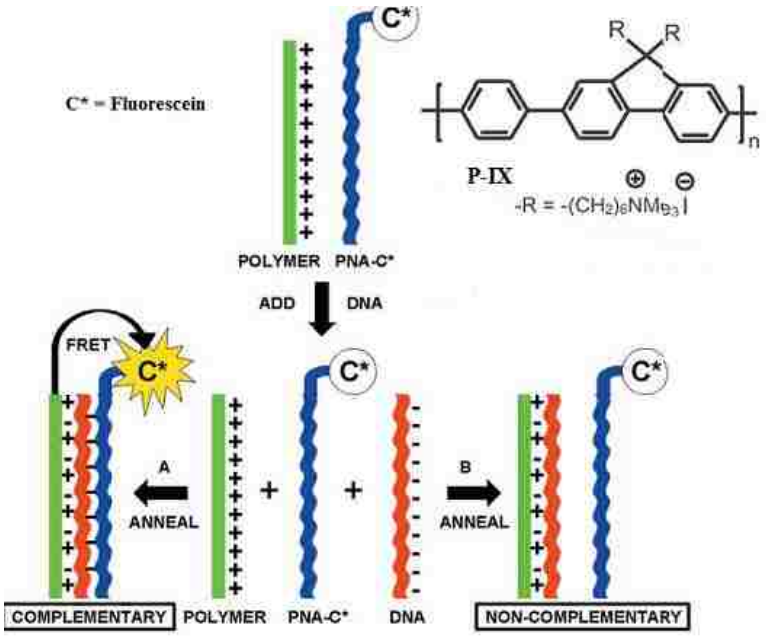

Figure 1.10. Schematic description of amplified fluorescent detection of a complimentary ssDNA strand (blue) by using FRET from CP (**P-IX)** (black) to fluorescein chromophore linked to a PNA reporter (red). Adding complementary DNA results in formation of a triplex where efficient FRET from CP to fluorescein produces an amplified fluorescent response; adding non-complementary DNA (green) produces no response. (Reproduced with permission from ref. 24. Copyright © 2002, The National Academy of Sciences.)

The donor polymer and fluorescein labeled PNA acceptor have spectral overlap required for efficient FRET but are not electrostatically attracted. However, when the DNA complementary to PNA is added, there is electrostatic attraction between the polymer and DNA as a result of which PNA labeled fluorescein becomes closer to the polymer. This brings them within the distance required for an efficient energy transfer from the polymer to fluorescein. Due

to this FRET, the emission from fluorescein was 25 times amplified relative to emission of the directly excited free fluorescein.

In another work by Bazan and group, the conjugated polymer (**P-IX**) behaved as a light-harvesting antenna unit which transferred excitation via FRET to a signaling fluorophore (Figure 1.11).[25] Figure A shows an efficient energy transfer after addition of a complementary target ssDNA to the fluorescein labeled ssDNA due to the formation of a double helix. The overall energy transfer from polymer through Fluorescein to Ethidium Bromide chromophore (EB) produces an amplified fluorescent signal. Figure B shows addition of a non-complementary ssDNA where base-pair hybridization does not occur and no EB intercalation and no energy transfer from the fluorescein labeled ssDNA to EB can be observed.

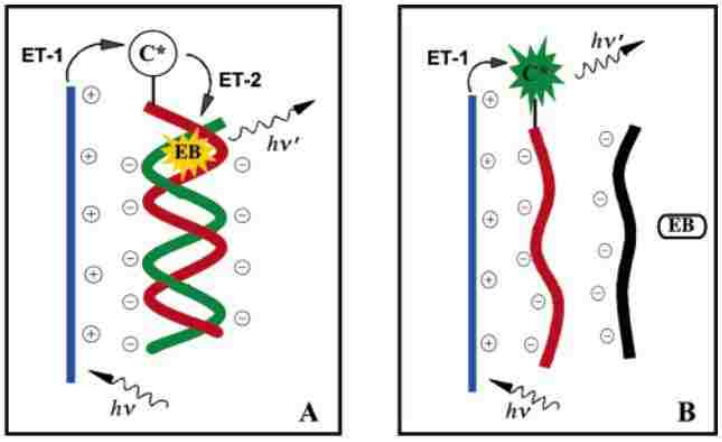

Figure 1.11. Strong FRET upon addition of a complementary target ssDNA vs weak FRET when noncomplementary ssDNA is used. (Reproduced with permission from ref.25. Copyright © 2004, American Chemical Society.)

1.5. Turn-On Amplification: Biosensing

Unlike intrinsically turn-on amplifying fluorescent CPs, quencher removal by analyte binding to produce an amplified turn-on response is a generally utilized strategy. Conjugated

Polymers with functionalized ionic chains (polyelectrolytes) are typically used in biosensing because of their improved solubility in aqueous medium. In a proof-of-concept demonstration, Whitten[26] and co-workers have used biotin-functionalized methyl viologen (MV^{2+}) adsorbed to the backbone that quenched the CP fluorescence which was recovered back after adding avidin. The original fluorescence quenching of the CP backbone was observed due to the electrostatic interaction between cationic MV^{2+} and the anionic polyelectrolyte (Figure 1.12). Upon the addition of avidin, the biotin-functionalized MV^{2+} was removed from CP thus restoring fluorescence of the CP. This scheme demonstrated signal amplification of up to 1,000,000 times (relative to the corresponding small molecule sensor).

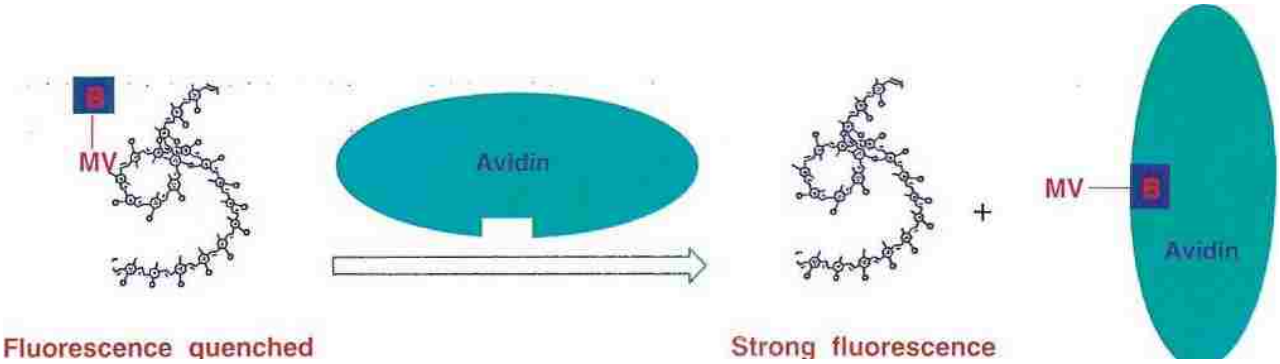

Figure 1.12. Whitten's quencher-tether-ligand-based strategy to biosensing. Addition of avidin to a solution of conjugated polyelectrolyte and biotin-functionalized quencher resulted in a turn-on (fluorescence recovery) response. (Reproduced with permission from ref. 26. Copyright © 1999, The National Academy of Sciences.)

In the quest to develop intrinsically amplifying turn-on CP-based sensors, two different groups, Swager[27] and Wang[28] designed conjugated polymers for fluoride ion sensing using turn-on mechanism. Wang used phenolic derivative of polyquinoline to detect fluoride ion that produced a 100 fold increase in a red shifted emission after exposure to fluoride ion (Figure 1.13).

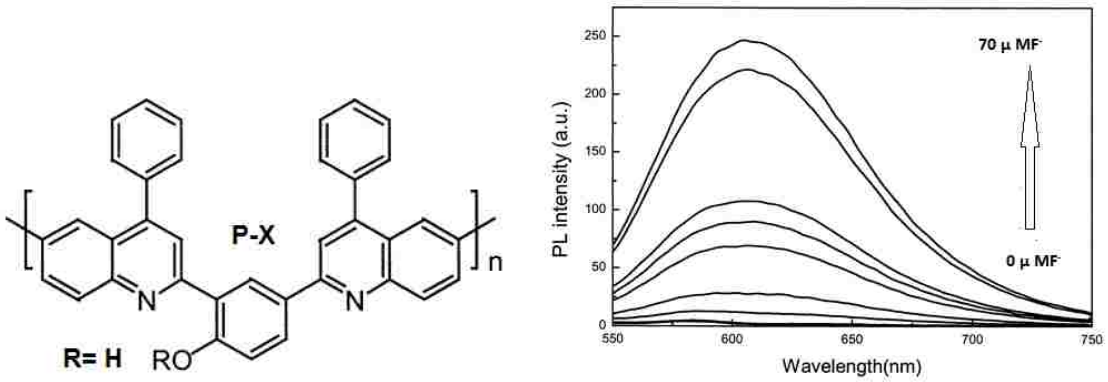

Figure 1.13. Wang's polymer **P X** which showed increase in fluorescent intensity after addition of fluoride ion. (Reproduced with permission from ref. 28. Copyright © 2003, American Chemical Society.)

Kim and Swager provided another example of signal amplification for the detection of fluoride. Their polymer was based on receptor having TIPS protected alcohol functionalized group that after interacting with analyte (TBAF) underwent cleavage of O-Si bond and subsequent formation of a highly emissive coumarin derivative (low energy defect site). The excitons formed upon backbone irradiation can find the defective site and migrate to that site producing an amplified signal at a different, higher wavelength relative to the initial polymer (Figure 1.14).

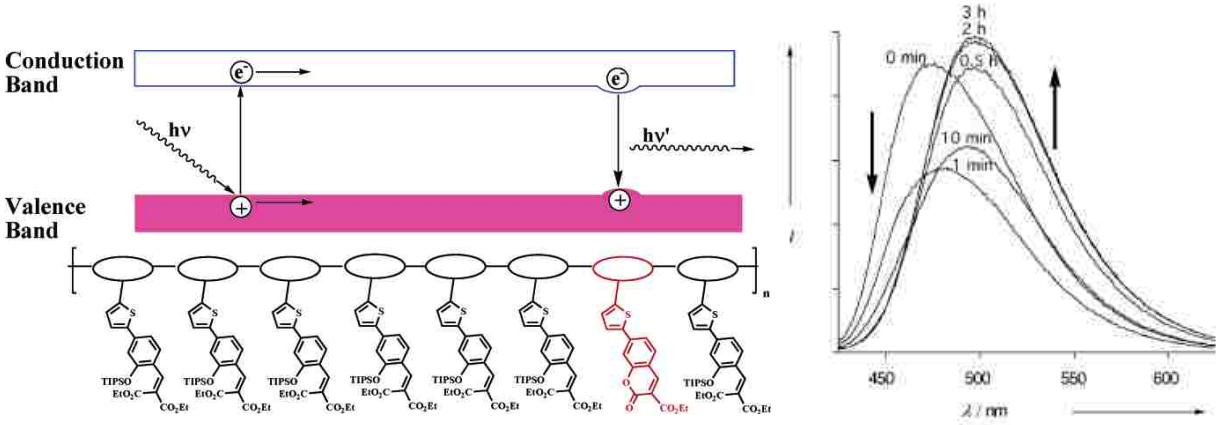

Figure 1.14. Fluoride-induced lactonization of side chains on the polymer backbone producing emissive sites with a smaller energy gap that gave a new amplified emission, increasing with time. (Reproduced with permission from ref. 27. Copyright © 2003, Wiley- VCH.)

1.6. Energy Transfer

The increased sensitivity (amplification) in amplifying fluorescent conjugated polymers is observed due to the CP ability to serve as an efficient manifold for the transport of excitons. In dilute solutions the efficient energy transfer in CP from the backbone to the binding site can occur intramolecularly by two different interplaying pathways: through-space Förster-type mechanism and/or through-bond (Dexter) Exchange Mechanism.[29]

The Förster energy transfer mechanism is a radiationless transition occurring through Coulombic interactions between electronic transition dipoles on donor and acceptor moieties. When this mechanism is operational, there is no need to have chemical bonding between the donor and acceptor chromophores, but there should be a significant overlap between the donor emission and acceptor absorption spectra. The rate of energy transfer by the Förster mechanism depends upon the distance (R) between the donor and acceptor moieties as a reciprocal sixth power (i.e $k_{ET} \sim 1/R^6$). [29]

In contrast, in the Dexter-mechanism the donor and acceptor moieties should be chemically bonded, meaning that the donor and acceptor should exhibit substantial overlap between MOs centered on donor and acceptor moieties, or have an array of interconnecting chemical bonds facilitating such an orbital interaction. The rate of the energy transfer by Dexter exchange mechanism shows exponential decrease with increasing distance between the donor and acceptor moieties, i.e $k_{ET} \sim \exp(-\beta R)$, where β is an attenuation coefficient, which depends upon the extent of electronic interaction between the donor and acceptor units.[30] In CPs, both mechanisms play an important role, with the role of the Dexter exchange mechanism increasing with increasing electronic delocalization in CPs.

1.7 Research Focus of This Dissertation

Photoexcitation of CP creates an excited state (exciton) that during its lifetime can move freely along the CP backbone until it finds a trapping lower energy site. As the exciton finds a lower energy site, it radiatively (or radiativelessly) deactivates to the ground state producing an amplified fluorescent signal in both turn-on and turn-off sensing schemes. In all the examples shown above, the amplification was obtained due to the migration of excitons from the higher energy gap CP backbone to a lower energy gap analyte-bound site. It is obvious that the energy migration is possible only from the higher to lower energy sites and not in the opposite direction. Therefore, in order for this amplification mechanism to be operational, the interaction between the receptor and analyte must create a lower energy site where the energy migration takes place producing an amplified signal.

An alternative and previously unexplored paradigm arises when an analyte binding with receptor creates a **higher energy gap site** on the CP backbone. It is well known that excitons can't funnel down to a higher energy site from a lower energy CP backbone, it is thermodynamically impossible. Our research focused on a possibility to produce signal amplification upon the creation of a higher energy gap site on the CP backbone after interaction of a receptor and an analyte. This stemmed from the idea that the higher-energy site would act as a "roadblock", which decreases the exciton migration efficiency and lowers excitons migration length thus resulting in the increasing fluorescent intensity of the CP. Overall, such amplification of relatively minor changes at the electronically interacting higher-energy receptor upon reacting with analyte would be an excellent manifestation of the generality and universality of conjugated polymers as a platform for fluorescent chemosensor development (Figure 1.15).

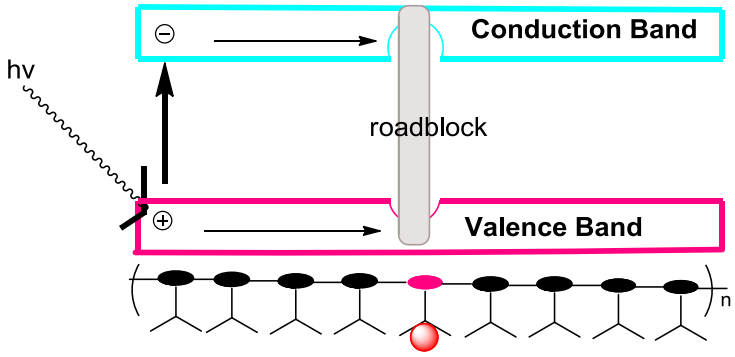

Figure 1.15. Illustration of decreasing exciton diffusion length due to a higher energy gap "roadblock" site.

To the best of our knowledge, there are no previous examples demonstrating this type of signal amplification mechanism. Usually turn-on response CP based sensors are obtained by removing the quenching site due to analyte binding. However, in our approach the signal amplification is obtained by the inverse electronic control, i.e. instead of funneling of excitons to the lower- energy site, the excitons are localized in the CP backbone.

In order to obtain the turn-on signal amplification via inverse electronic control, the interaction of a receptor and an analyte needs to create a new chromophore that will be higher in energy (blue shifted) relative to the initial interacting receptor. This would create "roadblocks" for exciton migration in the CP backbone and as a result the excitons formed due to photoexcitaton of CP get more localized, as their migration length would be essentially restricted by the newly created "roadblock" site.

When poly(*p*-phenylene vinylene) (PPV) is used as a CP, the newly created high band chromophore needs to absorb in the blue-green region (300-500 nm) of spectrum in order to satisfy requirement to be of higher energy than the CP itself. Coumarin, Benzothiazole and their derivatives are commonly used high-energy-gap chromophores in the detection of various analytes. Similarly, naphthalene also falls in the same category, therefore we decided to use

naphthalene as a receptor (chromophore) because it would be synthetically easier to functionalize for the incorporation into a CP backbone compared to benzothiazole and/or coumarin. The properly functionalized naphthalene would be a co-monomer to be used in the synthesis of a conjugated polymer, i.e poly(*p*-arylene vinylene). Functionalized naphthalene would act as a receptor unit where analyte binding would produce electronic perturbation at the backbone and this polymer would be used in the study of signal amplification phenomena.

The second chapter focuses on a proof-of-concept development of the signal amplifying polymer functioning on the principle of creating a higher energy gap site. The amplification is obtained due to the incorporation of a higher energy gap chromophore and resulting localization of excitons. From the practical standpoint, this polymer would be a good prototype of a sensor for the detection of toxic organophosphates warfare agents.

The third chapter focuses on applying the same concept of the higher energy gap signal amplification for the preparation of CP that would detect hydrogen sulfide (H_2S). H_2S is a toxic gas which is a third endogenous gas after nitric oxide (NO) and carbon monoxide (CO). Therefore, there is always a need of developing a chemosensor that shows better sensitivity and selectivity for this wide-spread analyte.

The fourth chapter focuses on the synthesis and studies of the novel Near-IR (NIR) conjugated polymers based on cyanine dyes that have potential applications for biosensing. Potential application of these NIR CPs in the biomedical field could stem from their cationic nature which increases the probability of binding with negatively charged biomolecules such as DNA. The electrostatic interaction could lead to the feasible detection of biomolecules such as proteins and DNA due to signal amplification in the CP based schemes. In addition, there is

always a better need of NIR chromophores and fluorophores for medical research as there is a much lower interference from cells and tissues in the NIR region.

1.8. References

[1] Shirakawa, H. The Discovery of Polyacetylene Film: The Dawning of an Era of Conducting Polymers. *Angew. Chem. Int. Ed*. **2001**, *40*, 2574-2580.

[2] MacDiamrmid, A. G. "Synthetic Metals": A Novel Role for Organic Polymers. *Angew. Chem. Int. Ed.* **2001**, *40*, 2581-2590.

[3] Kraft, A.; Grimsdale, A. C.; Holmes, A. B. Electroluminescent Conjugated Polymers - Seeing Polymers in a New Light. *Angew. Chem. Int. Ed*. **1998**, *37*, 402-428.

[4] Cheng, Y-J.; Yang, S. H.; Hsu, S. C. Synthesis of Conjugated Polymers for Organic Solar Cell Applications. *Chem. Rev*. **2009**, *109*, 5868–5923.

[5] McQuade, D. T.; Pullen, E. A.; Swager, T. M. Conjugated Polymer-Based Chemical Sensors. *Chem. Rev.* **2000**, *100*, 2537-2574.

[6] Swager, T. M. The Molecular Wire Approach to Sensory Signal Amplification. *Acc. Chem. Res.* **1998**, *31*, 201-207.

[7] Zhang, Z.; Yates, T. J. Band Bending in Semiconductors: Chemical and Physical Consequences at Surfaces and Interfaces. *Chem. Rev.* **2012**, *112*, 5520-5551.

[8] Dongwhagn, L.; Swager T. M. Defining Space Around Conjugated Polymers: New Vistas in Self-Amplifying Sensory Materials. *Syn. Lett*. **2004**, *1*, 149-154.

[9] Swager, T. M.; Gil, C. J.; Wrighton, M. S. Fluorescence Studies of Poly(p-phenyleneethynylene)s: The Effect of Anthracene Substitution *J. Phys. Chem*. **1995**, *99*, 4886-4893.

[10] Zhou, Q.; Swager, T. M. Fluorescent Chemosensors Based on Energy Migration in Conjugated Polymers: The Molecular Wire Approach to Increased Sensitivity. *J. Am. Chem. Soc*. **1995**, *117*, 12593-12602.

[11] Goldfinger, M. B.; Swager, T. M. Fused Polycyclic Aromatics via Electrophile-Induced Cyclization Reactions: Application to the Synthesis of Graphite Ribbons. *J. Am. Chem. Soc*. **1994,** *116*, 7895-7896.

[12] Thomas, S. W.; Joly, G. D.; Swager, T. M. Chemical Sensors Based on Amplifying Fluorescent Conjugated Polymers. *Chem. Rev.* **2007**, *107*, 1339-1386.

[13] Zhou, Q.; Swager, T. M. Methodology for Enhancing the Sensitivity of Fluorescent Chemosensors: Energy Migration in Conjugated Polymers. *J. Am. Chem. Soc*. **1995**, *117*, 7017-7018.

[14] Rochat, S.; Swager T. M. Conjugated Amplifying Polymers for Optical Sensing Applications. *ACS Appl. Mater. Interfaces* **2013,** *5*, 4488-4502.

[15] Yang, J.-S.; Swager, T. M. Fluorescent Porous Polymer Films as TNT Chemosensors: Electronic and Structural Effects. *J. Am. Chem. Soc.* **1998,** *120*, 11864-11873.

[16] Li, J.; Kendig, E. C.; Nesterov, E. E. Chemosensory Performance of Molecularly Imprinted Fluorescent Conjugated Polymer Materials. *J. Am. Chem. Soc*. **2007,** *129*, 15911-15918.

[17] Kim, J.; McQuade, D. T.; McHugh, S. K.; Swager, T. M. Ion – Specific Aggregation in Conjugated Polymers: Highly Sensitive and Selective Fluorescent Ion Chemosensors. *Angew.Chem. Int. Ed.* **2000,** *39*, 3868- 3871.

[18] Béra-Abérem, M.; Ho, H.-A.; Leclerc, M. Functional polythiophenes as optical chemo- and biosensors. *Tetrahedron* **2004,** *60*, 11169-11173.

[19] Liu, H.; Wang, S.; Luo, Y.; Tang, W.; Yu, G.; Li, L.; Chen, C.; Liu, Y.; Xi, F. Synthesis and properties of crown ether containing poly(p-phenylenevinylene). *J. Mater. Chem.* **2001,** *11*, 3063-3067.

[20] Kim, I.-B.; Bunz, U. H. F. Modulating the Sensory Response of a Conjugated Polymer by Proteins: An Agglutination Assay for Mercury Ions in Water. *J. Am. Chem. Soc.* **2006,** *128*, 2818-2819.

[21] Tang, Y.; He, F.; Yu, M.; Feng, F.; An, L.; Sun, H.; Wang, S.; Li, Y.; Zhu, D. A Reversible and Highly Selective Fluorescent Sensor for Mercury(II) Using Poly(thiophene)s that Contain Thymine Moieties. *Macromol. Rapid. Commun.* **2006,** *27*, 389-392.

[22] Kim, I.-B.; Erdogan, B.; Wilson, J. N.; Bunz, U. H. F. Sugar-poly(para-phenyleneethynylene) conjugates as sensory materials: Efficient quenching by Hg^{2+} and Pb^{2+} ions. *Chem.-Eur. J.* **2004**, *10*, 6247-6254.

[23] Liu, B.; Bazan, G. C. Homogenous fluorescence-based DNA detection with ionic Conjugated Polymers. *Chem. Mater.* **2004,** *16*, 4467-4476.

[24] Gaylord, B. S.; Heeger, A. J.; Bazan, G. C. DNA detection using water-soluble conjugated polymers and peptide nucleic acid probes. *Proc. Natl. Acad. Sci. U.S.A* **2002,** *99*, 10954-10957.

[25] Wang, S.; Gaylord, S. B.; Bazan C. G. Fluorescein Provides a Resonance Gate for FRET from Conjugated Polymers to DNA Intercalated Dyes. *J. Am. Chem. Soc.* **2004,** *126*, 5446-5451.

[26] Chen, L.; McBranch, D. W.; Wang, H.-L.; Helgeson, R.; Wudl, F.; Whitten, D. G. Highly sensitive biological and chemical sensors based on reversible fluorescence quenching in a conjugated polymer. *Proc. Natl. Acad. Sci. U.S.A* **1999,** *96*, 12287-12292.

[27] Kim, K. T.; Swager, T. M. A Fluorescent Self-Amplifying Wavelength Responsive Sensory Polymer for Fluoride Ions. *Angew. Chem. Int. Ed.* **2003,** *42*, 4803–4806.

[28] Tong, H.; Wang, L.; Jing, X.; Wang, F. "Turn-On" Conjugated Polymer Fluorescent Chemosensor for Fluoride Ion. *Macromolecules* **2003,** *36*, 2584- 2586.

[29] Dexter D. L. A Theory of Sensitized Luminescence in Solids. *J. Chem. Phys.* **1995,** *21*, 836-861.

[30] Turro, J. N. Modern Molecular Photochemistry; University Science Books, **1991.**

Chapter 2. "Higher Energy Gap" Control in Fluorescent Conjugated Polymers: Turn-On Amplified Detection of Organophosphorous Agents

2.1. Introduction

Fluorescent conjugated polymers (CPs) deliver a convenient and versatile platform for the design of fluorescent chemo- and biosensors. The significance of this class of organic materials for sensing applications largely stems from the intrinsic amplification of analyte binding events which is related to the efficient photoexcitation energy migration from the bulk of the polymer to the sites where analyte binding occurred. After the amplification phenomenon had been first reported by Swager in 1995, it became an important design paradigm in developing numerous fluorescent sensors for a broad range of analytes.[1,2] The amplification can be particularly significant in aggregates and thin films of conjugated polymers where it is facilitated by efficient intermolecular exciton migration by through-space dipole – induced dipole (Förster-type) mechanism due to the multitude of close intermolecular contacts.[3] Significant amplification can also be achieved in dilute solutions of conjugated polymers where it originates from intramolecular energy migration through the combination of Förster and through-bond Dexter-type exchange mechanisms.[4] Although amplification as high as 1,000,000 times was reported with strongly quenching analytes for conjugated polymers in dilute solutions,[5] typically it ranges from a few tens to a few hundreds times.[3] Most commonly, the amplification was encountered and studied in the case of turn-off sensors where non-specifically interacting analytes quench fluorescent emission of the polymers through photoinduced electron transfer mechanism (typical analytes in such a case are nitroaromatic explosives, quinones, gold nanoparticles, etc.),[6] or by inducing polymer aggregation.[7] The same approach can be used in the design of turn-on sensors

with operating principle based on the removal of a CP-attached quencher through the interaction with analyte. Since many practically important analytes do not act as CP fluorescence quenchers, the photonic amplification schemes which utilize Fluorescent Resonance Energy Transfer (FRET) effect for turn-on or ratiometric sensing of various non-quenching analytes (such as DNA and other biomolecules) have been developed.[8-10] Although FRET-based design has been successfully implemented for a variety of analytes, it has a number of intrinsic limitations, such as relative complexity of the sensing scheme, the necessity to employ chromophores with spectral characteristics matching the FRET requirements, as well as the need to functionalize one of the components of the sensor (or the CP itself) with a FRET acceptor fluorophore. A backward effect ("interrupted" FRET) in design of a pseudoratiometric sensor was also recently reported.[11]

A different paradigm to achieve turn-on amplification involves incorporation of an analyte-specific receptor electronically coupled to the band structure of the polymer π-electron conjugated system. Such design benefits from the efficient through-bond (by Dexter exchange mechanism) energy transfer which is independent on spectral overlap that controls the efficiency of FRET, and therefore would work in the situations where a FRET-based design would be inefficient. An excellent example of this approach is an amplified turn-on CP-based fluoride sensor developed by Kim and Swager, where fluoride-mediated cyclization of a pendant non-fluorescent precursor yielded a highly emissive low-energy coumarin chromophore electronically coupled to the CP backbone (Figure 2.1A). Indeed, such polymer demonstrated approximately 100-times amplification of fluoride detection (relative to the small-molecule receptor itself).[12]

Although this approach can lead to amplifying ratiometric fluorescent sensors, it is not widely used, possibly due to the fact that it is intrinsically limited to a relatively small subset of analytical reactions that yield high quantum yield fluorophores which are bathochromically

shifted relative to the CP backbone, i.e. generate a lower energy gap strongly fluorescent site (Figure 2.1A). This lower gap site acts as a trap for the randomly migrating excitons and produces a new higher wavelength emission band.

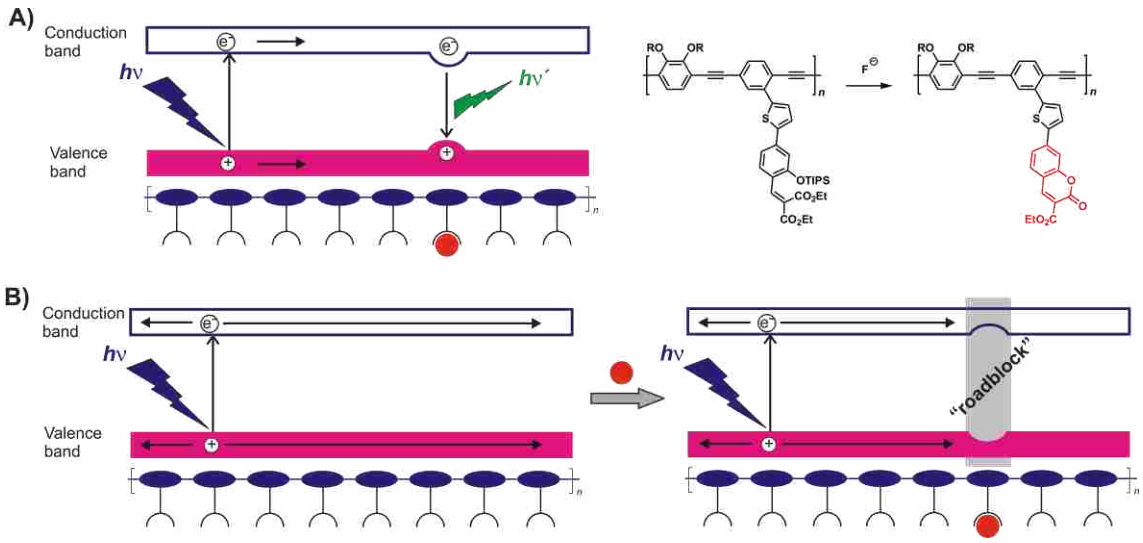

Figure 2.1. A) Schematic energy diagram illustrating the concept of amplified turn-on fluorescent sensing through the formation of a lower energy gap fluorophore and an example of CP turn-on sensor for fluoride detection developed by Kim and Swager.[12] B) Schematic diagram of the "higher energy gap" control of CP fluorescence: an analyte (red circle) binding creates a higher energy gap unit in the CP backbone which decreases the length of exciton migration in the polymer, therefore causing increase of the intensity of fluorescent emission.

Although exciton migration to a lower energy gap or quenching site represents a well-understood mechanism to utilize the amplification phenomenon, one can envision an alternative mechanism leading to amplifying turn-on fluorescent sensors in situations where a reaction with analyte produces a hypsochromically shifted chromophore. Within this paradigm, analyte binding to a receptor chromophore electronically coupled to the CP band structure creates a higher energy gap site on the CP backbone (Figure 2.1B). This higher energy gap site cannot act as an acceptor of the migrating excitons generated in the bulk of the CP. However, this perturbed site would act as a "roadblock" for the excitons and hinder their random migration along the CP backbone. This

"roadblock" effect would be operational because of the fine balance between two mechanisms responsible for exciton migration in an isolated conjugated polymer chain: through-space Förster and through-bond Dexter mechanisms. The higher energy "roadblock" site would predominantly affect the through-bond migration, and the exciton in principle still would be able to bypass the "roadblock" by through-space hopping. However, loss of the through-bond component would make bypassing the higher energy "roadblock" less favorable, and thus of a lower probability to happen. One seemingly counterintuitive consequence of the limiting intramolecular exciton migration is that in some cases this should enhance fluorescent intensity of the CP chromophore. Indeed, it is well known that fluorescence efficiency of CPs can be reduced due to the increased mobility of excitons which upon their migration encounter low-energy defect sites within isolated polymer chains and dissipate their energy radiationlessly. Typical on-chain fluorescence-quenching defects may include conformational defects, chemically oxidized species (or molecular oxygen bound sites), as well as transient defects such as triplet states, photogenerated free charge carriers, or charge-separated states, etc.[13] Therefore, restricting exciton migrating ability should result in decreasing the probability for the exciton quenching through encounter with such on-chain quenching sites, and increasing fluorescence efficiency of CP. Such fluorescent intensity enhancement was experimentally observed in cases where exciton migration in CPs was intentionally restricted by decreasing π-electron conjugation across the polymer backbone.[14] Importantly, such enhancement should occur independent on whether the reaction with analyte produces fluorescent or non-fluorescent chromophore – a major advantage over the conventional scheme relying on formation of a lower energy gap highly fluorescent unit. Since the fluorescence enhancement is directly related to exciton migration in the conjugated polymer, one would expect similar kind of signal gain as in the cases of amplifying polymers utilizing

migration to a lower energy gap unit. Another characteristic feature of this mechanism is that, at least at low analyte concentrations, formation of the higher energy gap site is not expected to change wavelength of the CP emission (as long as the exciton delocalization length does not exceed the distance between the "roadblock" sites, which may only happen at unrealistically high conversion at high analyte concentrations). Thus, this "higher energy gap" electronic control effect would result in an amplified turn-on response on the otherwise small electronic perturbation at the receptor site. Overall, such amplification of a relatively minor electronic perturbation at the higher-energy receptor upon reacting with analyte would be an excellent manifestation of the generality and universality of conjugated polymers as a platform for amplifying fluorescent chemosensors. Surprisingly, to the best of our knowledge, this natural counterpart to the traditional "lower energy gap" paradigm has not been experimentally demonstrated.

To test this hypothesis, we decided to utilize a naphthalene based hydroxy oxime chromophore **1** as an analytical receptor (Scheme 2.1). This compound was recently developed by Rebek as a small-molecule detector for organophosphorous chemical warfare agents.[15] Reaction with organophosphate reagents results in a facile conversion of the oxime **1** into the corresponding isoxazole **2**. Both the oxime **1** (λ_{max}(abs) 354 nm, λ_{max}(em) 392 nm) and product isoxazole **2** (λ_{max}(abs) 326 nm, λ_{max}(em) 361 nm) are higher energy gap chromophores compared to typical fluorescent CPs (such as poly(*p*-phenylene vinylene), PPV, λ_{max}(em) >500 nm[16]). Importantly, product isoxazole chromophore **2** possesses a noticeably higher energy gap relative to the oxime **1** as can be judged from the hypsochromic shifts of both absorption and emission maxima in the **1** to **2** conversion.

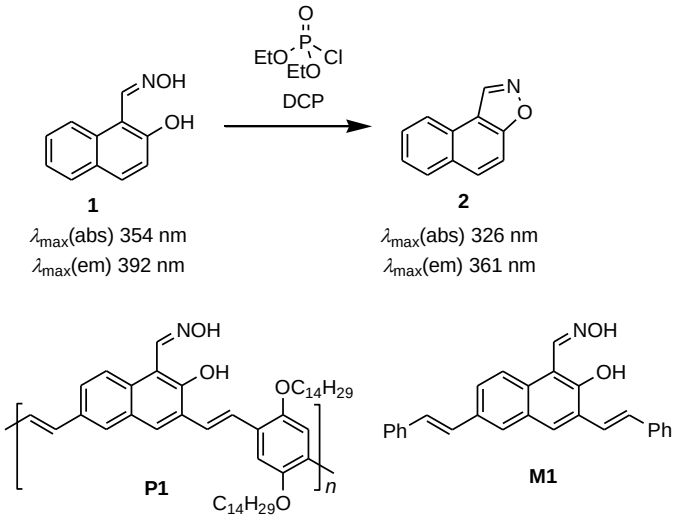

Scheme 2.1. Reaction of DCP with hydroxy- oxime **1** produces isoxazole **2**. Chemical structures of small molecule **M1** and polymer **P1**.

Therefore, incorporation of such a chromophore into a PPV backbone would yield an excellent system for the experimental testing of the "higher energy gap" control hypothesis. In addition, the practical importance of a rapid and robust detection of low concentrations of organophosphates – simple chemicals which can be readily manufactured and belong to the class of the most dangerous chemical warfare agents, cannot be overestimated.[17] Numerous sensors for chromogenic and fluorogenic detection of organophosphates have been reported to date,[18] however they are mostly based on small molecules, and do not benefit from the possibility of signal amplification stemming from the use of conjugated polymers. Therefore, we decided to prepare a poly(arylene vinylene) conjugated polymer **P1** based on the receptor chromophore **1**, and test in detail the "higher energy gap" control paradigm in designing a turn-on amplifying sensor, as well as to determine the extent of signal gain stemming from using the polymer as opposed to using a small molecule counterpart **M1**.

2.2 Synthesis

Preparation of the polymer **P1** required designing a synthetic strategy toward the naphthalene oxime **1** functionalized with appropriate "handles" for incorporation into the CP backbone. The synthesis of dibromo monomer **6** started with bromination of the commercially available 6-bromo-2-naphthol to yield tetrabromoketone **3** which upon reduction with $SnCl_2$ in acetic acid gave 1,3,6-tribromo-2-naphthol **4** (Scheme 2.2). Further selective reduction of **4** with $SnCl_2$ in refluxing ethanol yielded 3,6-dibromo-2-naphthol **5** in 51% overall yield. Increased nucleophilicity of carbon 1 in the naphthalene ring enabled selective installation of an aldehyde group via Reimer-Tiemann reaction to give the required monomer **6** in 58% yield.

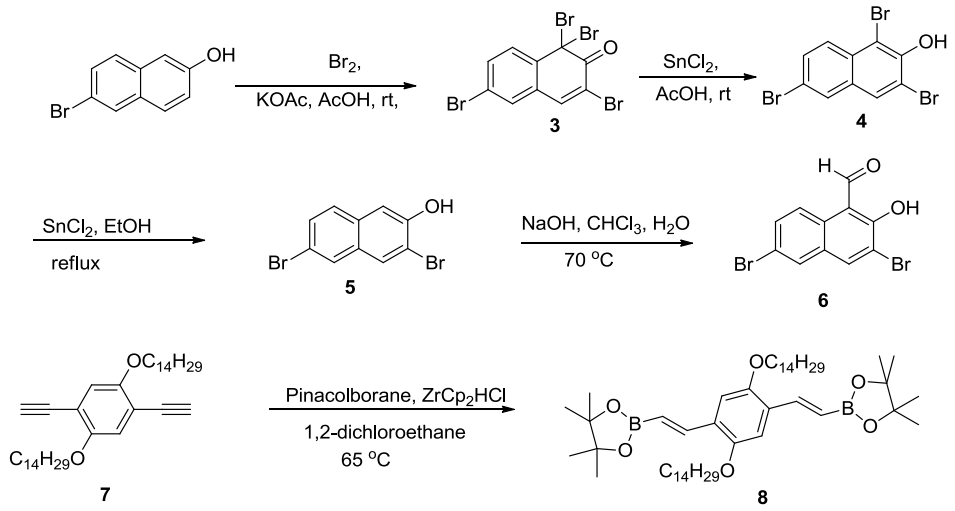

Scheme 2.2. Preparation of monomers **6** and **8**.

In our synthetic design, we decided to use the aldehyde **6** as a monomer for polymerization, instead of converting **6** to the corresponding oxime monomer first, as high nucleophilicity of the oxime would likely make it incompatible with metal-catalyzed conditions required for subsequent polymerization. We chose Suzuki coupling for the preparation of the precursor polymer **P2** as this reaction requires mild reaction conditions. This determined the

second co-monomer – *trans*-bis-vinylboronate **8** (Scheme 2.2), which was prepared in a good yield by using $ZrCp_2HCl$ catalyzed hydroboration of the precursor bis-acetylene **7**.[19] The choice of tetradecyl solubilizing groups was dictated by the need to incur enough solubility to the polymer **P1** in common organic solvents.

Preparation of the precursor polymer **P2** was carried out by emulsion polymerization at a water-organic interface, and furnished the required polymer in 50% yield as a dark-red solid material (Scheme 2.3). GPC characterization of the polymer (THF, calibrated vs. polystyrene standards) revealed number-average molecular weight M_n 10 kDa, with polydispersity 1.7. Post-polymerization conversion of **P2** into the target hydroxy oxime polymer **P1** was accomplished by the reaction with excess hydroxylamine hydrochloride, and furnished yellow-green polymer **P1** which was found moderately soluble in common organic solvents such as CH_2Cl_2.

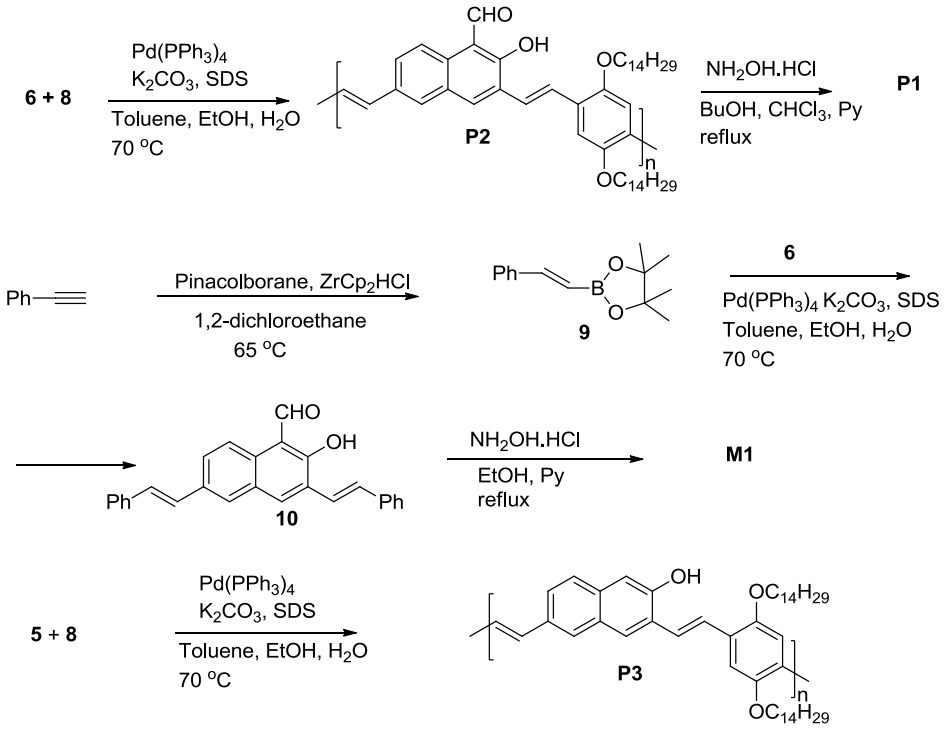

Scheme 2.3. Preparation of small molecule sensor **M1** and polymers **P1** and **P3**.

Completeness of the conversion of aldehyde to oxime was confirmed by ^{1}H NMR monitoring which showed disappearance of the two distinct signals at 13.81 and 10.84 ppm (corresponding to naphthol OH and aldehyde protons in **P2**, respectively), and appearance of the new signals corresponding to the hydroxy oxime functionality.

As a reference compound, we also prepared a small-molecule counterpart **M1**. In its preparation, we used Suzuki coupling of the dibromide monomer **6** with two equivalents of the vinylboronate compound **9**, which in turn was prepared via $ZrCp_2HCl$-catalyzed hydroboration of phenylacetylene (Scheme 2.3). Precursor aldehyde **10** was converted to the target hydroxy oxime **M1** using the same procedure as for the polymer **P1**. In addition, we prepared polymer **P3** (by emulsion polymerization of dibromide **5** and diboronate **8**) which was structurally similar to **P1** but lacked oxime functionality, to use in control experiments (*vide infra*).

2.3. Spectroscopic Properties

The extended electronic delocalization in **P1** was evident upon comparison of UV/vis absorption spectra of dilute solutions of **P1** and its small-molecule counterpart **M1** (Figure 2.2). **P1** exhibited a substantial bathochromic shift of 95 nm of the maximum in the absorption spectrum (λ_{max} 426 nm for **P1** *vs.* λ_{max} 331 nm for **M1**). The main absorption band of **M1** showed a distinct vibronic structure, whereas **P1** showed a featureless band characteristic of poly(arylene vinylene) polymers. Also in agreement with the high π-electron delocalization in **P1**, its fluorescence spectrum was 80 nm bathocromically shifted relative to **M1** (λ_{max} 524 nm for **P1** *vs.* λ_{max} 444 nm for **M1**); in addition, **P1** showed five times higher fluorescence quantum yield. Both absorption and fluorescent spectroscopic characteristics of **P1** were in the range expected for typical PPV polymers.

An unusual spectroscopic feature of **M1** was that the wavelength of its main UV/vis absorption band maximum (331 nm) was below that of the parent compound **1** (λ_{max}(abs) 354 nm). One would expect that extended via the two styryl groups π-electron delocalization in **M1** would result in a bathochromic shift of the absorption band, and therefore the actually observed hypsochromic shift was counterintuitive. Closer inspection of the UV/vis absorption spectrum of **M1** revealed a low-intensity shoulder at around 400 nm (Figure 2.2). This shoulder could originate from an electronically delocalized chromophore but the low intensity (extinction coefficient around 6000 M^{-1} cm^{-1} at 400 nm) likely indicates a partially forbidden electronic transition. In such a case, **M1** would contain two weakly interacting individual chromophores: a naphthalene-localized higher-energy chromophore, and a lower-energy chromophore resulting from the extended π-electron delocalization. It appears that the lower-energy partially forbidden transition in the delocalized chromophore becomes essentially allowed in the polymer **P1** and corresponds to its main absorption band (Figure 2.2).

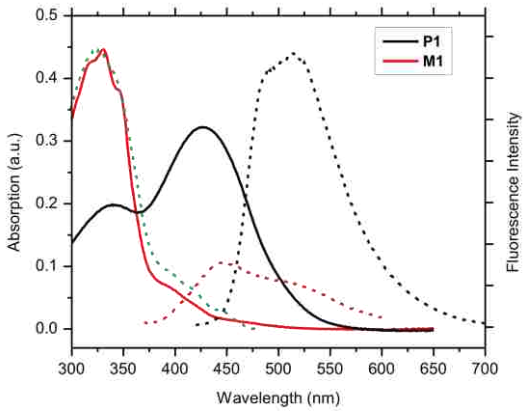

Figure 2.2**.** Absorption (solid traces) and fluorescence (dashed traces) spectra of 9.5 μM solutions of CP **P1** and small-molecule counterpart **M1** in DMF (concentration of **P1** is based on repeating unit). Dashed green trace corresponds to an excitation spectrum of **M1**. For **P1** ε = 33900 M^{-1} cm^{-1} at λ_{max} 426 nm; emission λ_{max} 524 nm, quantum yield Φ = 0.11; for **M1** ε = 47000 M^{-1} cm^{-1} at λ_{max} 331 nm; emission λ_{max} 444 nm, quantum yield Φ = 0.02.

Despite apparently weak electronic coupling between the two electronic transitions in **M1**, the striking similarity between absorption and excitation spectra pointed out the very efficient energy transfer between the higher- and lower-energy chromophores. While better and more accurate understanding of the spectroscopic features of **M1** requires further study, comparison between the spectra of **M1** and **P1** indicated an efficient electronic delocalization through the naphthalene units in **P1** which is an important requirement for unhindered intramolecular exciton migration by through-bond mechanism.

2.4. DCP Sensing Studies

Since actual organophosphorous agents are highly toxic, a common test compound used to mimic them is diethylchlorophosphate (DCP) which has similar reactivity but lacks the efficacy of the warfare agents. We first studied the reaction of DCP with **M1**. Unexpectedly, we could not observe any reaction upon adding together solutions of DCP and **M1** in a non-polar solvent (CH_2Cl_2), even in the presence of excess triethylamine base. This could be due to the thermodynamically unfavorable equilibrium of the hydroxy oxime – isoxazole transformation in this case, possibly because of the poor stabilization of ionic phosphate by-product by the non-polar solvent.

After having tried different combinations of solvents, we found that isoxazole formation occurred readily and completely when a DCP solution in CH_2Cl_2 was added to a solution of **M1** in DMF, with no external base present. Indeed, after letting to sit for 30 min, pouring the reaction mixture into an aqueous $NaHCO_3$ solution followed by extraction with CH_2Cl_2 produced isoxazole product in quantitative yield as was monitored by ^1H NMR spectroscopy (Figure 2.3).

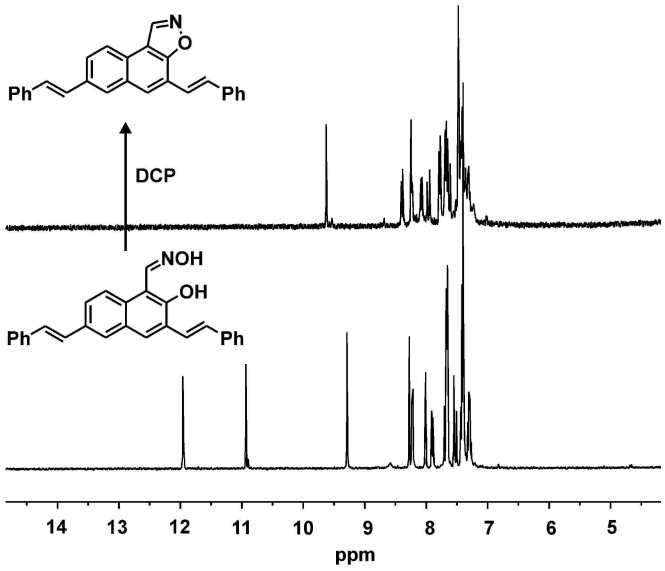

Figure 2.3. ^{1}H NMR spectra (in acetone-D6, 400 MHz)) of **M1** (bottom) and the product after treatment of DMF solution of **M1** with DCP in CH_2Cl_2 followed by pouring in aqueous $NaHCO_3$ and extraction with CH_2Cl_2 (top).

The completeness of the hydroxy oxime to isoxazole conversion was evident from disappearance of the two singlets at 11.96 and 10.94 ppm (OH and N-OH), and downfield shift of the =C-H singlet from 9.29 to 9.63 ppm. The isoxazole product was found not very stable and readily convertible back to **M1** by hydrolysis in acidic conditions; indeed if the isoxazole containing reaction mixture was poured into water (instead of aqueous $NaHCO_3$ solution), only starting **M1** was detected by ^{1}H NMR.

We then proceeded to study the response of CP **P1** in reaction with DCP. Addition of small amounts of DCP (as solutions in CH_2Cl_2) to a dilute solution of polymer **P1** in DMF produced a pronounced spectroscopic response (Figure 2.4). In UV/vis absorption spectrum, there was a small hypsochromic shift of the absorption band maximum at higher DCP concentrations along with a hypsochromic shift of the long wavelength onset of the spectra, which indicated an overall small increase in the CP energy gap upon increasing density of the transformed hydroxy oxime sites in the CP chain.

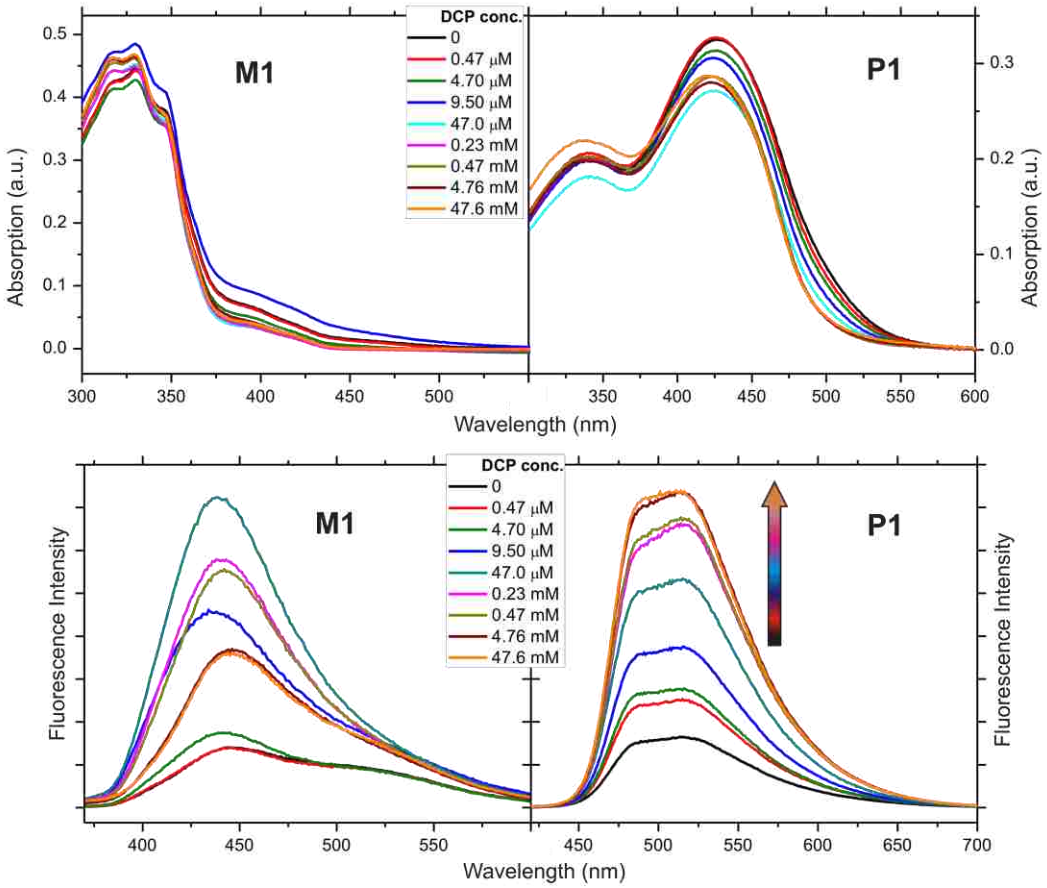

Figure 2.4. Absorption (top) and fluorescence (bottom) spectra of 9.5 μM solutions of **M1** and **P1** in DMF (concentration of **P1** is based on repeating unit) upon addition of the increasing concentration DCP solutions in CH_2Cl_2. For fluorescence spectra, excitation wavelength was 310 nm for **M1** and 400 nm for **P1**. The spectra were acquired in 30 min after addition of DCP.

The relatively insignificant changes in the UV/vis absorption spectra (particularly at the low concentrations of DCP) were consistent with only a minor change in the electronic structure of CP **P1** upon hydroxy oxime to isoxazole conversion. This minor effect was expected since such a conversion could not strongly affect the energy gap of **P1** which is mainly controlled by the extended electronic delocalization through the polymer chain which remains decoupled from the changes in the naphthalene-centered chromophore (see discussion about the spectroscopic features of **M1** above). In stark contrast to the insignificant changes in absorption spectrum, addition of DCP produced a significant enhancement of the fluorescence intensity without

causing a wavelength shift, in excellent agreement with our initial "higher energy gap control" hypothesis.

Although quantitative kinetic studies on the reaction of polymer **P1** with DCP were not possible (as fluorescence quantum yield of **P1** varies with changing conversion), it was clear that the reaction was relatively fast, as intensity of the fluorescent band would stop growing in about 20 min after addition of DCP (Figure 2.5).

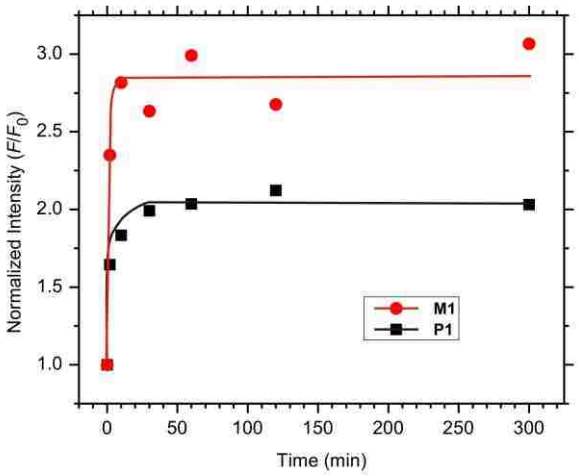

Figure 2.5. **.** Normalized fluorescence intensity (F/F_0) vs. time in reaction of DCP with polymer **P1** and small-molecule sensor **M1** in DMF (100 μl of a 0.2 mM stock solution of DCP in CH_2Cl_2 was added to 2 ml of 10 μM solution of **P1** or **M1** in DMF). The lines show exponential fit to the experimental data using first-order kinetic treatment (R^2 0.93 for both **M1** and **P1**, first-order rate constant for **M1** k_{obs} = 0.66 min^{-1}).

In the case of polymer **P1**, adding increasing concentrations of DCP produced steady increase in the fluorescent intensity (Figure 2.4). In contrast, the fluorescent intensity of the small-molecule counterpart **M1** initially increased upon addition of lower concentrations of DCP (up to an equimolar amount of added DCP), however, the intensity dropped precipitously at higher DCP concentrations (Figure 2.4). The reason for this drop is unclear at this time, and could possibly be related to secondary reactions of the isoxazole unit with excess DCP.

Further comparison between the fluorescent responses of **P1** and **M1** on DCP addition revealed striking differences related to the effect of signal amplification in the case of CP (and the lack of amplification in the case of **M1**). Upon excitation at the wavelength of the main absorption band (310 nm), the small-molecule sensor **M1** showed a relatively narrow analyte detection range with the maximum level of detectable DCP concentrations roughly coinciding with the solution concentration of **M1** (which reflected 1:1 stoichiometry of the hydroxy oxime reaction with DCP), with a rapid drop of the fluorescent signal after adding more than equimolar amount of DCP. Excitation of **M1** at the wavelength of the lower-energy absorption shoulder (possibly corresponding to the π-electron delocalized chromophore) produced overall very low quantum yield fluorescence, with a very insignificant response on added DCP (Figure 2.6).

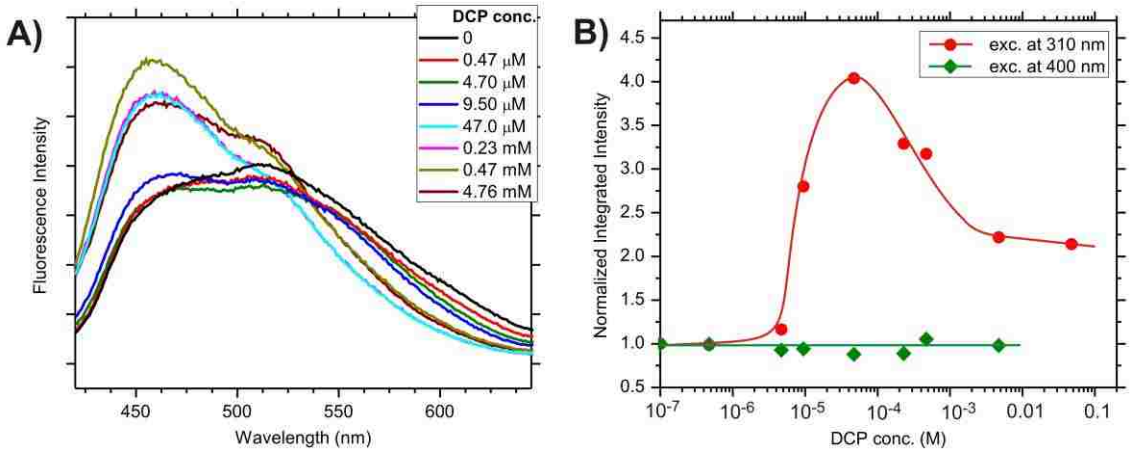

Figure 2.6 A) Fluorescence spectra of 9.5 μM solution of **M1** in DMF acquired at 400 nm excitation upon addition of the increasing concentration DCP solutions in CH_2Cl_2. The spectra were acquired in 30 min after addition of DCP. B) Dependence of fluorescent response of small-molecule sensor **M1** on excitation wavelength (310 nm *vs.* 400 nm). The traces show change in integrated fluorescence intensity of 9.50 μM solution of **M1** upon addition of increasing concentrations of DCP. The intensity is expressed as a ratio of integrated area of a fluorescent band at each DCP concentration divided by the area of the fluorescent band in the absence of DCP (F/F_0). The plot uses logarithmic scale for DCP concentration axis.

In contrast, the same concentration solution of polymer **P1** showed a steadily increasing fluorescent response in the very broad range of analyte concentrations ranging a few orders of magnitude from high nanomolar to high millimolar concentrations. This can be best seen in Figure 2.7, which shows fluorescent response on added DCP and utilizes a logarithmic scale for the DCP concentration axis. Such a broader analyte detection range is a clear advantage of CP based detection schemes. The enhanced DCP sensitivity of **P1** due to signal amplification is clearly evident from the much lower DCP concentration required to achieve a noticeable fluorescent response in the case of **P1** as compared to using solutions of **M1** with exactly the same concentration (Figure 2.7). One can estimate that **P1** is at least 20-30 times more sensitive than the small-molecule counterpart **M1**, the number which represents its intrinsic amplification. This signal gain estimate is in agreement with previously reported values for other CP-based schemes in dilute solutions.[3,20]

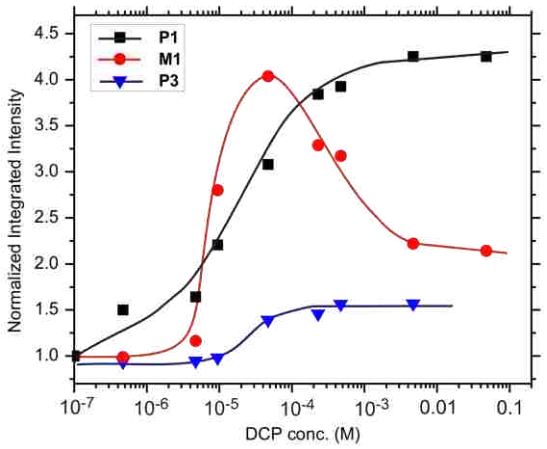

Figure 2.7. Change in integrated fluorescence intensity of 9.50 μM solutions of polymers **P1** and **P3**, and small-molecule sensor **M1** upon addition of increasing concentrations of DCP. The intensity is expressed as a ratio of integrated area of a fluorescent band at each DCP concentration divided by the area of the fluorescent band in the absence of DCP (F/F_0). The plot uses logarithmic scale for the DCP concentration axis.

The amplified response polymer **P1** showed on addition of DCP prompted us to check if such a response was specifically associated with formation of isoxazole units within the CP chain, as other alternatives such as hydroxyl group phosphorylation by DCP, or electrophilic aromatic substitution in the naphthalene unit could potentially be involved. Polymer **P3** with the same structure as **P1** but without the oxime group in the naphthol unit was prepared and studied in reaction with DCP exactly in the same conditions that were used with the polymer **P1**. Although **P3** did show some response (Figure 2.8), the response was of much lower magnitude than the response obtained with CP **P1** (Figure 2.7). Most likely, the response of **P3** was due to phosphorylation of the hydroxyl group by DCP. Such phosphorylation could either directly affect the electronic gap of the naphthol chromophore, or preclude possible fluorescence quenching via excited-state intramolecular proton transfer (ESIPT)[21] which is often encountered due to the high acidity of photoexcited naphthols. Irrespective of what caused the response, the magnitude of the response was minor and not comparable to the magnitude of the response observed with CP **P1**. Thus, the amplified turn-on response observed for **P1** was indeed due to the formation of the higher energy gap isoxazole units electronically coupled to the polymer band gap.

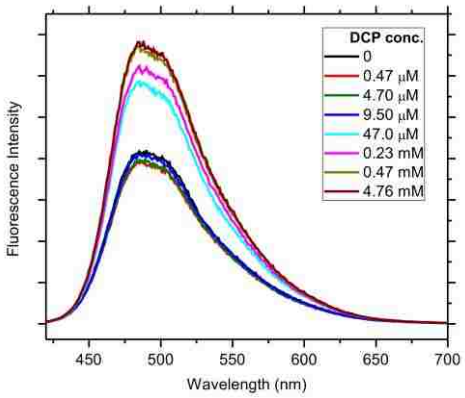

Figure 2.8. Fluorescence spectra of 9.5 μM solutions of **P3** in DMF (concentration based on repeating unit) upon addition of the increasing concentration DCP solutions in CH_2Cl_2. The spectra were acquired in 30 min after addition of DCP.

Signal amplification in chemosensors based on dilute solutions of CPs stems from one-dimensional exciton migration in isolated polymer chains. Since much higher efficiency of exciton migration can be achieved in thin films of conjugated polymers (where exciton migration occurs as a three-dimensional process due to involvement of the intermolecular Förster-type mechanism), this typically means much higher signal amplification in thin film CP-based sensors relative to the CP sensors operating in dilute solutions (although restricted analyte diffusion often limits practical applications of thin-film CP sensors). The increased amplification reflects a higher probability for a three-dimensionally walking exciton to visit a quenching or a lower energy gap site generated by the analyte binding. In contrast to conventional amplifying CP sensors with operating principle based on exciton migration to a quenching site or a lower energy gap chromophore, fundamental feature of the turn-on fluorescent sensors described herein is that thin films of such sensors should display no response, or even a turn-off response on the same analytes that cause amplified turn-on response with dilute solutions of the sensor. The lack of response in the case of the "higher energy gap" control mechanism is directly related to the enhanced exciton migration efficiency in thin films. Indeed, generating a "roadblock" (higher energy gap site) in the CP thin film will have little effect on exciton migration length as the exciton can effectively bypass the "roadblock" through intermolecular "hopping". Thus, amplified turn-on fluorescent response in dilute solutions, and lack of response (or even turn-off fluorescent response) in thin films can be predicted as a definitive characteristic feature of the "higher energy gap" control mechanism.

Thin films of CP **P1** could be readily prepared by spin-casting from a solution of this polymer in chloroform, and the absorption and fluorescence spectra of thin films were similar to the corresponding spectra in dilute solutions (Figure 2.9). DCP has relatively high vapor pressure

(0.1 mm Hg at room temperature), therefore exposure of thin films to DCP vapor was carried out by placing the films in a closed vial with a drop of DCP at the bottom. Exposure of the films to DCP did not produce turn-on response, instead we observed significant drop of the fluorescent intensity even after short-time DCP exposure (Figure 2.9).

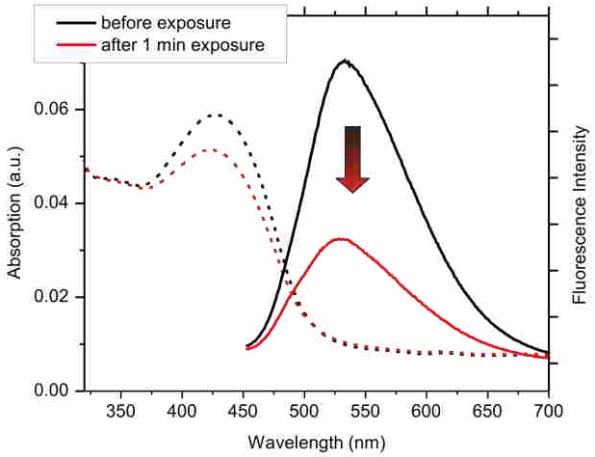

Figure 2.9. Absorption (dashed traces) and fluorescence (solid traces) spectra of a thin film of **P1** before and after exposure for 1 min to saturated vapor of DCP at room temperature.

This observation clearly indicated that the reaction of **P1** with DCP did happen in the solid state (despite potential complications due to a limited analyte diffusion in the film, or restricted chemical reactivity in the solid state) and was in exact agreement with the initial prediction; therefore it serves to support the involvement of the "higher energy gap" control mechanism which is responsible for turn-on signal amplification in dilute solutions. It may be possible to vary the extent of intermolecular exciton migration in thin films by incorporating steric spacers in the CP backbone to reduce intermolecular separation between individual chains. When the intermolecular exciton migration is substantially diminished, one can expect re-emergence of the amplified turn-on response in thin film. This will be tested in the future studies.

2.5.Conclusions

We designed and demonstrated the principle of the "higher energy gap" control of fluorescence intensity in amplifying conjugated polymers. This novel concept relies on shortening exciton migration length within the polymer conjugated backbone by generating higher energy gap sites which act as "roadblocks" for the migrating excitons. The shorter exciton migration length causes an increase in fluorescent intensity (turn-on response), and the amplification of such a response is an intrinsic feature of CP-based sensors. We illustrated this concept by preparation of an amplifying turn-on chemosensor for the detection of organophosphorous nerve agent mimics. The sensor showed both substantial signal gain and broad analyte detection range when compared to an analogous small-molecule sensor. The fundamental feature of the "higher energy gap" control mechanism (which contrasts it with previously developed amplification schemes) is that amplified turn-on response can only be achieved in dilute solutions of CP sensors, and not in thin films. Although photonic amplification in dilute solutions of CPs is intrinsically limited by one-dimensional nature of exciton diffusion, the current study developed an important concept which adds to the universality of the signal amplification phenomenon in CPs and can be used in the design of efficient turn-on amplifying sensors for other practically important analytes. Additional experimental studies on various factors capable of influencing the amplification, as well as gaining deeper understanding of the nature and origin of the "higher energy gap" control phenomenon are required to optimize the performance of these materials in chemosensing and will be done in future studies.

2.6. References

[1] Swager, T. M. The molecular wire approach to sensory signal amplification. *Acc. Chem. Res.* **1998,** *31*, 201-207.

[2] McQuade, D. T.; Pullen, A. E.; Swager, T. M. Conjugated polymer-based chemical sensors. *Chem. Rev.* **2000,** *100*, 2537-2574.

[3] Thomas III, S. W.; Joly, G. D.; Swager, T. M. Chemical Sensors Based on Amplifying Fluorescent Conjugated Polymers. *Chem. Rev.* **2007,** *107*, 1339-1386.

[4] Feng, X.; Liu, L.; Wang, S.; Zhu, D. Water-soluble fluorescent conjugated polymers and their interactions with biomacromolecules for sensitive biosensors. *Chem. Soc. Rev.* **2010,** *39*, 2411-2419.

[5] Kim, H. N.; Guo, Z.; Zhu, W.; Yoon, J.; Tian, H. Recent progress on polymer-based fluorescent and colorimetric chemosensors. *Chem. Soc. Rev.* **2011,** *40*, 79-93.

[6] Liu, Y.; Ogawa, K.; Schanze, K. S. *J. Photochem. Photobiol.,C.* Conjugated polyelectrolytes as fluorescent sensors. **2009,** *10*, 173-190.

[7] Schwartz, B. J. Conjugated polymers as molecular materials: How Chain Conformation and Film Morphology Influence Energy Transfer and Interchain-Interactions. *Annu. Rev. Phys. Chem.* **2003,** *54*, 141-172.

[8] Beljonne, D.; Pourtois, G.; Silva, C.; Hennebicq, E.; Hertz, L. M.; Friend, R. H.; Scholes, G. D.; Setayesh, S.; Müllen, K.; Brédas, J. L. Interchain vs. intrachain energy transfer in acceptorcapped conjugated polymers. *Proc. Nat. Acad. Sci. USA* **2002,** *99*, 10982-10987.

[9] Murphy, C. B.; Zhang, Y.; Troxler, T.; Ferry, V.; Martin, J.; Jones, W. E., Jr. Probing Förster and Dexter Energy-Transfer Mechanisms in Fluorescent Conjugated Polymer Chemosensors *J. Phys. Chem. B* **2004,** *108*, 1537-1543.

[10] Collini, E.; Scholes, G. D. Coherent Intrachain Energy Migration in a Conjugated Polymer at Room Temperature. *Science* **2009,** *323*, 369-373.

[11] Becker, K.; Lupton, J. M.; Feldmann, J. F.; Setayesh, S.; Grimsdale, A. C.; Müllen, K. Efficient Intramolecular Energy Transfer in Single Endcapped Conjugated Polymer Molecules in the Absence of Appreciable Spectral Overlap *J. Am. Chem. Soc.* **2006,** *128*, 680-681.

[12] Averbeke, B. V.; Beljonne, D.; Hennebicq, E. Energy Transport along Conjugated Polymer Chains: Through-Space or Through-Bond. *Adv. Funct. Mater.* **2008,** *18*, 492-498.

[13] Chen, L.; McBranch, D. W.; Wang, H.-L.; Helgeson, R.; Wudl, F.; Whitten, D. G. Highly sensitive biological and chemical sensors based on reversible fluorescence quenching in a conjugated polymer. *Proc. Natl. Acad. Sci. USA* **1999,** *96*, 12287-12292.

[14] Yang, J.-S.; Swager, T. M. Fluorescent Porous Polymer Films as TNT Chemosensors: Electronic and Structural Effects. *J. Am. Chem. Soc.* **1998,** *120*, 11864-11873.

[15] Rose, A.; Zhu, Z.; Madigan, C. F.; Swager, T. M.; Bulović, V. Sensitivity gains in chemosensing by lasing action in organic polymers. *Nature* **2005,** *434*, 876-879.

[16] Toal, S. J.; Trogler, W. C. Polymer sensors for nitroaromatic explosives detection. *J. Mater. Chem.* **2006,** *16*, 2871-2883.

[17] Zhou, Q.; Swager, T. M. Fluorescent Chemosensors Based on Energy Migration in Conjugated Polymers: The Molecular Wire Approach to Increased Sensitivity. *J. Am. Chem. Soc.* **1995,** *117*, 12593-12602.

[18] Fan, C.; Wang, S.; Hong, J. W.; Bazan, G. C.; Plaxco, K. W.; Heeger, A. Beyond superquenching: Hyper-efficient energy transfer from conjugated polymers to gold nanoparticles. *Proc. Natl. Acad. Sci. USA* **2003,** *100*, 6297-6301.

[19] Disney, M. D.; Zheng, J.; Swager, T. M.; Seeberger, P. H. Detection of Bacteria with Carbohydrate-Functionalized Fluorescent Polymers. *J. Am. Chem. Soc.* **2004,** *126*, 13343-13346.

[20] Kim, I.-B.; Erdogan, B.; Wilson, J. N.; Bunz, U. H. F. Sugar–Poly(*para*-phenylene ethynylene) Conjugates as Sensory Materials: Efficient Quenching by $Hg^{2+}$and Pb^{2+}Ions *Chem. Eur. J.* **2004,** *10*, 6247-6254.

[21] Xie, D.; Parthasarathy, A.; Schanze, K. S. Aggregation-Induced Amplified Quenching in Conjugated Polyelectrolytes with Interrupted Conjugation. *Langmuir* **2011,** *27*, 11732-11736.

[22] Gaylord, B. S.; Heeger, A. J.; Bazan, G. C. DNA detection using water-soluble conjugated polymers and peptide nucleic acid probes. *Proc. Natl. Acad. Sci. USA* **2002,** *99*, 10954-10957.

[23] Liu, B.; Bazan, G. C. Homogeneous fluorescence-based DNA detection with water-soluble conjugated polymers. *Chem. Mater.* **2004,** *16*, 4467-4476.

[24] Traina, C. A.; Bakus, II, R. C.; Bazan, G. C. Design and Synthesis of Monofunctionalized, Water-Soluble Conjugated Polymers for Biosensing and Imaging Applications. *J. Am. Chem. Soc.* **2011,** *133*, 12600-12607.

[25] Ho, H.-A.; Najari, A.; Leclerc, M. Optical Detection of DNA and Proteins with Cationic Polythiophenes. *Acc. Chem. Res.* **2008,** *41*, 168-178.

[26] Ho, H. A.; Doré, K.; Boissinot, M.; Bergeron, M. G.; Tanguay, R. M.; Boudreau, D.; Leclerc, M. Direct Molecular Detection of Nucleic Acids by Fluorescence Signal Amplification. *J. Am. Chem. Soc.* **2005,** *127*, 12673-12676.

[27] Duan, X.; Liu, L.; Feng, F.; Wang, S. Cationic Conjugated Polymers for Optical Detection of DNA Methylation, Lesions, and Single Nucleotide Polymorphisms *Acc. Chem. Res.* **2010,** *43*, 260-270.

[28] Pinto, M. R.; Schanze, K. S. Amplified fluorescence sensing of protease activity with conjugated polyelectrolytes. *Proc. Natl. Acad. Sci. USA* **2004,** *101*, 7505-7510.

[29] Cox, J. R.; Müller, P.; Swager, T. M. Interrupted Energy Transfer: Highly Selective Detection of Cyclic Ketones in the Vapor Phase. *J. Am. Chem. Soc.* **2011,** *133*, 12910-12913.

[30] Kim, T.-H.; Swager, T. M. A Fluorescent Self-Amplifying WavelengthResponsive Sensory Polymer for Fluoride Ions. *Angew. Chem. Int. Ed.* **2003,** *42*, 4803-4806.

[31] Lupton, J. M. Single-Molecule Spectroscopy for Plastic Electronics: Materials Analysis from the Bottom-Up. *Adv. Mater.* **2010,** *22*, 1689-1721.

[32] Bolinger, J. C.; Traub, M. C.; Brazard, J.; Adachi, T.; Barbara, P. F.; Vanden Bout, D. A. Conformation and Energy Transfer in Single Conjugated Polymers. *Acc. Chem. Res.* **2012,** *45*, 1992-2001.

[33] Choi, J.; Ruiz, C. R.; Nesterov E. E. Temperature-Induced Control of Conformation and Conjugation Length in Water-Soluble Fluorescent Polythiophenes. *Macromolecules* **2010,** *43*, 1964-1974.

[34] Kim, J.; Swager, T. M. Control of conformational and interpolymer effects in conjugated polymers. *Nature* **2001,** *411*, 1030-1034.

[35] Schindler, F.; Lupton, J. M. Electrothermal Manipulation of Individual Chromophores in Single Conjugated Polymer Chains: Controlling Intrachain FRET, Blinking, and Spectral Diffusion. *Nano Lett.* **2010,** *10*, 2683-2689.

[36] Dale, T. J.; Rebek, Jr., J. Hydroxy Oximes as Organophosphorus Nerve Agent Sensors. *Angew. Chem. Int. Ed.* **2009,** *48*, 7850-7852.

[37] Kerkines, I. S. K.; Petsalakis, I. D.; Theodorakopoulos, G.; Rebek, Jr. J. Excited-State Intramolecular Proton Transfer in Hydroxyoxime-Based Chemical Sensors. *J. Phys. Chem. A* **2011,** *115*, 834-840.

[38] Grimsdale, A. C.; Holmes, A. B. In *Handbook of Conducting Polymers, 3rd ed., Conjugated polymers: theory, synthesis, properties, and characterization*; Skotheim, T. A., Reynolds, J. R., Eds.; CRC Press: Boca Raton, **2007;** pp. 4-1–4-22.

[39] Kim, K.; Tsay, O. G.; Atwood, D. A.; Churchill, D. G. Destruction and Detection of Chemical Warfare Agents. *Chem. Rev.* **2011,** *111*, 5345-5403.

[40] Zhang, S.-W.; Swager, T. M. Fluorescent Detection of Chemical Warfare Agents: Functional Group Specific Ratiometric Chemosensors *J. Am. Chem. Soc.* **2003,** *125*, 3420-3421.

[41] Knapton, D.; Burnworth, M.; Rowan, S. J.; Weder, C. Fluorescent Organometallic Sensors for the Detection of Chemical-Warfare-Agent Mimics. *Angew. Chem. Int. Ed.* **2006,** *45*, 5825-5829.

[42] Dale, T. J.; Rebek, Jr., J. Fluorescent Sensors for Organophosphorus Nerve Agent Mimics. *J. Am. Chem. Soc.* **2006,** *128*, 4500-4501.

[43] Bensic-Nagale, S.; Sternfeld, T.; Walt, D. R. Microbead Chemical Switches: An Approach to Detection of Reactive Organophosphate Chemical Warfare Agent Vapors. *J. Am. Chem. Soc.* **2006,** *128*, 5041-5048.

[44] Clavaguera, S.; Carella, A.; Caillier, L.; Celle, C.; Pécaut, J.; Lenfant, S.; Vuillaume, D.; Simonato, J.-P. Sub-ppm Detection of Nerve Agents Using Chemically Functionalized Silicon Nanoribbon Field-Effect Transistors. *Angew. Chem. Int. Ed.* **2010,** *49*, 4063-4066.

[45] Gotor, R.; Costero, A. M.; Gil, S.; Parra, M.; Martínez-Máñez, R.; Sancenón, F. A Molecular Probe for the Highly Selective Chromogenic Detection of DFP, a Mimic of Sarin and Soman Nerve Agents. *Chem. Eur. J.* **2011,** *17*, 11994-11997.

[46] Hewage, H. S.; Wallace, K. J.; Anslyn, E. V. Novel chemiluminescent detection of chemical warfare simulant. *Chem. Commun.* **2007,** *38* 3909-3911.

[47] Pereira, S.; Srebnik, M. Hydroboration of Alkynes with Pinacolborane Catalyzed by HZrCpzCl. *Organometallics* **1995,** *14*, 3127-3128.

[48] Li, J.; Kendig, C. E.; Nesterov, E. E. Chemosensory Performance of Molecularly Imprinted Fluorescent Conjugated Polymer Materials. *J. Am. Chem. Soc.* **2007,** *129*, 15911-15918.

[49] Andrew, T. L.; Swager, T. M. Structure- Property relationships for exciton transfer in conjugated polymers. *J. Polym. Sci., Part B: Polym. Phys.* **2011,** *49*, 476-498.

[50] Paul, B. K.; Guchhait, N. 1-Hydroxy-2-naphthaldehyde: A prospective excited-state intramolecular proton transfer (ESIPT) probe with multi-faceted applications *J. Lumin.* **2012,** *132*, 2194-2208.

[51] Wu, J.; Liu, W.; Ge, J.; Zhang, H.; Wang, P. New sensing mechanisms for design of fluorescent chemosensors emerging in recent years *Chem. Soc. Rev.* **2011,** *40*, 3483-3495.

Chapter 3. "Higher Energy Gap" Control Principle in the Design of an Amplifying Fluorescent Sensory Polymer for H_2S Detection

3.1. Introduction

The use of the "higher energy gap" control paradigm to obtain an amplified signal in chemosensing applications of fluorescent conjugated polymers was discussed in chapter 2. As a proof of concept, we used a hydroxy oxime poly(*p*-arylene vinylene) polymer. In order to provide further experimental support for this concept, this chapter describes our attempts towards another example of the signal amplification by using the same "higher energy gap" mechanism for the detection of hydrogen sulfide.

Hydrogen sulfide (H_2S) is well known as toxic gas with an unpleasant smell which happens to be the third endogenous gas after nitric oxide (NO) and carbon monoxide (CO).[1,2] H_2S is involved in wide range of physiological functions such as modulation of cardiovascular system, respiratory system, gastrointestinal system and endocrine system.[3] The abnormal level of H_2S is associated with a number of health conditions such as Alzheimer's disease, Diabetes and Downs syndrome.[5,6] Therefore, it is very important to quantitatively and accurately detect this small molecule at ultra-low concentrations as well as in a broad range of concentrations. The current methods for the detection include colorimetric analysis[7], gas chromatography[8], gravimetry[9] and using of fluorescent probes[10] and they often require damaging and/or destruction of living tissues or cells.

The use of fluorescent probes for the detection of H_2S has gained more popularity than the other methods because fluorescent detection is very reliable, fast, selective and sensitive. The chemical strategies to the development of fluorescent probes are very similar, and they usually start with a non-fluorescent or masked fluorophore which, upon exposure to H_2S, is converted to a fluorescent moiety. Typical chemical transformations used in detection are azide to amine

reduction, nucleophilic addition of H_2S to the fluorophore and reduction of nitro to amine group of the fluorophore in the presence of H_2S.

Chang and co-workers used an azide masked rhodamine fluorophore in the closed lactone form which is not fluorescent. Upon exposure to the source of H_2S, the azide was reduced to amine, as a result the lactone ring opened up and became fluorescent.[9] This probe was also selective as it did not show any response towards other biological thiols such as cysteine and gluthathione, however it took almost an hour to reach the highest level of fluorescence intensity. Wang and co-workers developed a dansyl fluorophore with sufonyl azide which was converted to sulfonylamide upon exposure to H_2S.[10] As a result, there was a significant increase in the fluorescence almost instantaneously and the probe was also selective towards other biological thiols and did not undergo displacement reactions with amino groups or other nucleophilic anions nor it reacted with reducing species, even at very high concentrations (Figure 3.1).

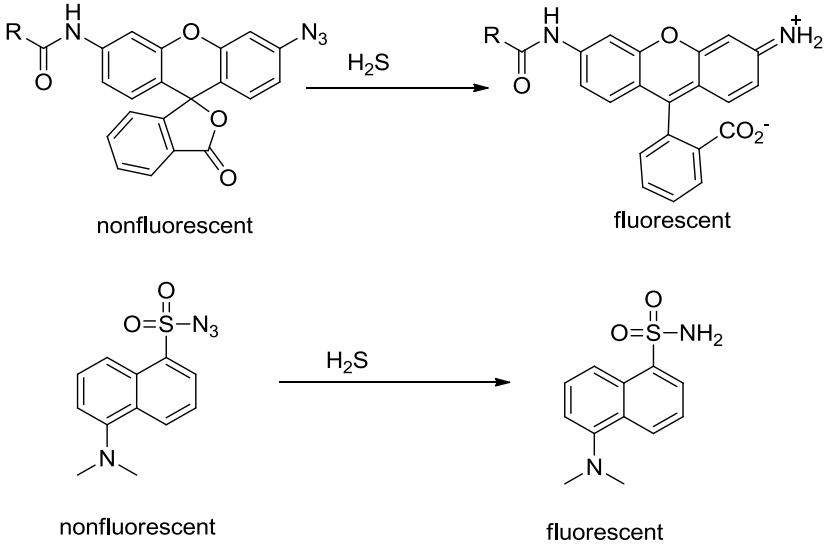

Figure 3.1. Fluorescent H_2S probes based on reduction of azide to amino group by H_2S.

The other commonly used method is the nucleophilic addition of H_2S to the probe which results in cyclization generating a fluorescent unit. He, Jiao and co-workers used this approach to convert non-fluorescent 1,3,5-triaryl-2-pyrazoline and BODIPY moieties into fluorophores upon exposure to H_2S.[11]

Xian and co-workers used the nucelophilic addition strategy to develop a sensor using a non-fluorescent fluorescein chromophore masked by an ester group with a disulfide linkage. Upon exposure to H_2S, the nucleophilic substitution between H_2S and disulfide bond of the masked fluorescein probe created an intermediate, which spontaneously underwent cyclization by cleaving the masked ester moiety and regaining its fluorescence (Figure 3.2).[12] This is a turn-on sensor but the detection time was slow and it was not selective with respect to other biological thiols such as cysteine derivatives. Similarly, Chen and co-workers reported a NIR based fluorescent probe using a nitro group functionalized Cyanine-7 dye that was converted to a fluorescent amine compound when exposed to H_2S.[13]

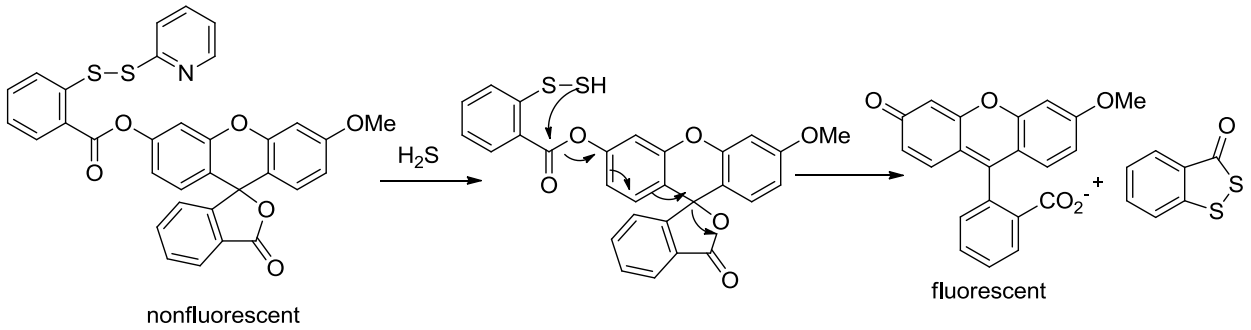

Figure 3.2. An example of Nucleophilic addition of H_2S to a non-fluorescent probe to generate a fluorescent species.

One more example of fluorescent H_2S sensor has been recently reported by Guo and co-workers. They used a hybrid chromophore of coumarin and an indolenium block called (CouMC) to achieve ratiometric H_2S sensing. This probe was fast and selective with respect to other biological thiols and more importantly, it could be used in vivo imaging, e.g. imaging of H_2S in

mitochondria. Upon addition of H_2S, the fluorescence from the merocyanine decreased whereas there was an increase in emission from the coumarin part of the molecule (Figure 3.3).[14]

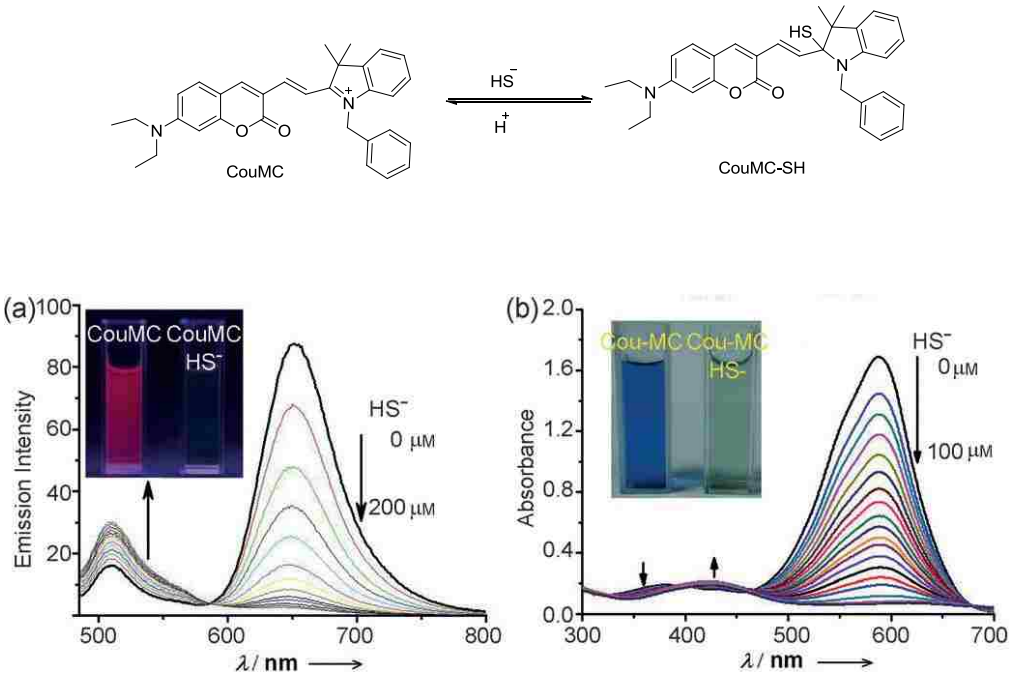

Figure 3.3. Proposed H_2S sensing reaction mechanism of CouMC probe and ratiometric fluorescence (left) and absorbance (right) response upon addition of H_2S. (Reproduced with permission from ref. 14. Copyright © 2013, Wiley- VCH.)

All the examples described above were small-molecule sensors. However, to the best of our knowledge, there was no conjugated polymer based sensor for the detection of H_2S. There is an advantage of using CP based sensors over small molecule sensors because of signal amplification intrinsic to the conjugated polymers. Therefore, we designed an H_2S sensor using naphthalene based spiropyran conjugated polymer. We decided to incorporate this chromophore in a poly(arylene vinylene) backbone to be used as an H_2S amplifying fluorescent sensor. First, this would be a practical CP based sensor for the detection of H_2S, and second, even more important, would be another example to demonstrate the generality of the "higher energy gap"

concept for obtaining signal amplification. The excitons produced by photoexcitation of the CP walk randomly along the conjugated backbone. Upon exposure to H_2S, the ring opens up as shown in Figure 3.4 causing conversion of the low-gap spyropyran unit into a higher-energy gap ring opened chromophore.

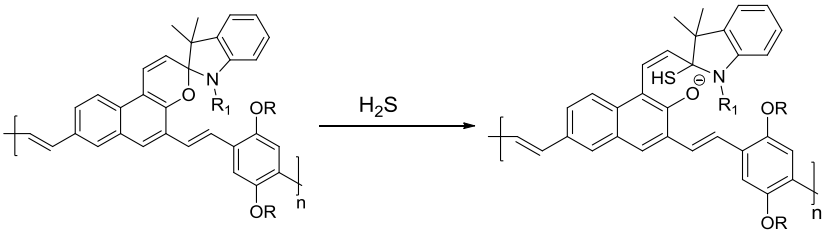

Figure 3.4. Proposed reaction mechanism for the detection of H_2S using fluorescent CP.

The higher energy gap chromophore in the polymer would act as a "roadblock" for randomly migrating excitons, thus causing their localization. The exciton localization is expected to produce enhanced fluorescence, according to the "higher energy gap" concept described in detail in chapter 2.

3.2. Synthesis

The monomer **15** is a versatile monomer that would be used in the synthesis of all the polymers as one of the co-monomers. All the measurements and studies would be performed in solution, therefore it is very important to have a good solubility of the polymers.

The required co-monomer **15** was prepared by following the Scheme 3.1. The synthesis began with the preparation of the tri(ethylene glycol) tosylate **11** and bromination of the commercially available hydroquinone to afford **12**. Reaction between **11** and **12** yielded dibromide **13** which was then subjected to Sonogashira coupling with TMS-acetylene and subsequent acetylene deprotection to afford **14**. Finally, hydroboration of bis-acetylene **14** was carried out in presence of $HZrCp_2Cl$ catalyst to afford monomer **15**.

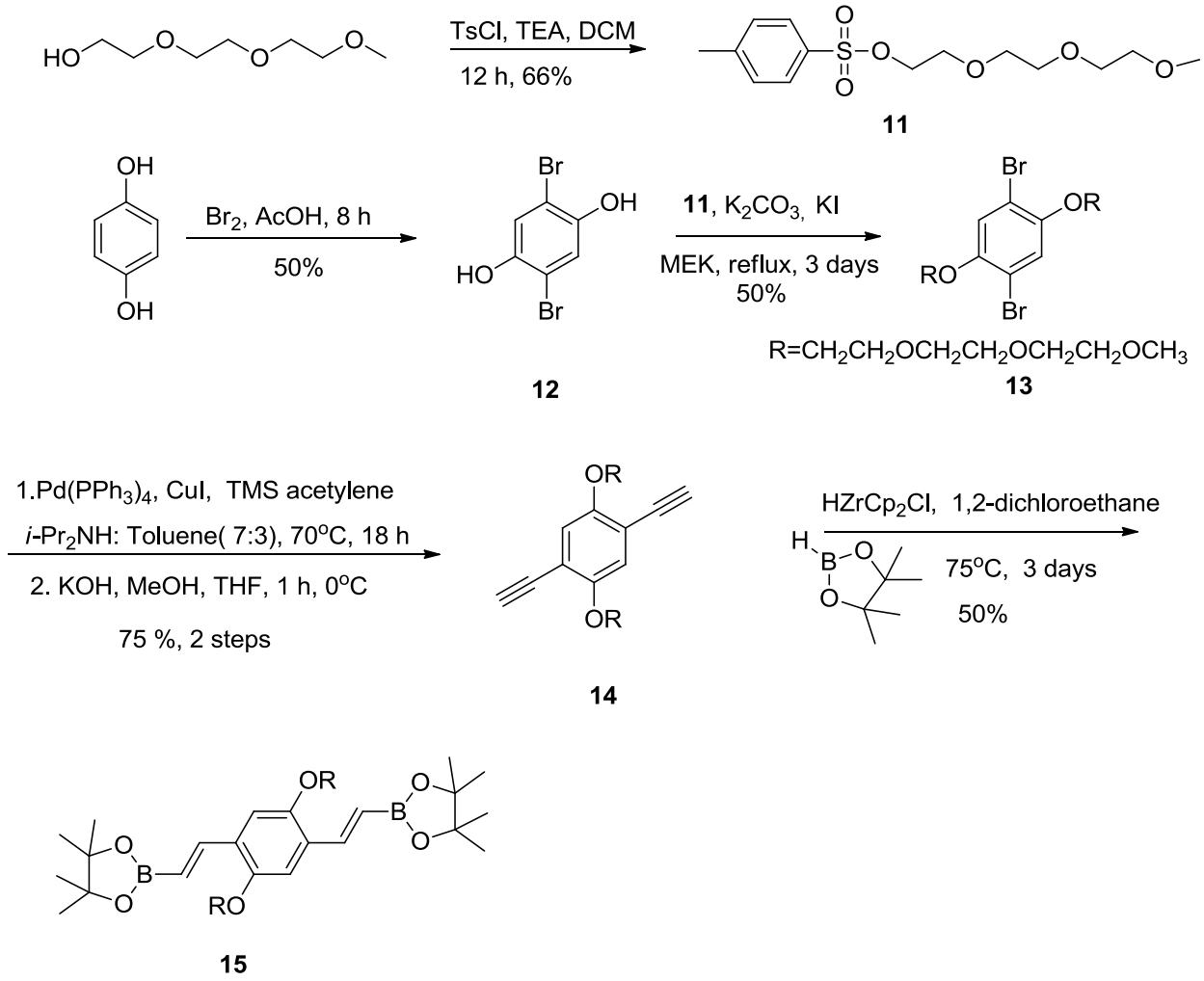

Scheme 3.1. Synthesis of the monomer **15**.

Preparation of polymer **P4** was attempted using two methods, first using the pre-functionalized monomer **20a** or **b** and second using post-functionalization of the aldehyde polymer **P5**.

In the first approach, the commercially available tetramethylindolenium salt **17** and 2,5-dibromobenzaldehyde **19** were refluxed in ethanol with catalytic amount of pyridine to afford the monomer **20a**. For increased aqueous solubility, the sulfonated indolenium compound **18**[16] was condensed with aldehyde **19** using the same procedure. The merocyanine (MC) monomer **20a** or

20b was then co-polymerized with monomer **15**, but the polymerization was not successful, producing only degradation products (Scheme 3.2).

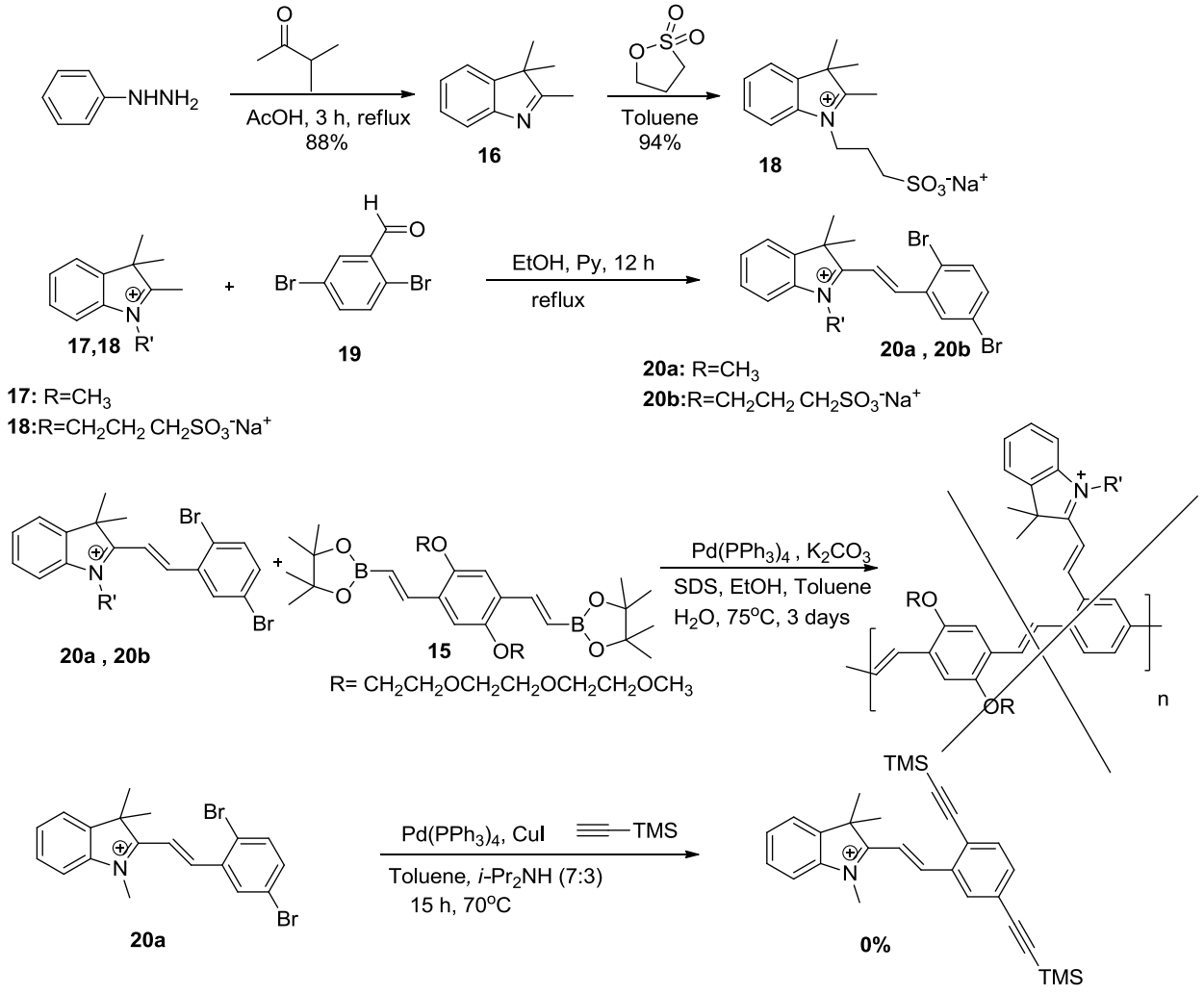

Scheme 3.2. Attempted synthesis of polymer **P4** using pre-functionalized monomer.

The reaction time and conditions were varied, still the polymerization was not successful, most likely because MC-monomers (**20a** or **b**) were not stable in the reaction conditions used in Suzuki coupling. In order to test stability of the compound **20a** in such conditions, it was subjected to Sonogashira coupling with TMS-acetylene which resulted only in the degradation products, thus proving the futility of further attempts to use this route. Since the MC-monomer

was unstable in Suzuki or Sonogashira coupling using palladium catalyst, the post-polymerization functionalization method was attempted. First, aldehyde functionalized polymer **P5** was synthesized using Suzuki coupling conditions followed by post-polymerization treatment with compound **17** or **18** in the presence of catalytic amount of pyridine in the mixture of n-butanol and chloroform as a solvent (Scheme 3.3).

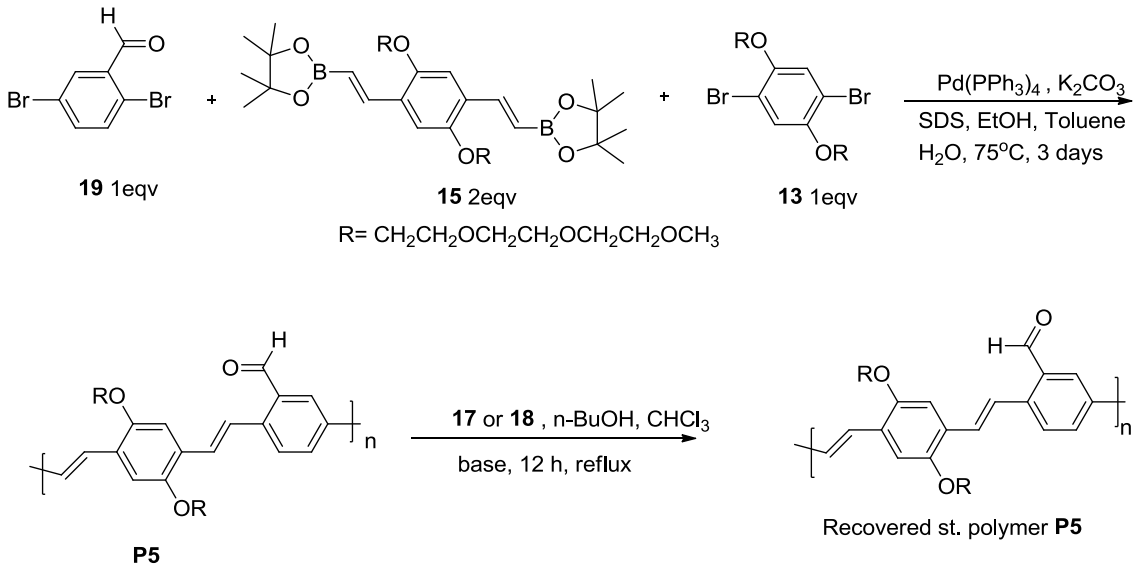

Scheme 3.3. Attempted synthesis of polymer **P4** using post-functionalization method.

Initially, the polymer **P5** was prepared from monomers **19** and **15** (taken in 1:1 ratio) using Suzuki coupling reaction conditions. The polymer **P5** obtained was characterized by GPC which showed number average molecular weight M_n 15 kDa. The polymer was found sufficient soluble for characterization by ^{1}H NMR spectroscopy which did show an aldehyde peak at 10.4 ppm. The post-polymerization functionalization using **17** or **18** attempted in n-butanol and chloroform mixture resulted in the recovery of the starting aldehyde polymer **P5**. Since the reaction was carried out in heterogeneous conditions, aldehyde polymer did not completely dissolve that could have some impact on the course of the reaction.

In order to increase solubility of the polymer **P5** in organic solvents, the fraction of the solubilizing groups was increased. Thus, a mixture of 25% of **19**, 25% of **13** and 50% of **15** was subjected to Suzuki polymerization conditions to afford a well-soluble polymer **P5** with average molecular weight M_n 10 kDa, according to GPC analysis (Scheme 3.3). Finally, polymer **P5** was subjected to post-polymerization functionalization with **18** in mixture of chloroform and n-butanol (1:1) in presence of catalytic amount of pyridine. However, numerous attempts using different bases such as pyridine, piperidine, NaOH, diisopropylamine were not successful. Depending upon the reaction time either starting material (**P5**) or products of polymer degradation were recovered.

Even after several attempts to synthesize the desired polymer **P4** using different methods such as pre-functionalized monomer, post-functionalization of aldehyde polymer **P5**, the polymer could not be obtained. In the first method, the MC monomer was not stable under palladium catalyzed reaction conditions whereas in the second, the post-functionalization was not successful. Therefore, the synthetic scheme needed to be changed to obtain the polymer that would show response to H_2S.

After screening some monomers, we decided to build the spiropyran functionalized conjugated polymer using previously synthesized monomer compound **6**. Preparation of polymer **P7** started with Suzuki coupling of monomers **6** and **15** using $Pd(PPh_3)_4$ as a catalyst in mixture of EtOH, H_2O and Toluene as a solvent and SDS as a surfactant (Scheme 3.4) to afford an aldehyde polymer **P6** (M_n 6kDa by GPC vs. polystyrene standards). The polymer **P6** was subjected to condensation with **18** to afford polymer **P7**.

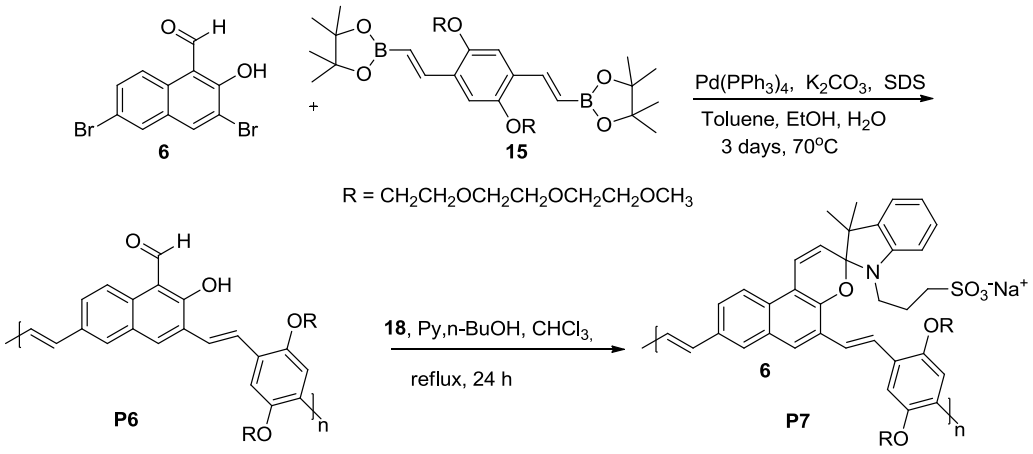

Scheme 3.4. Synthesis of the Polymer **P7**.

An alternative polymer **P8** was synthesized using Sonogashira coupling reaction conditions (Scheme 3.5). The polymer **P8** was characterized by ^{1}H NMR and number average molecular weight of 20 kDa was found by GPC (vs. polystyrene standards).

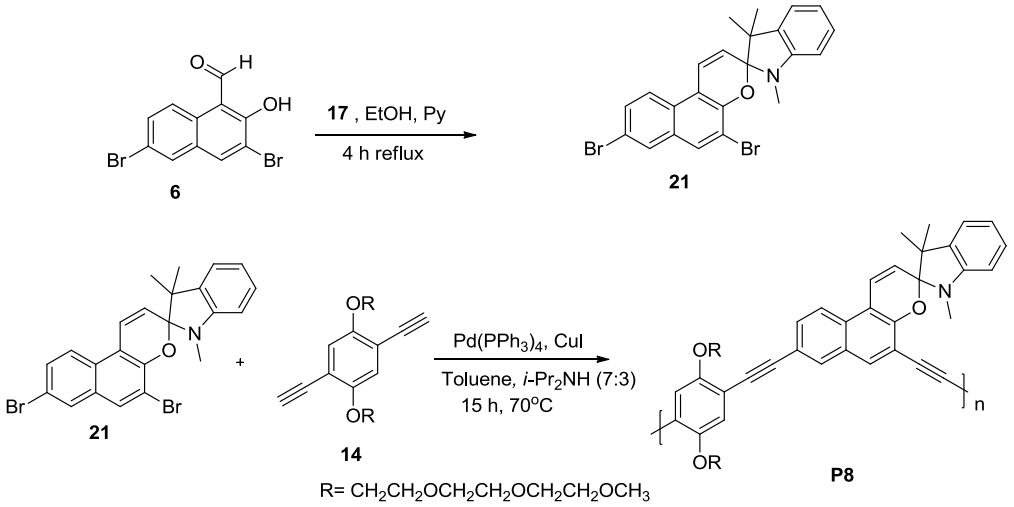

Scheme 3.5. Synthesis of the Polymer **P8**.

3.3. Spectroscopic Characterizations

The absorbance and emission spectra of different polymers are shown in Figure 3.5. The **P5-** polymer showed absorbance maximum at 450 nm and emission maximun at 575 nm whereas the napthyl-aldehyde polymer **P6** had absorbance maximum at 420 nm and emission maxium at

580 nm. The polymer **P8** had absorbance maximum at 440 nm and emission maximum at 500 nm.

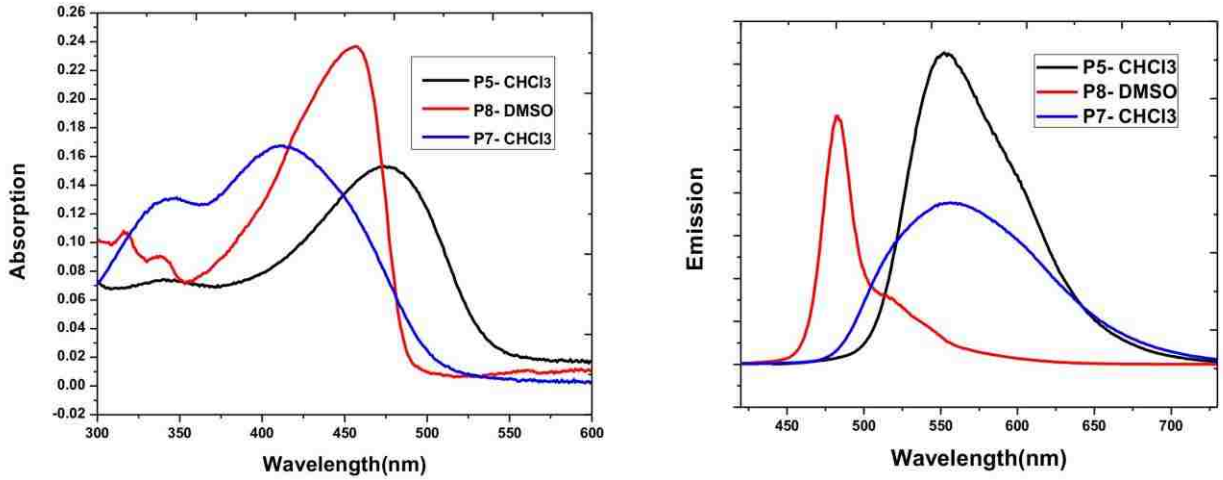

Figure 3.5. Absorption and Emission spectra of different CPs to be used in H_2S sensing.

The polymers **P7** and **P8** were used to study their response to H_2S addition. The stock solution of the polymers were prepared in DMSO and then diluted with methanol because these polymers did not dissolve in methanol. NaSH dissolved in MeOH was used as an H_2S source for the studies. All these measurements were carried out as preliminary tests, therefore actual concentrations of the samples were not determined.

As can be seen from Figure 3.6, there was a significant increase in the fluorescence intensity after addition of H_2S to a solution of the polymer **P7** whereas in the case of **P8**, there was a small decrease in the intensity. The decrease in the fluorescence intensity of **P8** was likely due to dilution of the sample whereas the increase in the intensity of **P7** was most likely due to the formation of a higher energy gap chromophore in good agreement with the original hypothesis. As expected, the polymer **P8** did not produce an appreciable response on exposure to

H_2S because there was no creation of a "higher energy gap" chromophore in the polymer backbone that could acts as a "roadblock" for exciton migration. As a result, there was almost no change in fluorescence of the polymer **P8** after exposure to an H_2S source.

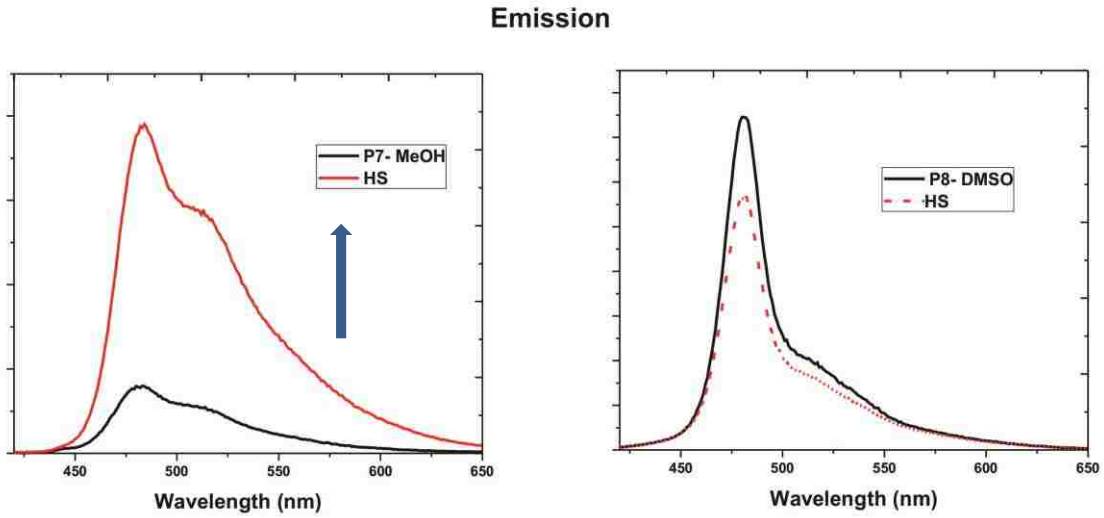

Figure 3.6. Change in Fluorescence intensity of polymers **P7** and **P8** after addition of NaSH in MeOH. The left graph corresponds to polymer **P7** and the right graph corresponds to polymer **P8**.

3.4. Future Work

The future studies will require synthesizing a water soluble polymer analogue of **P7** so that all the measurements could be carried out in aqueous medium which would make it a good candidate for in vivo applications. More accurate quantitative studies and detailed characterization (using time resolved spectroscopic techniques) will be required to undoubtfully establish "the higher energy gap" paradigm as a general and universal concept in amplifying fluorescent conjugated polymers.

3.5. References

[1] Obermajer, N.; Wong J. L.; Edwards, P. R.; Chen, K.; Scott, M.; Khader, S.; Kolls, J, K.; Odunsi, K.; Billiar, T. R.; Kalinski, P. Induction and stability of human Th17 cells require endogenous NOS2 and cGMP-dependent NO signaling. *J. Exp. Med*. **2010,** *10*, 1433-1445.

[2] Morita, T.; Perrella, A. M.; Lee, E. M.; Kourembanas, S. Smooth muscle cell-derived carbon monoxide is a regulator of vascular cGMP. *Proc. Natl. Acad. Sci. USA* **1995,** *92*, 1475-1479.

[3] Lefer, D. J. A new gaseous signaling molecule emerges: Cardioprotective role of hydrogen sulfide. *Proc. Natl. Acad. Sci. USA* **2007,** *104*, 17907-17908.

[4] Martelli, A.; Testai, L.; Bresch, C. M.; Blandizzi, C.; Virdis, A.; Teddei, S.; Calderone, V. Hydrogen Sulphide: Novel Opportunity for Drug Discovery. *Med. Res. Rev.* **2012,** *6*, 1093-1130.

[5] Kamoun, P.; Belardinelli, M. C.; Chabli, A.; Lallouchi, K.; Chadefaux-Vekemans, B. Endogenous hydrogen sulfide overproduction in Down syndrome. *Am. J. Med. Genet. Part A* **2003,** *116*, 310-311.

[6] Eto, K.; Asada, K.; Arima, K.; Makifuchi, T.; Kimura, H. Brain hydrogen sulfide is severely decreased in Alzheimer's disease. *Biochem. Biophys. Res. Commun*. **2002,** *293*, 1485-1488.

[7] Jimenez, D.; Martinez-Manez, R.; Sancenon, F.; Ros-Lis, J. V.; Benito, A.; Soto, J. A New Chromo-chemodosimeter Selective for Sulfide Anion. *J. Am. Chem. Soc*. **2003,** *125*, 9000-9001.

[8] Bérubé, R. P.; Parkinson, D. P.; Hall, R. E. A Measurement of reduced sulphur compounds contained in aqueous matrices by direct injection into a gas chromatograph with a flame photometric detector. *J. Chromatogr. A* **1999,** *830*, 485-489.

[9] Lippert, R. A.; Elizabeth, J.; New, J. E.; Chang, J. C. Reaction-Based Fluorescent Probes for Selective Imaging of Hydrogen Sulfide Living Cells. *J. Am. Chem. Soc*. **2011,** *113*, 10078-10080.

[10] Kumar, N.; Bhalla, V.; Kumar M. Recent developments of fluorescent probes for the detection of gasotransmitters (NO, CO, H_2S). *Coord. Chem. Rev*. **2013,** *257*, 2335-2347.

[11] Qian, Y.; Karpus, J.; Kabil, O.; Zhang, S. Y.; Zhu, H. L.; Banerjee, R.; Zhao, J.; He, C. Selective fluorescent probes for live-cell monitoring of sulphide. *Nat. Commun*. **2011,** *2*, 495-499.

[12] Liu, C.; Pan, S.; Li, S.; Zhao, Y.; Wu, L. Y.; Berkman, C. E.; Whorton, A. R.; Xian, M. Capture and Visualization of Hydrogen Sulfide by a Fluorescent Probe. *Angew. Chem. Int. Ed.* **2011,** *50*, 10327–10329.

[13] Wang, R.; Yu, F.; Chen, L.; Chen, H.; Wang, L.; Zhang, W. A highly selective turn-on near-infrared fluorescent probe for hydrogen sulfide detection and imaging in living cells. *Chem. Commun*. **2012,** *48*, 11757-11759.

[14] Chen, Y.; Zhu, C.; Yang, Z.; Chen, J.; He, Y.; Jiao, Y.; He, W.; Qiu, L.; Cen, J.; Guo, Z. A Ratiometric Fluorescent Probe for Rapid Detection of Hydrogen Sulfide in Mitochondria. *Angew. Chem. Int. Ed.* **2013,** *52*, 1688–1691.

[15] Chan, Y. P.; Fan, L.; You, Q.; Chan, W. H.; Lee, W. M. A.; Shuang, S. Ratiometric pH responsive fluorescent probes operative on ESIPT. *Tetrahedron* **2013,** *69*, 5874-5879.

[16] Richard, J. A.; Massonneau, M.; Renard, Y-P.; Romieu, A. 7-Hydroxycoumarin-Hemicyanine Hybrids: A New Class of Far-Red Emitting Fluorogenic Dyes. *Org. Lett*. **2008,** *10,* 4175-4178.

Chapter 4. Polycyanines – Near-Infrared Fluorescent Conjugated Polymers

4.1. Introduction

Near Infrared (NIR) fluorescent materials have gained interest as fluorescent tags for bioimaging and chemosensing and also for use in NIR organic light emitting diodes (OLED's).[1,2,3] It is always desirable to have a fluorophore that absorbs and emits in the 650 to 1100 nm wavelength range because of the better spectral separation from autofluorescence and low light scattering of cells and tissues in biosensing and bioimaging applications.[4] Similarly, these far-red or NIR emitting fluorophores are of great interest in the field of OLEDs because of their potential applications in photodynamic therapy, night vision, defense security and telecommunications.[5]

Conjugated polymers have gained popularity as NIR materials because of the ease of altering their chemical and photophysical/spectroscopic properties which can be done by changing the band gap of the materials. Various factors such as resonance effect, planarity, interchain and bond length alternation also play a significant role in tuning the band gap. To obtain far-red or NIR absorption and emission, there are two different methods that have been utilized. One well-known strategy is elongation of the π-electron system of polymethine dyes by increasing the number of methine units, whereas another approach includes incorporation of alternating donor (D) and acceptor (A) units in the conjugated backbone of CP.[6,7,8]

NIR emitting polymers have been demonstrated by using 2,1,3-benzoselenadiazole (PCPDTBSe).[9] Anderson also used a similar approach using a D-A-D scheme to synthesize NIR-CPs (LBPP-1) with an emission band at 950 nm and showed potential use of this polymer in fabricating solar cells.[10] CPDT-based polymer was developed that provides dual functions as a low-gap polymer for NIR photovoltaics and light-emitting diodes (Figure 4.1).[21]

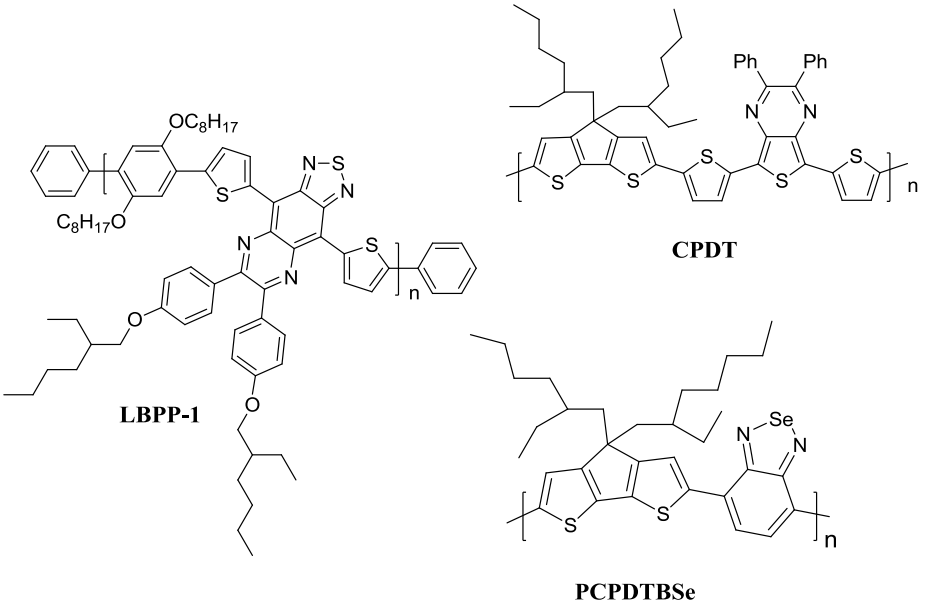

Figure 4.1. Representation of NIR- conjugated polymers for potential use in fabricating OLEDs and photovoltaic cells.

Different small molecule dyes with π-electron systems have been widely explored and used to reach the far red region, e.g cyanines, phthalocyanines and porphyrin derivatives, functionalized BODIPY's and squaraines.[11] Along the same line, there are multiple examples of conjugated polymers to obtain NIR absorption and emission. Usually dyes like squaraines and oxazines and functionalized BODIPY are used to achieve spectral properties in the far-red to NIR region. Zhu, Cheng et al. synthesized and studied fluorescent properties of NIR emissive polymers incorporating BODIPY and binapthyl units that would be useful in biological and cellular imaging.[12] Lambert and his group synthesized polysquaraine NIR CPs by condensation of squaric acid with electron rich aromatic co-monomers and studied their spectral properties which showed absorption in the red to near infrared (NIR) region with narrow NIR fluorescence (Figure 4.2).[13]

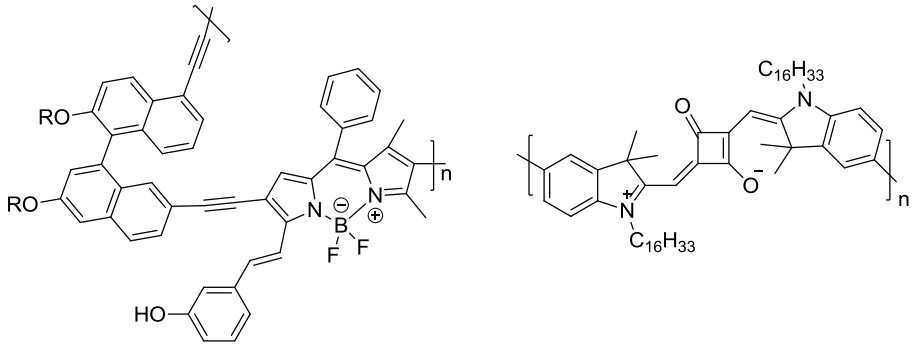

Figure 4.2. Incorporation of red-fluorescent dyes in constructing NIR conjugated polymers.

Cyanine dyes have gained more popularity for the applications in NIR region because of their broad wavelength tunability, high to moderate quantum yields and large molar extinction coefficients. These dyes have been known for more than 100 years. They are characterized by two heterocyclic units connected by a polymethine bridge having an odd number of carbons, where the two terminal heterocyclic units can be identical or different. Generic cyanine dyes consist of two nitrogen centers, one of which is positively charged and is linked by a conjugated chain of carbon atoms to the other neutral nitrogen (Figure 4.3). The spectral properties of cyanine dyes can be tuned from the visible region to far-red or NIR by changing the bridge length and heterocyclic units.[3,14]

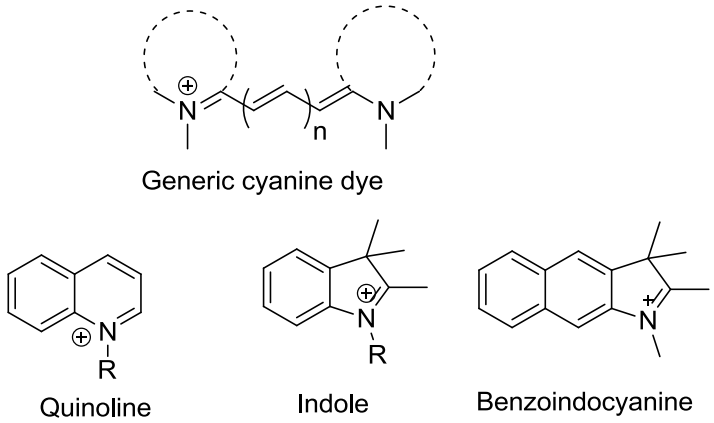

Figure 4.3. Generic structure and examples of the most common heterocyclic components found in cyanine dyes.

Cyanine dyes in solution are known to form aggregates characterized by distinct spectroscopic properties. There are a variety of factors that contribute to the formation of cyanine aggregates, such as solvent polarity, concentration, temperature, pH and ionic strength.[18] The molecules of cyanine dyes may aggregate in parallel fashion (plane-to-plane stacking) to form sandwich- type or H-aggregates which results in the hypsochromically shifted absorption bands relative to the monomer molecule. In contrast, J- aggregates result from head-to-tail (end-to-end) stacking and produce bathochromically shifted absorption bands relative to the monomer. This type of change in spectral properties has wide range of applications in many different areas such as photography, photodynamic therapy, optoelectronics, and photoelectric cells.[14]

As their ground and excited state geometries are close to each other, cyanine dyes exhibit narrow absorption and fluorescence bands with relatively small Stokes shifts. Although the π-conjugated electrons in the cyanine dyes appear to be mostly delocalized within the polymethine bridge, the terminal heterocyclic aromatic moieties also participate in the π-electron delocalization.[15]

For example, increase in conjugation length with accompanying bathochromic spectral shifts were observed when naphthalene aromatic termini (as in benzindocyanine compounds) were used instead of benzene units (as in indocyanine dyes) (Figure 4.4).[16] Encouraged by this observation, we hypothesized that linking indocyanines as monomeric units into a polycyanine chain would produce fluorescent CPs with extended π- electron delocalization, therefore shifting their absorption and emission into NIR region.[19] Due to the relative conformational flexibility around the bonds that interconnect the adjacent monomeric repeating units, photophysical properties of such polymers could be very sensitive to the environment, making them highly

attractive for sensing applications. In addition to that, these positively charged cyanine polymers would be an ideal candidate for the detection of negatively charged biomolecules such as DNA.

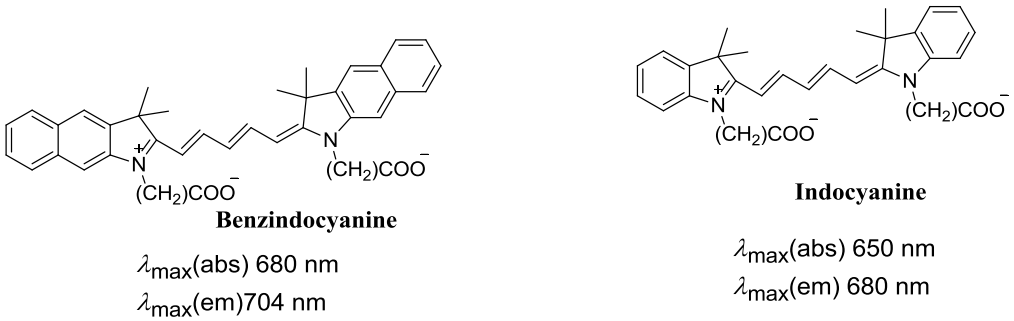

Figure 4.4. Chemical structures of Benzindocyanine and Indocyanine dyes and their spectroscopic characterization in methanol.[16, 20]

4.2. Design and Synthesis

The design and initial synthesis of the poly(cyanine) **P9** was started by a former group member Dr. Jinwoo Choi. The Yamamoto polymerization conditions were used in the synthesis of the polymer and monomers and its precursors were synthesized as shown in Scheme 4.1.

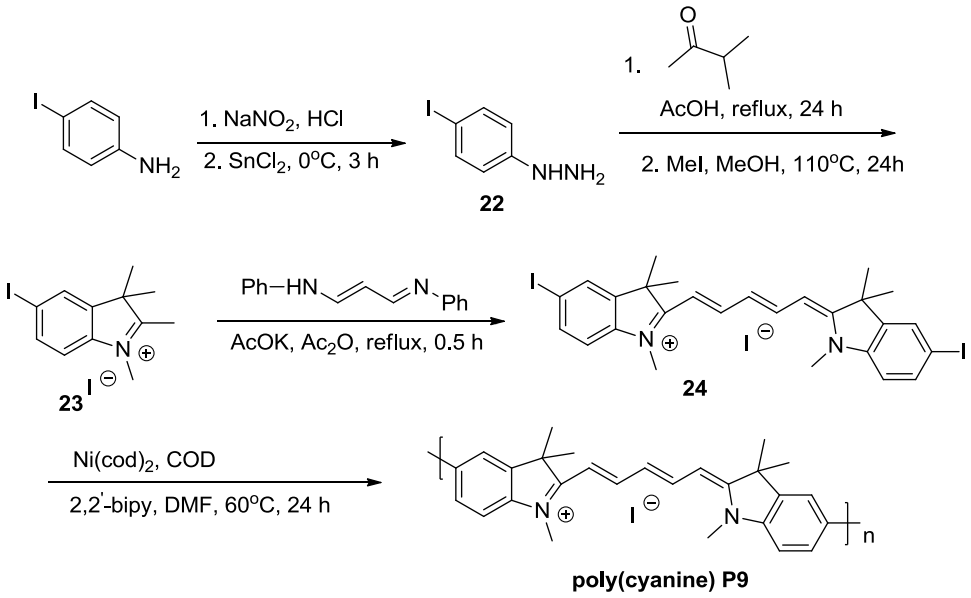

Scheme 4.1. Earlier reaction scheme for the synthesis of the poly(cyanine) polymer, **P9**.

The synthesis of polymer started with commercially available 4-iodoaniline which was converted to 4-iodophenylhydrazine **22**. The hydrazine was condensed with isopropyl methyl ketone and methylated with CH_3I to afford **23** followed by condensation with malonaldehyde bis(phenylimine) monohydrochloride to yield monomer **24** with two iodo "handles" for further polymerization. The Yamamoto polymerization using stoichiometric $Ni(cod)_2$ was carried out to afford the poly(cyanine) **P9**. The polymer obtained was dark blue powder as expected for a NIR material and had fairly good solubility in polar aprotic solvents like DMF, DMSO or in Methanol. The polymer showed reasonable thermal stability in solid state. Indeed, there was no substantial degradation found in TGA studies until 200 ^oC, and DSC measurements showed a broad endothermic peak centered around 95 ^oC. This phase transition could be due to melting of the polymer in a broad temperature range (Figure 4.5)

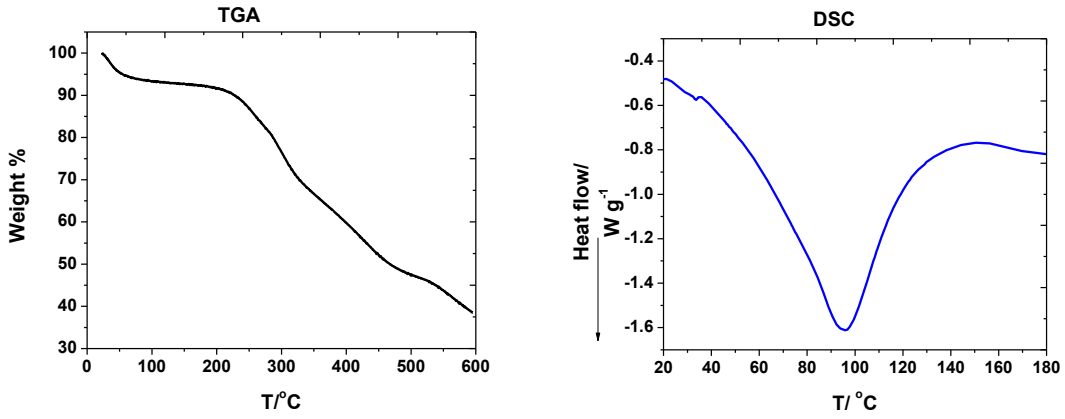

Figure 4.5. TGA and DSC measurements for polymer **P9** prepared as outlined in Scheme 4.1. Data were acquired at the heating rate of 10 ^oC min^{-1} in N_2 atmosphere.

Due to the charged nature of the molecule of **P9**, it was difficult to determine its molecular weight using GPC because it did not pass through the column when DMF was used to dissolve the cyanine polymer and also as an eluent for the chromatography. Therefore, we

decided to prepare well-defined oligomers such as dimer and tetramer of the monomer **24** in order to study the π-electron delocalization and to determine the effect of increasing molecular length on the spectroscopic properties.

The novel compounds monomer **30**, dimer **31** and tetramer **34** of cyanine dyes were synthesized from commercially available starting material biphenylbenzimine dihydrochloride **25**. The synthesis of the oligomers of the cyanine dye is outlined in the Scheme 4.3 whereas the synthesis of the required intermediates is outlined in Scheme 4.2.

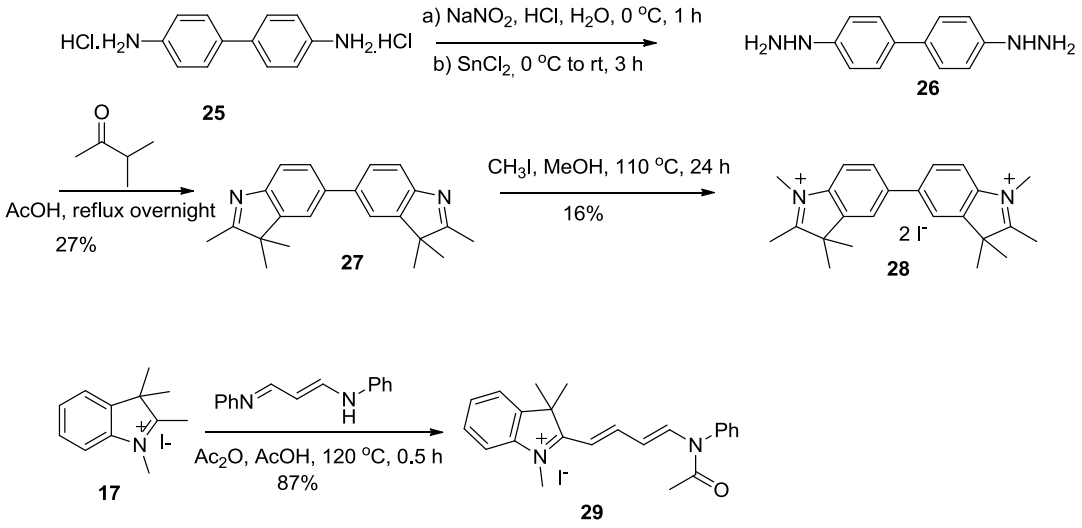

Scheme 4.2. Synthesis of the intermediates.

The biphenylbenzimine hydrochloride **25** was first converted to bis-hydrazine **26** and then condensed with excess isopropyl methyl ketone to afford **27** followed by N-methylation to afford **28**. Condensation of **17** with malonaldehyde bis(phenylimine) monohydrochloride in acetic anhydride and acetic acid afforded **29**, a half dye. These two compounds **28** and **29** were the main intermediates for the synthesis of oligomers and were used in a newly designed synthesis of the polymer (Scheme 4.4).

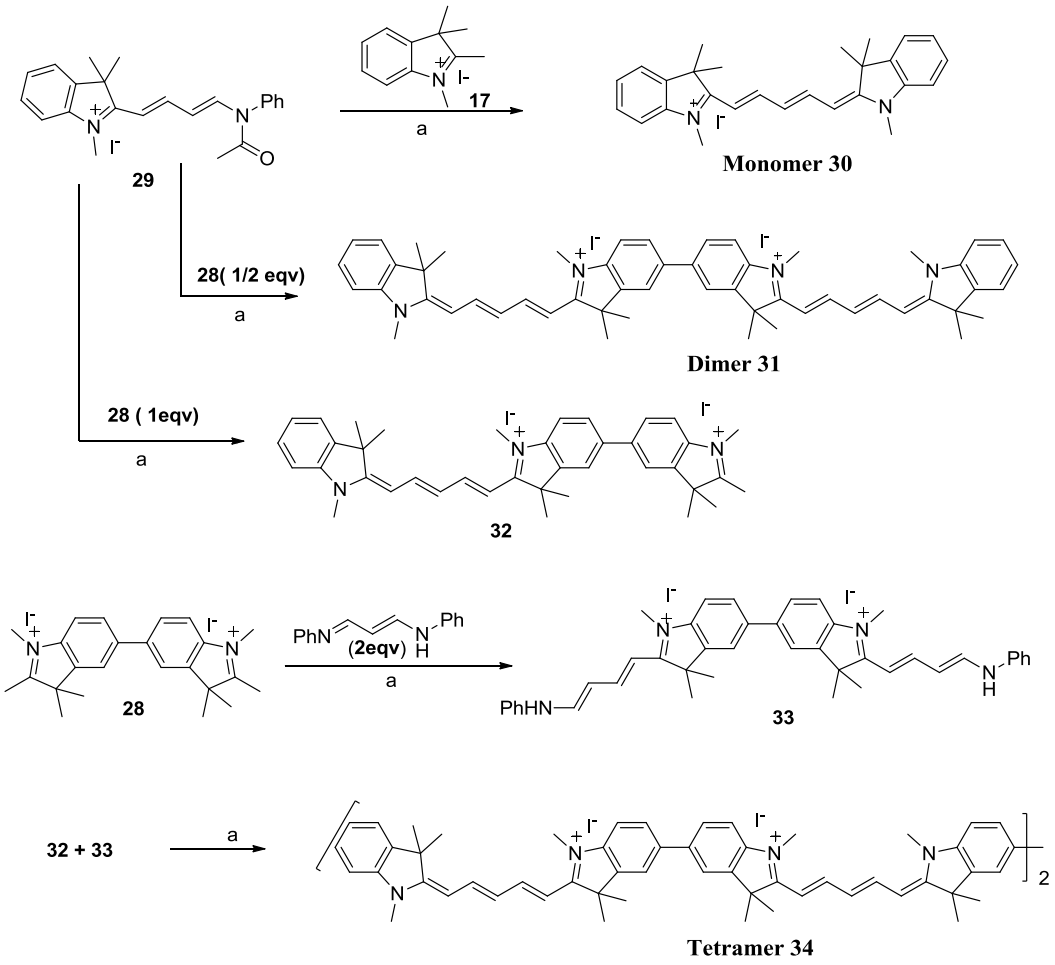

Reaction conditions a) Ac_2O, AcOH, 2 h, 140 ^oC.

Scheme 4.3. Synthesis of Monomer, Dimer and Tetramer

Condensation between **29** and **17** afforded the monomer **30** whereas condensation of **28** (1eqv) and **29** (2eqv) yielded the dimer **31**. The synthesis of the monomer and the dimer was straightforward, on the other hand for the synthesis of tetramer **34** a few more intermediates were required. First, **29** was condensed with 1 eqv of **28** to afford **32**, and **28** was then reacted with 2 eqv of malonaldehyde bis(phenylimine) monohydrochloride to afford second intermediate **33**. Finally, intermediates **33** and **32** were condensed together to afford tetramer **34** (Scheme 4.3).

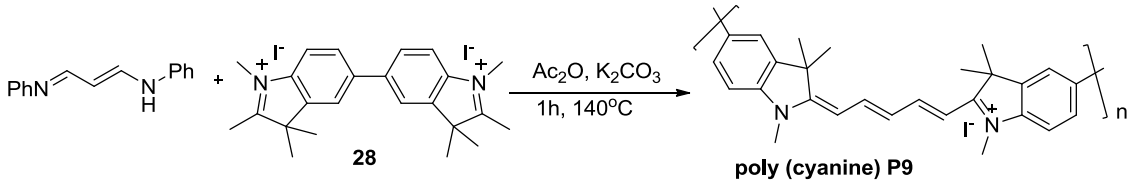

Scheme 4.4. Synthesis of polymer **P9**.

The synthesis of the polymer was relatively simple and was done in one step under basic conditions. The condensation of 1eqv of **28** with 1eqv of malonaldehyde bis(phenylimine) monohydrochloride in the presence of potassium carbonate in acetic anhydride at 140 ^{o}C for 2 h afforded **P9** as a dark blue powder.

4.3. Spectral Properties

The cyanine polymer **P9** optical spectra were significantly broadened as compared to the monomer **30** and appeared to consist of at least two overlapping bands. The first absorbance band at 625 nm was similar to the monomer **30** whereas the second band at 750 nm was red shifted by almost 100 nm (Figure 4.6 and Table 4.1). Similarly, the emission also showed dual bands, first at 650 nm and the second band at 700 nm.

Table 4.1.Spectroscopic properties of cyanine oligomers and polymer **P9** in DMSO

	Monomer (30)	**Dimer(31)**	**Tetramer(34)**	**Polymer P9**
Absorption (λ_{max})	620 nm	700 nm	680 nm	625 nm,750 nm
Emission (λ_{max})	650 nm	660 nm	675 nm	650 nm, 700 nm
ε, M^{-1} cm^{-1}	$1.5x10^5$	$1.1x10^5$	$1.0x10^5$	$0.5x10^5$
Quantum yield, %	38%	2%	0.2%	0.1%

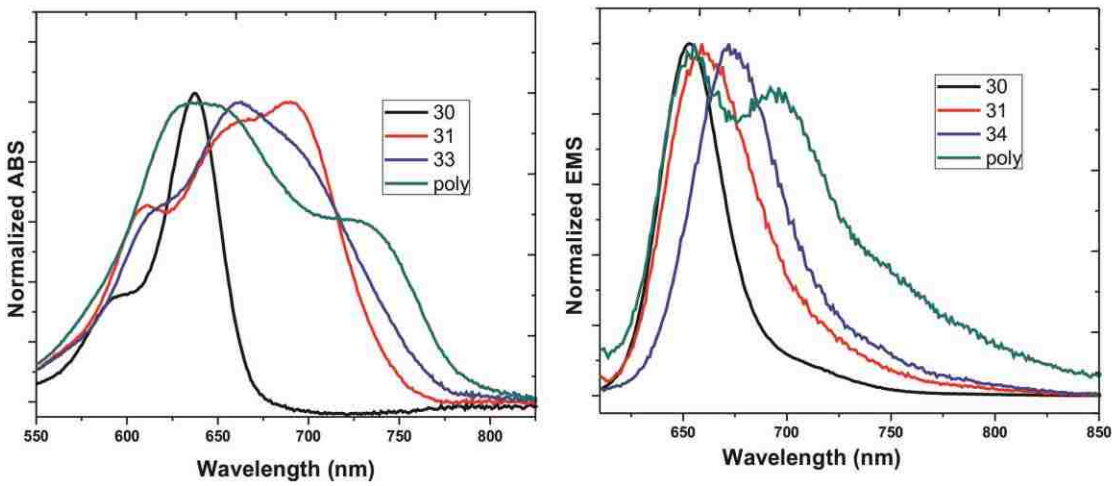

Figure 4.6. Normalized absorption and emission spectra of the monomer **30**, dimer **31**, tetramer **34** and polymer **P9** in DMSO.

As expected, fluorescent bands of the polymer were red shifted compared to the monomer because of the increase in π-conjugation length. Similarly, fluorescent spectrum of the cyanine polymer **P9** showed bathochromic shifts of 25 nm or 30 nm compared to dimer **31** or tetramer **34**, respectively. The origin of the dual band of these cyanines is currently not clear. It is known the oligomeric and polymeric cyanine dyes are prone to aggregate in solution resulting in production of both hypsochromically and bathochromically shifted new bands due to the formation of H and J aggregates, respectively. This kind of aggregation pattern is greatly affected by concentration of the sample, as with concentration increase, intensity of J and H aggregate bands tend to increase. In order to gain a deeper knowledge of the origin of the dual bands, absorption spectra of cyanine oligomers and polymer were obtained at different concentrations, from a very dilute to a highly concentrated sample (Figure 4.7). As can be seen from the normalized absorption graphs below, there was no change in the shape of the absorption bands,

from this it can be concluded that the dual bands were intrinsic to the molecules, and not originating from intermolecular aggregation.

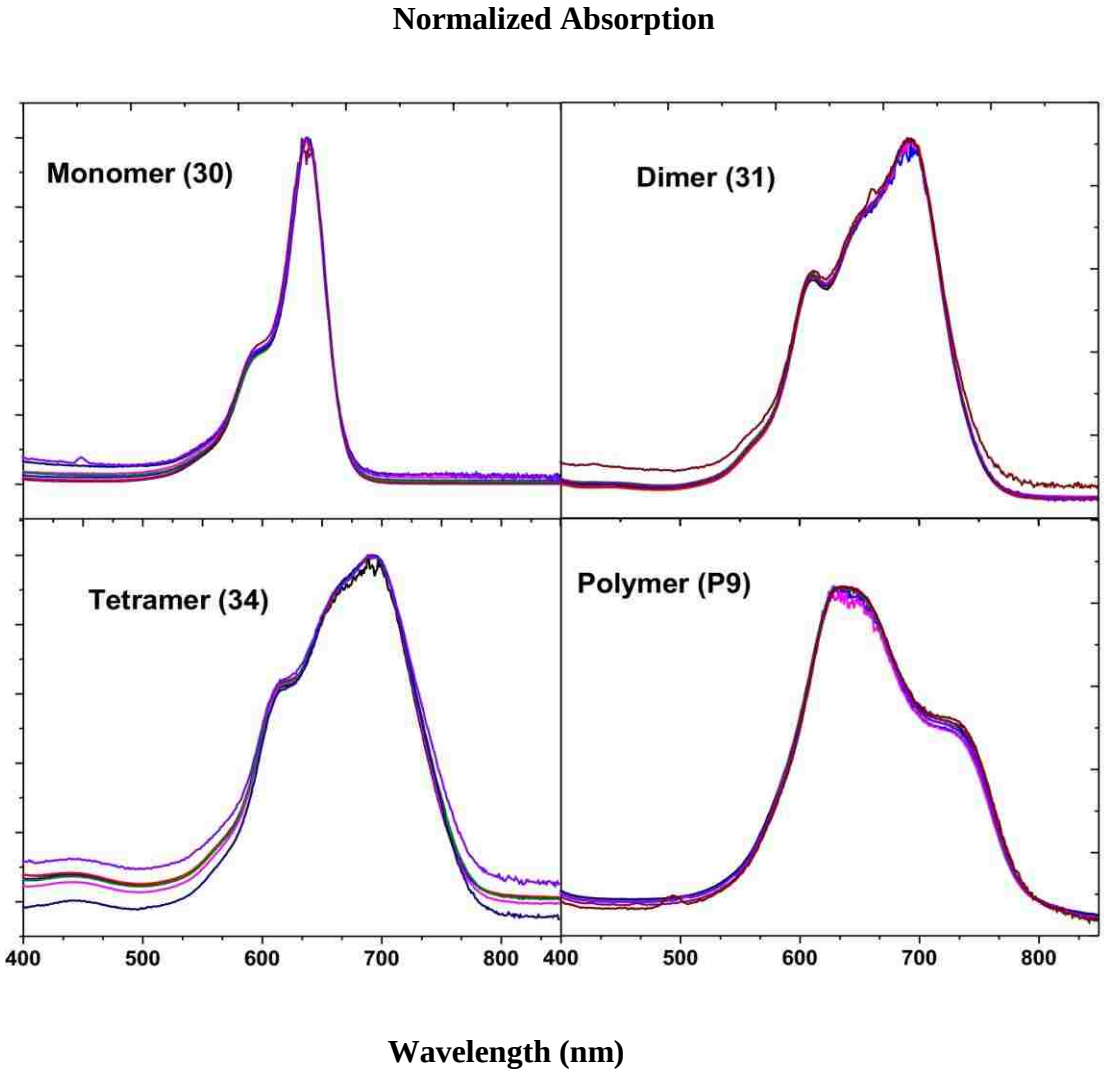

Figure 4.7. Normalized UV/Vis Absorption spectra of Monomer, Dimer, Tetramer and Polymer **P9** at concentrations ranging from 100uM to 0.01uM.

From this experiment, one can conclude that, although cyanine dyes are traditionally known to produce aggregates, the red shifted emission observed was due to the increase in the conjugation length from the monomer to the polymer. Another important observation was that wavelength did not show any further bathochromic shift upon moving from tetramer to the

polymer. This probably indicated that conjugation length in the poly(cyanine) polymers is limited by no more than 4 repeating units.

4.4. ^{1}H-NMR Studies

Variable temperature NMR: At low or room temperature, NMR spectra of the polymer **P9** were not very clear as the aromatic protons were overlapping with each other which made the spectra difficult to interpret. However, at the elevated temperature (around 40°C and higher) in DMSO, as shown in the Figure 4.8, an acceptable spectrum of polymer **P9** was obtained. The chemical shift of the aromatic protons of the cyanine polymer was very similar to the chemical shift of the analogous signals in the monomer **30**.

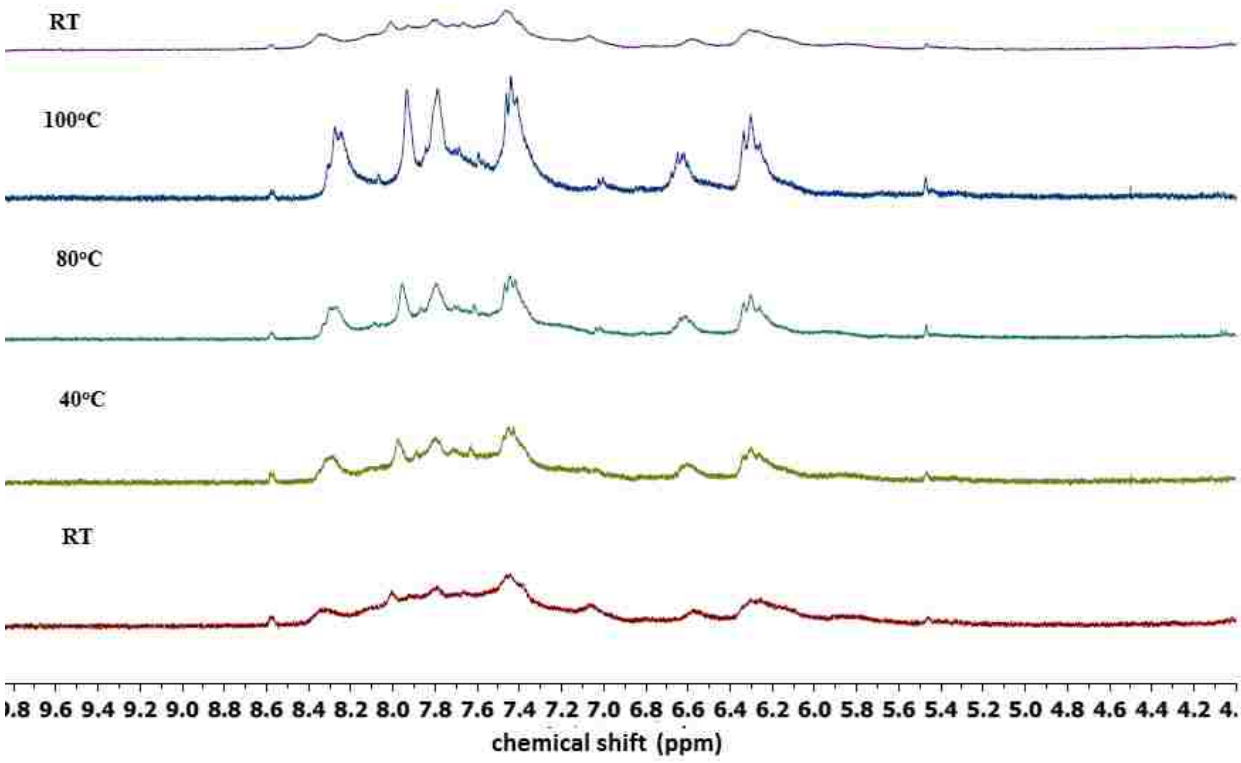

Figure 4.8. Variable- temperature ^{1}H NMR spectra of cyanine polymer **P9**. The top spectra is obtained after cooling the sample from 100 °C to RT.

Comparison between the NMR spectra of monomer and polymer: The polymethine bridge protons (δ 8.3, 6.6, 6.25 ppm) were observed in both monomer **30** and cyanine polymer **P9** at the same chemical shift whereas aromatic protons were slightly downfield shifted in **P9** compared to monomer **30** (Figure 4.9). Integration of the aromatic protons of the polymer showed two fewer protons in the aromatic region compared to the monomer as these two positions were used to form the polymer chain. On the other hand, comparison of the NMR spectrum of the polymer with shorter oligomers showed distinctly different spectra, neither matching the aromatic protons nor polymethine bridge. From this observation, it can be concluded that polymer **P9** was at least larger than the tetramer **34**.

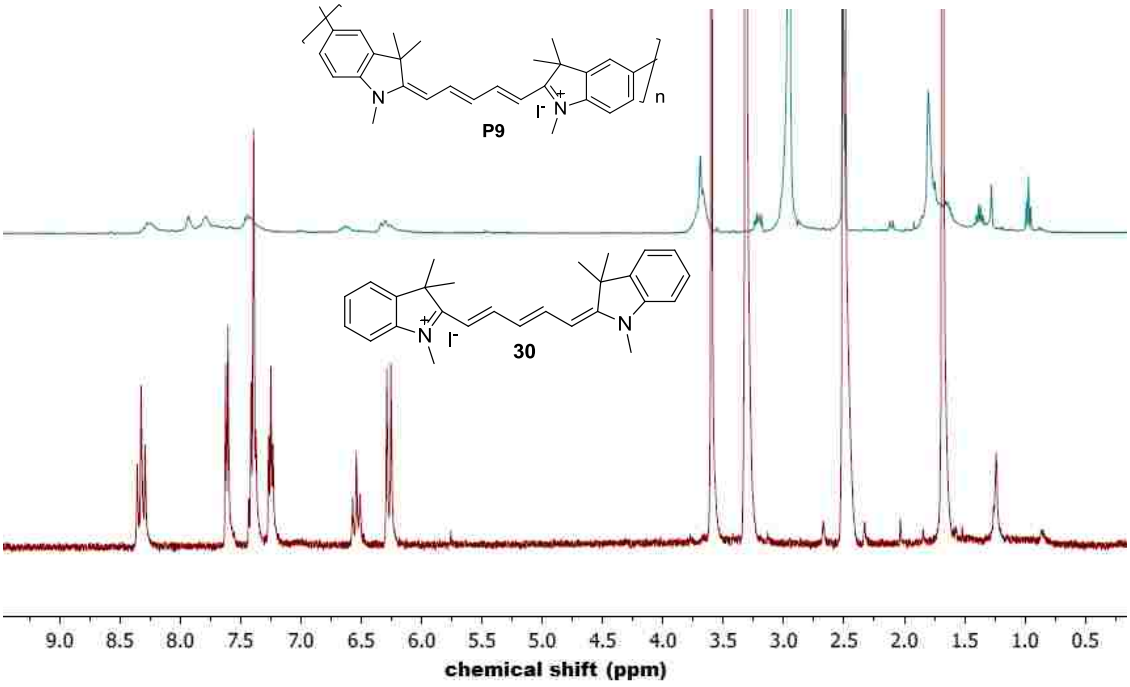

Figure 4.9. Comparison of ^{1}H NMR spectra of monomer **30** and cyanine polymer **P9**.

Diffusion NMR. The lack of consistent information about the chain length from either GPC or NMR studies lead us to rely upon the diffusion NMR to estimate the relative size of the polymer

and compare the value to the tetramer and dimer. Diffusion pulse-gradient NMR can allow determination of diffusion coefficient. The diffusion coefficient provides further information about the size of the molecule, as the bigger the molecule, the smaller the diffusion constant and vice versa. The correlation between the molecular size and experimental diffusion constant can be seen from the Table 4.2.

Table 4.2. Diffusion coefficient of cyanine oligomers and polymer **P9** in DMSO

	Monomer(30)	**Dimer(31)**	**Tetramer (34)**	**Polymer P9**
Diffusion Coefficient	$3.815 \times 10^{-10} m^2/s$	$1.711 \times 10^{-10} m^2/s$	$1.408 \times 10^{-10} m^2/s$	$6.814 \times 10^{-11} m^2/s$

According to the data in Table 4.2, one can conclude that the polymer showed diffusion coefficient approximately 6 times smaller than the diffusion coefficient of the monomer. This kind of measurement is usually performed for bigger molecules (such as DNA and proteins), although it can also be used for organic polymers to estimate the relative size. The significant difference in diffusion coefficients of polymer **P9** and oligomers indicated that the polymer was at least larger than the largest oligomer (tetramer **34**). Thus, this data was consistent with polymeric nature of **P9**.

4.5 Conclusions

After comparison of the optical properties, NMR spectra and Diffusion coefficient of cyanine polymer **P9** and related oligomers one can conclude that polymer was indeed larger than the tetramer, the longest of the prepared oligomers. More importantly, independent of how much the molecular length was extended, the absorption and emission spectra of the polymer **P9** did not show much difference relative to the tetramer **34**, and could not be shifted further to the NIR region. Nevertheless, the polymer **P9** did show some electronic delocalization (and far-red

spectroscopic properties). This principle should enable using such polymers as amplifying scaffold to construct NIR fluorescent amplifying chemo and biosensors. This and other opportunities should be studied as part of the future research program.

4.6. References

[1] Weil, T.; Vosch, T.; Hofkens, J.; Peneva, K.; Müllen, K. The Rylene Colorant Family—Tailored Nanoemitters for Photonics Research and Applications. *Angew. Chem. Int. Ed*. **2010,** *49*, 9068-9063.

[2] Williams, E. L.; Li, J.; Jabbour, G. E. Organic light-emitting diodes having exclusive near-infrared electrophosphorescence. *Appl. Phys. Lett.* **2006**, *89*, 0835061-0835063.

[3] Fabian, J. Near-infrared absorbing dyes. *Chem Rev*. **1992**, *92*, 1197-1226.

[4] Oushiki, D.; Kojima, H.; Terai, T.; Arita, M.; Hanaoka, K.; Urano, Y.; Nagano, T. Development and Application of a Near-Infrared Fluorescence Probe for Oxidative Stress Based on Differential Reactivity of Linked Cyanine Dyes. *J. Am. Chem. Soc*. **2010,** *132*, 2795–2801.

[5] Steckler, T. T.; Fenwick, O.; Lockwood ,T.; Anderson , M. R.; Cacialli, F. Near-Infrared Polymer Light-Emitting Diodes Based on Low-Energy Gap Oligomers Copolymerized into a High-Gap Polymer Host. *Macromol. Rapid Commun*. **2013,** *34*, 990−996.

[6] Umezawa, K.; Matsui, A.; Nakamura, Y.; Citterio, D.; Suzuki, K. Bright, Color-Tunable Fluorescent Dyes in the Vis/NIR Region: Establishment of New "Tailor-Made" Multicolor Fluorophores Based on Borondipyrromethene. *Chem. Eur. J.* **2009,** *15*, 1096–1106.

[7] Roncali, J. Synthetic Principles for Bandgap Control in Linear π-Conjugated Systems. *Chem. Rev*. **1997,** *97*, 173−205.

[8] Qian, G.; Zhong, Z.; Luo, M.; Yu, Z.; Zhang, Z.; Wang, Y.; Ma, D. Simple and Efficient Near-Infrared Organic Chromophores for Light-Emitting Diodes with Single Electroluminescent Emission above 1000 nm. *Adv. Mater.* **2009,** *21*, 111-116.

[9] Yang, R.; Tian, R.; Yang, J.; Hou, Q.; Yang, W.; Zhang, C.; Cao, Y. Deep-Red Electroluminescent Polymers: Synthesis and Characterization of New Low-Band-Gap Conjugated Copolymers for Light-Emitting Diodes and Photovoltaic Devices. *Macromolecules* **2005,** *38*, 244-253.

[10] Perzon, E.; Zhang, F.; Andersson, M.; Mammo, M.; Inganäs, O.; Andersson, M. R. A Conjugated Polymer for Near Infrared Optoelectronic Applications. *Adv. Mater*. **2007,** *19*, 3308–3311

[11] Escobedo, J. O.; Rusin, O.; Lim, S.; Strongin, R . M. NIR dyes for bioimaging applications. *Current Opinion in Chemical Biology.* **2010,** *14*, 64–70

[12] Wu, Y.; Mao X.; Ma, X.; Huang, X.; Cheng, Y.; Zhu, C. Synthesis and Fluorescence Properties of Chiral Near-Infrared Emissive Polymers Incorportating BODIPY Drivatives and (S)- Binapthyl. Macromol. *Chem. Phys*. **2012,** *213*, 2338-2245.

[13] Völker, S. F.; Lambert, C. Exciton Coupling Effects in Polymeric cis-Indolenine Squaraine Dyes. *Chem. Mater*. **2012,** *24*, 2541−2553.

[14] Mishra, A.; Behera, R. K.; Behera, K. P.; Mishra, B. K.; Behera, G. B. Cyanines during the 1990s: A Review. *Chem. Rev*. **2000,** *100*, 1973−2011.

[15] Ohira, S.; Hales, J. M.; Thorley, K. J.; Anderson, H. L.; Perry, J. W.; Brédas, J.-L. A New Class of Cyanine-like Dyes with Large Bond-Length Alternation. *J. Am. Chem. Soc.* **2009,** *131*, 6099-6101.

[16] Mujumdar, S. R.; Mujumdar, R. B.; Grant, C. M.; Waggoner, A. S. Bioconjugate Chem. Cyanine-Labeling Reagents: Sulfobenzindocyanine Succinimidyl Esters. **1996,** *7*, 356-362.

[17] Eisfeld, A.; Briggs, J. S. The J- and H-bands of organic dye aggregates. *Chemical Physics* **2006,** 324 376–384.

[18] Chowdhury, A.; Wachsmann-Hogiu, S.; Bangal, P. R.; Raheem, I.; Peteanu, L. A. Characterization of Chiral H and J Aggregates of Cyanine Dyes Formed by DNA Templating Using Stark and Fluorescence Spectroscopies. *J. Phys. Chem. B.* **2001,** *105*, 12196-12201.

[19] Geiger, T.; Benmansour, H.; Fan, B. ; R. Nüesch, H. F. Low-Band Gap Polymeric Cyanine Dyes Absorbing in the NIR Region. *Macromol.Rapid Commun.* **2008,** *29*, 651-658.

[20] Mader, O.; Reiner, K.; Egelhaaf, H-J.; Fischer, R.; Brock, R. Structure Property Analysis of Pentamethine Indocyanine Dyes: Identification of a New Dye for Life Science Applications. *Bioconjugate Chem*. **2004,** *15*, 70−78.

[21] Li, P.; Fenwick, S.; Yilmaz,S.;Dietrich Breusov, D.; Caruana, D. J.; Allard, S.; Scherf, U.; Caciall, F. Dual functions of a novel low-gap polymer for near infra-red photovoltaics and light-emitting diodes. *Chem. Commun*. **2011**, *47*, 8820–8822

Chapter 5. Experimental Details

5.1.General Procedures

All reactions were performed under an atmosphere of dry nitrogen, except those that required Schlenk techniques, which were performed under an atmosphere of ultrapure argon. Chromatographic separations were carried out on silica gel (EMD, 60 Å, 40-63 μM, pH 6.8-7.0) slurry packed into glass columns. Toluene, hexane, dichloromethane and THF were dried by passing through columns of activated alumina, and *N*,*N*-dimethylformamide (DMF) was dried by passing through a column of molecular sieves using a PS-400 Solvent Purification System from Innovative Technologies, Inc. The water content in the solvents was confirmed by coulometric titration (using a DL32 coulometric titrator from Mettler Toledo). High purity $Pd(PPh_3)_4$ was obtained from Strem Chemicals, Inc., while all other reagents were obtained from Sigma-Aldrich and Alfa Aesar and used as received. ^{1}H NMR spectra were recorded at 400 MHz, unless noted otherwise, and are reported in parts per million downfield from tetramethylsilane. UV-Visible spectra were recorded either on a Varian Cary 50 (solutions) or an Agilent Cary 5000 (thin films) spectrophotometer. Fluorescence studies were carried out using a PTI QuantaMaster4/2006SE spectrofluorimeter. Absolute quantum yields were determined using a "small" integrating sphere from PTI interfaced with the spectrofluorimeter. GPC analysis of polymers was performed with Agilent 1100 chromatograph equipped with two PLgel 5 μm MIXED-C and one PLgel 5 μm 1000 Å columns connected in series, using THF as a mobile phase, and calibrated against polystyrene standards. Thin-film samples for spectroscopic studies were prepared using Laurell Technologies WS-400B-6NPP spin processor. High-resolution mass spectra were obtained at the Mass Spectrometry Facility at LSU Chemistry Department using an ESI-TOF method with peak matching protocol to determine the mass and error range of the molecular ion

5.2. Synthetic Details

1,3,6-Tribromo-2-napthol (**4**) was prepared following the modified literature procedure.[1] A mixture of 10.0 g (0.045 mol) of 6-bromo-2-napthol and 22.0 g (0.22 mol) of potassium acetate was dissolved in 75 ml of glacial acetic acid upon slight heating and 37.2 g (12.0 ml, 0.22 mol) of liquid Br_2 was added slowly to the solution. The reaction mixture was stirred for 3 h at room temperature that resulted in the formation of yellow precipitate of compound **3**. The solid precipitate was collected by filtration and washed with water. It was dissolved in 150 ml of glacial acetic acid and 40.0 g (0.22 mol) of $SnCl_2$ (anhydrous) was added to the solution, and the resulting mixture was stirred for 10 h at room temperature. The reaction mixture was poured into 200 ml of 20% HCl and the solid precipitate was collected by filtration and dried in vacuo to afford 15.0 g of **4** as a colorless solid which was used in the next step without further purification. ^{1}H NMR ($CDCl_3$, 250 MHz) δ 7.97 (s, 1H), 7.94 (d, J = 9.2 Hz, 1H), 7.88 (d, J = 2.0 Hz, 1H), 7.65 (dd, J_1 = 9.2, J_2 = 2.0 Hz, 1H), 6.24 (s, 1H).

3,6-Dibromo-2-napthol (**5**) was prepared following the modified literature procedure.[1] A solution of 15.0 g (0.04 mol) of **4** and 20.0 g (0.11 mol) of anhydrous $SnCl_2$ in 110 ml of ethanol – conc. HCl (10:1) mixture was refluxed for 4 h. After cooling to room temperature, the reaction mixture was poured into ice-cold water, which yielded a colorless precipitate. The precipitate was collected by filtration, dissolved in dichloromethane and dried over Na_2SO_4. Concentration in vacuo afforded 7.0 g (51% over two steps) of **5** as a colorless fluffy solid, mp. 121-123 °C. ^{1}H NMR ($CDCl_3$) δ 7.94 (s, 1H), 7.85 (s, 1H), 7.57 (d, J = 8.9 Hz, 1H), 7.51 (dd, J_1 = 8.9, J_2 = 1.8 Hz, 1H), 7.35 (s, 1H), 5.70 (broad s, 1H).

3,6-Dibromo-2-hydroxy-1-napthaldehyde (**6**). A mixture of 5.0 g (0.016 mol) of **5**, 5.3 g (0.13 mol) of NaOH, 6 ml of chloroform and 7 ml of water was stirred upon heating at 75 °C for 18 h. After allowing to cool to room temperature, the reaction mixture was poured into 100 ml of 8% HCl and stirred for 30 min, and extracted with ethyl acetate (100 ml). The organic phase was washed successively with water, brine and dried over Na_2SO_4. Concentration in vacuo afforded a crude product which was purified by column chromatography on silica gel (eluent CH_2Cl_2 – hexane 2:1). A fraction with R_f 0.50 afforded 1.2 g of the starting material **5**, and a fraction with R_f 0.70 afforded 2.4 g (58%) of **6** as a yellow fluffy solid, mp. 151-152 °C. ^{1}H NMR ($CDCl_3$) δ 13.78 (s, 1H), 10.74 (s, 1H), 8.25-8.19 (m, 2H), 7.91 (d, J = 2.0 Hz, 1H), 7.74 (s, 1H), 7.72 (dd, J_1 = 9.1, J_2 = 2.0 Hz, 1H). HRMS (ESI-TOF) *m/e* 327.8649 M^+ (calcd. for $C_{11}H_6Br_2O_2$ 327.8735).

1,4-diethynyl-2,5-bis(tetradecyloxy)benzene (7). A mixture of 3.0 g (4.54 mmol) of **S1**, 1.2 g (1.7 ml, 11.4 mmol) of TMS-acetylene, 0.26 g (0.22 mmol) of $Pd(PPh_3)_4$, and 50 mg (0.22 mmol) of CuI in 50 ml of toluene – *i*-Pr_2NH (7:3) mixture was stirred in a sealed Air-free flask at 70 °C for 15 h. After allowing to cool to room temperature, the crude product was concentrated in vacuo and passed through a short plug of silica gel using chloroform as an eluent to afford 2.4 g of a yellow solid. The solid was dissolved in 50 ml of THF, and a solution of 2.0 g (35.0 mmol) of KOH in 25 ml of methanol was added dropwise at 0 °C to the THF solution and the resulting mixture was stirred for 1 h. The reaction mixture was poured into water and extracted with ethyl acetate. The organic phase was washed with water, brine and dried over Na_2SO_4. Concentration in vacuo afforded a crude product which was purified by column chromatography on silica gel (eluent CH_2Cl_2 – hexanes 1:1) to afford 1.76 g (75% over 2 steps) of **7** as colorless

oil that slowly solidified into a sticky colorless solid, R_f 0.60. ^{1}H NMR characterization was in agreement with the previously published data.[4]

Bis-1,4-[2-(4,4,5,5-tetramethyl-1,3,2-dioxaborolan-2-yl)-(1*E*)-ethenyl]-2,5-bis(tetradecyloxy)benzene (8). A mixture of 1.0 g (1.8 mmol) of compound **7**, 0.57 g (0.65 ml, 4.5 mmol) of pinacolborane, 46 mg (0.18 mmol) of $ZrCp_2HCl$ in 20 ml of 1,2-dichloroethane was stirred in a sealed Air-free flask at 65 °C for 3 days. After allowing to cool to room temperature, the reaction mixture was poured into water and extracted with ethyl acetate. The organic phase was washed successively with water, brine and dried over Na_2SO_4. Concentration in vacuo afforded crude product as brown oil. The crude product was purified by column chromatography on silica gel (eluent EtOAc – hexanes 1:4) to yield 0.8 g (50%) of **8** as a yellow solid, R_f 0.50, mp. 59-61 °C. ^{1}H NMR ($CDCl_3$) δ 7.71 (d, J = 18.6 Hz, 2H), 7.06 (s, 2H), 6.16 (d, J = 18.6 Hz, 2H), 3.94 (t, J = 6.7 Hz, 4H), 1.90-1.70 (m, 4H), 1.48-1.15 (m, 68H), 0.93-0.85 (m, 6H). HRMS (ESI-TOF) *m/e* 807.6843 $[M+H]^+$ (calcd. for $C_{50}H_{89}B_2O_6$ 807.6845).

(*E*)-4,4,5,5-tetramethyl-2-styryl-1,3,2-dioxaborolane (9) was prepared following a modified literature procedure.[5] A mixture of 0.5 g (4.9 mmol) of phenylacetylene, 0.8 g (0.9 ml, 6.37 mmol) of pinacolborane, 70 mg (0.27 mmol) of $ZrCp_2HCl$ in 10 ml of 1,2-dichloroethane was stirred in a sealed Air-free flask at 65 °C for 2 days. After allowing to cool to room temperature, the reaction mixture was poured into water and extracted with ether. The organic phase was washed successively with water, brine and dried over Na_2SO_4. Concentration in vacuo afforded a crude oil product which was purified by passing through a short plug of silica gel using CH_2Cl_2 – hexanes (2:1) as an eluent to afford 0.8 g (70%) of compound **9** as yellow oil. ^{1}H NMR characterization was in agreement with the previously published data.[6]

2-Hydroxy-3,6-di-(*E*)-styryl-1-napthaldehyde (10). A mixture of 0.23 g (1.0 mmol) of compound **9**, 0.15 g (0.45 mmol) of compound **6**, 10 mg (8.7 μmol) of $Pd(PPh_3)_4$, 0.31 g (2.25 mmol) of K_2CO_3 and 50 mg (2.25 mmol) of sodium dodecyl sulfate (SDS) in 15 ml of a mixture of toluene – ethanol – water (1:4:10) was stirred at 1000 rpm in a sealed Air-free flask at 75 °C for 48 h. After allowing to cool to room temperature, the reaction mixture was poured into water and extracted with ethyl acetate. The organic phase was successively washed with water, brine and dried over Na_2SO_4. Concentration in vacuo afforded crude product as a yellow solid which was purified by column chromatography on silica gel (eluent CH_2Cl_2 – hexanes 2:1) to afford 120 mg (70%) of **10** as a bright-yellow solid, R_f 0.50, mp. 205-207 °C. ^{1}H NMR ($CDCl_3$) δ 13.78 (s, 1H), 10.84 (s, 1H), 8.31 (d, J = 9.0, Hz, 1H), 8.26 (s, 1H), 7.88 (d, J = 1.8 Hz, 1H), 7.84 (dd, J_1 = 9.0, J_2 = 1.8 Hz, 1H), 7.65-7.55 (m, 5H), 7.48-7.35 (m, 5H), 7.33-7.26 (m, 2H), 7.24 (s, 2H).

2-Hydroxy-3,6-di-(*E*)-styryl-1-napthaldehyde oxime (M1). A mixture of 0.05 g (0.13 mmol) of **10**, 0.03 g (0.5 mmol) of hydroxylamine hydrochloride, 5 ml of ethanol and 0.5 ml of pyridine was refluxed for 2 h. After allowing to cool to room temperature, the reaction mixture was poured into water and extracted with ethyl acetate. The organic phase was washed with water and dried over Na_2SO_4. Concentration in vacuo afforded 0.045 g (85%) of **M1** as a bright-yellow solid powder, mp. 240-243 °C. ^{1}H NMR (acetone-D6) δ 11.96 (s, 1H), 10.94 (s, 1H), 9.29 (s, 1H), 8.27 (s, 1H), 8.23 (d, J = 8.2 Hz, 1H), 8.01 (s, 1H), 7.90 (d, J = 8.2 Hz, 1H), 7.76-7.60 (m, 5H), 7.53 (d, J = 15.0 Hz, 1H), 7.44-7.38 (m, 6H), 7.33-7.27 (m, 2H). HRMS (ESI-TOF) *m/e* 392.1644 $[M+H]^+$ (calcd. for $C_{27}H_{22}NO_2$ 392.1645).

Polymer P2. Polymerization was carried out using a literature procedure.[7] A mixture of 50 mg (0.15 mmol) of **6**, 128 mg (0.16 mmol) of **8**, 20 mg (0.015 mmol) of $Pd(PPh_3)_4$, 230 mg (1.5 mmol) of K_2CO_3, and 290 mg (1.5 mmol) of sodium dodecyl sulfate (SDS) in 30 ml of the mixture of water – toluene – ethanol (15:8:2) was stirred at 1000 rpm in a sealed Schlenk flask at 75 °C for 72 h. After cooling down to room temperature, the reaction mixture was poured into acetone, centrifuged, and supernatant solution was discarded. The solid residue was washed with water, centrifuged and supernatant solution was discarded. Again, the solid was dissolved in chloroform and precipitated into methanol twice to afford solid polymer. Finally, the product was dried in vacuo to afford 60 mg (50%) of the polymer **P2** as an orange powder, M_n 10 kDa, PDI 1.7. ^{1}H NMR ($CDCl_3$) δ 13.81 (broad s, 1H), 10.84 (broad s, 1H), 8.32-8.26 (m, 2H), 7.95-7.50 (m, 6H), 7.30-7.15 (m, 2H), 4.12 (broad s, 4H), 1.92 (broad s, 4H), 1.60-1.22 (m, 44H), 0.85 (broad s, 6H).

Polymer P1. A mixture of 60 mg (0.08mmol) of polymer **P2** and 100 mg (0.81 mmol) of hydroxylamine hydrochloride was dissolved in 10 ml of *n*-butanol – chloroform (1:1). Pyridine (0.5 ml) was added and the resulting mixture was refluxed for 2 h. After allowing to cool down to room temperature, the reaction mixture was poured into methanol, centrifuged, and supernatant solution was discarded. The solid residue was dissolved in chloroform and precipitated into methanol. The process was repeated twice and the resulting solid was dried in vacuo to afford 40 mg (50%) of polymer **P1** as a yellow-green powder, M_n 10 kDa, PDI 1.5. ^{1}H NMR ($CDCl_3$) δ 11.28 (broad s, 1H), 9.16 (broad s, 1H), 8.15-8.06 (m, 2H), 7.95-7.60 (m, 7H), 7.30-7.15 (m, 2H), 4.10 (broad s, 4H), 1.92 (broad s, 4H), 1.60-1.22 (m, 44H), 0.85 (broad s, 6H).

Polymer P3 was prepared following the procedure described for the polymer **P2**. A reaction of 25 mg (0.08 mmol) of **5**, 70 mg (0.09 mmol) of **8**, 15 mg (0.012 mmol) of $Pd(PPh_3)_4$, 75 mg (0.8 mmol) of K_2CO_3, and 80 mg (0.8 mmol) of sodium dodecyl sulfate in 15 ml of water – toluene – ethanol (15:8:2) mixture afforded 20 mg (25%) of the polymer **P3** as a dark-green powder, M_n 5 kDa, PDI 1.5. ^{1}H NMR ($CDCl_3$) δ 7.99 (broad s, 1H), 7.88-7.10 (m, 11H), 4.03 (broad s, 4H), 1.88 (broad s, 4H), 1.60-1.10 (m, 44H), 0.87 (broad s, 6H).

Reaction of M1 with DCP. A solution of DCP in CH_2Cl_2 (0.5 ml of 0.01 mM stock solution) was added to 10 mg (0.025 mmol) of **M1** in 4 ml of DMF, and the resulting mixture was left at room temperature for 30 min, followed by pouring into 8 ml of aqueous solution of $NaHCO_3$. It was extracted with CH_2Cl_2, and the organic phase was washed with water, and dried over Na_2SO_4. Concentration in vacuo afforded a crude solid product which was passed through a short plug of silica gel using CH_2Cl_2 – hexanes (1:1) as an eluent. The product was immediately analyzed by ^{1}H NMR. The analysis showed quantitative conversion to the corresponding isoxazole.

Analytical studies in dilute solutions. An aliquot of 2.0 ml of 10 μM stock solution of polymer **P1** (or **P3**, or small-molecule analogue **M1**) in DMF was added into separate vials. The 100 μl aliquots of stock solutions of DCP in CH_2Cl_2 (with concentration ranging from 10 μM to 0.1 M) were added into the polymer solutions to keep the total volume of the final solution at 2.1 ml. The final solutions were allowed to stay at room temperature for 30 min, and then were used to acquire UV/vis and fluorescence spectra.

Analytical studies in thin film of P1. A thin film of **P1** was prepared by spin-casting from a solution in $CHCl_3$ onto a 22×22 mm microscope glass cover slides at 1000 rpm in nitrogen

atmosphere. After UV/vis and fluorescence spectra have been acquired, a slide was placed on the wall inside a glass beaker containing a drop of DCP in the bottom. The beaker was closed, and the slide was kept inside for 1 min, removed, and immediately used to acquire UV/vis and fluorescence spectra.

Tri(ethylene glycol)-p-toluenesulfonate (11). A solution of 10.0 g (8.6 ml, 0.06 mol) of tri(ethylene glycol), 11.5 g (0.06 mol) of TsCl and 8.6 ml (0.06 mol) of triethylamine in 50 ml of dry DCM was stirred at room temperature for 12 h. The reaction mixture was poured into water and extracted with DCM followed by washing with water, $NaHCO_3$ and brine. The organic phase was then dried over Na_2SO_4 and concentrated in vacuo to afford 15 g (66%) of **11** as a colorless oil. ^{1}H NMR ($CDCl_3$) δ 7.79 (d, *J* = 9 Hz, 2H), 7.33 (d, *J* = 9 Hz, 2H), 4.15 (t, *J* = 9.6 Hz, 3H), 3.68 (t, *J* = 9.6 Hz, 3H), 3.61-3.58 (m, 6H), 3.53-3.31 (m, 3H), 3.3 (s, 3H).

1,4-Dibromo-2,5-bis(2-(2-(2-methoxyethoxy)ethoxy)ethoxy)benzene (13). A mixture of 2.0 g (0.074 mol) of **12**, 9.5 g (0.03 mol) of **11**, 4.1 g (0.03 mol) of K_2CO_3, 4.9 g (0.03 mol) of KI mixed in 100 ml of methyl ethyl ketone was refluxed for 2 days. After cooling to room temperature, the precipitate was removed by filtration and the liquid was concentrated in vacuo. The brown liquid obtained was then poured into aqueous $NaHCO_3$ and extracted with DCM, washed with water and brine and the organic phase obtained was dried over Na_2SO_4. Concentration in vacuo afforded a crude product which was purified by column chromatography on silica gel (eluent CH_2Cl_2) to afford 2.5 g (60%) of **13** as a colorless solid, R_f 0.60, mp. 35-36 ^{o}C. ^{1}H NMR ($CDCl_3$) δ 7.14 (s, 2H), 4.10 (t, *J* = 9.5 Hz, 4H), 3.88 (t, *J* = 9.6 Hz, 4H), 3.75-3.65 (m, 4H), 3.58-3.55 (m, 4H), 3.39 (s, 3H).

1,4-Diethynyl-2,5-bis(2-(2-(2-methoxyethoxy)ethoxy)ethoxy)benzene (14). A mixture of 1.72 g (4.54 mmol) of **13**, 0.73 g (0.9 ml, 7.45 mmol) of TMS-acetylene, 0.2 g (0.19 mmol) of $Pd(PPh_3)_4$, and 36 mg (0.19 mmol) of CuI in 30 ml of toluene – *i*-Pr_2NH (7:3) mixture was stirred in a sealed Air-free flask at 70 °C for 15 h. After allowing to cool to room temperature, the crude product was concentrated in vacuo and passed through a short plug of silica gel using ethyl acetate as an eluent to afford 1.5 g of a yellow solid. The solid was dissolved in 100 ml of THF, and a solution of 1.4 g (25.0 mmol) of KOH in 50 ml of methanol was added dropwise at 0 °C to the THF solution and stirred for 1.5 h. The reaction mixture was poured into water and extracted with chloroform. The organic phase was washed with water, brine and dried over Na_2SO_4. Concentration in vacuo afforded a crude product which was purified by column chromatography on silica gel (eluent ethyl acetate) to afford 0.8 g (60% over 2 steps) of **14** as colorless oil that slowly solidified into a sticky colorless solid, R_f 0.60. ^{1}H NMR ($CDCl_3$) δ 6.99 (s, 2H), 4.15 (t, J = 9.7 Hz, 4H), 3.87 (t, J = 9.8 Hz, 4H), 4.16-4.13 (m, 4H), 3.67-3.65 (m, 8H), 3.56-3.55 (s, 4H), 3.54 (s, 6H) 3.33 (s, 2H).

2,2'-((1E,1'E)-(2,5-bis(2-(2-(2-methoxyethoxy)ethoxy)ethoxy)-1,4-phenylene)bis(ethene-2,1-diyl))bis(4,4,5,5-tetramethyl-1,3,2-dioxaborolane) (15). A mixture of 0.5 g (1.0 mmol) of compound **14**, 0.3 g (0.36 ml, 2.5 mmol) of pinacolborane, 30 mg (0.1 mmol) of $ZrCp_2HCl$ in 15 ml of 1,2-dichloroethane was stirred in a sealed Air-free flask at 65 °C for 3 days. After allowing to cool to room temperature, the reaction mixture was poured into water and extracted with ethyl acetate. The organic phase was washed successively with water, brine and dried over Na_2SO_4. Concentration in vacuo afforded crude product as brown oil. The crude product was purified by column chromatography on silica gel (eluent EtOAc – hexanes 4:1) to yield 0.4 g (50%) of **15** as a yellow sticky solid, R_f 0.50. ^{1}H NMR ($CDCl_3$) δ 7.71 (d, J = 18.6 Hz, 2H), 7.1 (s, 2H), 6.15 (d,

J = 18.6 Hz, 2H), 4.15-4.13 (m, 4H), 3.90-3.87 (m, 4H), 3.78-3.69 (m, 18H), 3.57- 3.55 (m, 6H) 1.31-1.25 (m, 12H).

2,3,3-Trimethyl-3H-indole (16). A solution of 5 g (4.6 ml, 0.046 mol) of phenylhydrazine and 4.1 g (4.8 ml, 0.04 mol) of 3-methylbutanone in 25 ml of acetic acid was refluxed for 3 h. After cooling to room temperature, the reaction mixture was neutralized to pH 7 using aqueous $NaHCO_3$ and extracted with DCM. The organic phase was washed with water, brine and then dried over Na_2SO_4, and concentrated in vacuo to afford 6.5 g (88%) of **16** as a brown oil. ^{1}H NMR ($CDCl_3$) δ 7.53 (d, *J* = 7.5 Hz, 1H), 7.32-7.28 (m, 2H), 7.19 (t, *J* = 14.2 Hz, 1H), 2.28 (s, 3H), 1.30 (s, 6H).

3-(2,3,3-trimethyl-3H-indol-1-ium-1-yl)propane-1-sulfonate, sodium salt (18). A solution of 0.5 g (3.1 mmol) of **16** and 0.56 g (4.56 mmol) of 1,3-propane sultone in 5 ml of toluene was refluxed for 18 h. After cooling to room temperature, the crude product was concentrated in vacuo to afford red sticky solid. Further purification was carried by recrystallization from ethanol to afford 0.85 g (94%) of **18** as a red amorphous powder. ^{1}H NMR characterization was in agreement with the previously published data.[8]

(E)-2-(2,5-dibromostyryl)-1,3,3-trimethyl-3H-indol-1-ium iodide (**20a**). A solution of 0.11 g (0.38 mmol) of **17**, 0.1 g (0.38 mmol) of **19** and few drops of pyridine in 8 ml of ethanol was refluxed for 15 h. After cooling to room temperature, the crude product was concentrated in vacuo to afford a red solid. The red solid was then dissolved in chloroform, washed with water, brine and dried over Na_2SO_4 to afford 0.1 g (52%) of compound **20a** as a red powder, mp 187-193 ^{o}C. ^{1}H NMR ($CDCl_3$) δ 9.01 (s, 1H) 8.44 (d, *J* = 16 Hz, 1H), 8.25 (d, *J* = 16 Hz, 1H), 7.71-7.65 (m, 1H), 7.64-7.60 (m, 3H), 7.55-7.50 (m, 2H), 4.62 (s, 3H), 1.90 (s, 6H).

(E)-3-(2-(2,5-dibromostyryl)-3,3-dimethyl-3H-indol-1-ium-1-yl)propane-1-sulfonate (20b). A solution of 0.083 g (0.28 mmol) of **18**, 0.075 g (0.29 mmol) of **19** and few drops of pyridine in 5 ml of ethanol was refluxed for 15 h. After cooling to room temperature, the crude product was concentrated in vacuo to afford a red solid. Further purification was carried out by recrystallization from ethanol to afford 0.85 g (45%) of compound **20b** as a bright red powder, mp >400 ^{o}C. ^{1}H NMR ($CDCl_3$) δ 9.01 (s, 1H) 8.44 (d, *J* =16 Hz, 1H), 8.25 (d, *J* =16 Hz, 1H), 7.71-7.65 (m, 1H), 7.64-7.60 (m, 3H), 7.55-7.50 (m, 2H), 4.62 (s, 3H), 1.90 (s, 6H).

5,8-Dibromo-1',3',3'-trimethylspiro[benzo[f]chromene-3,2'-indoline] (21). A solution of 0.1 g (0.3 mmol) of **18**, 0.09 g (0.3 mmol) of **17a** and few drops of pyridine in 10 ml of ethanol was refluxed for 3 h. After cooling to room temperature, the crude product was concentrated in vacuo to afford dark purple solid. Further purification was carried out by recrystallization from ethanol to afford 0.1 g (68%) of **21** as shiny colorless crystals, mp 171-175^{o}C. ^{1}H NMR ($CDCl_3$) δ 7.86 (d, *J* = 8.8, 1H), 7.81 (d, *J* = 6.4 Hz, 2H), 7.57 (d, *J* = 8.6 Hz, 1H), 7.50 (d, *J* = 10.1 Hz, 1H) , 7.19 (t, *J* = 15.7 Hz, 1H) , 7.0 (d, *J* = 7.0 Hz, 1H,), 6.87 (t, *J* =14.6 Hz, 1H), 6.55 (d, *J* =7.4 Hz, 1H), 5.87 (d, *J* =10.7 Hz, 1H) , 2.71 (s, 3H), 1.34 (s, 3H), 1.23 (s, 3H).

Attempted Synthesis of polymer (P4). A mixture of 30.0 mg (0.05 mmol) of **20a**, 39.0 mg (0.051mmol) of **15**, 75.0 mg (0.5 mmol) of K_2CO_3, 155.0 mg (0.05 mmol) of SDS, 10.0 mg (0.005mmol) of $Pd(PPh_3)_4$ in 15 ml of a mixture of water – toluene – ethanol (15:8:2) was stirred at 1000 rpm in a sealed Air-free flask at 75 °C for 72 h. The reaction mixture was then cooled to room temperature and poured into acetone and centrifuged. The liquid was decanted and the red solid precipitate did not dissolve in any organic solvents, i.e THF, DCM, $CHCl_3$, DMSO, and

DMF. Similarly, polymerization between **20b** and **15** using same reaction conditions and time was carried out, after the reaction was complete, a red insoluble powder was obtained.

Aldehyde Polymer (P5). A mixture of 18.0 mg (0.068 mmol) of **19**, 48.0 mg (0.07 mmol) of **15**, 96.0 mg (0.7 mmol) of K_2CO_3, 188.0 mg (0.07 mmol) of SDS, 10.0 mg (0.005 mmol) of $Pd(PPh_3)_4$ in 15 ml of a mixture of water – toluene – ethanol (15:8:2) was stirred at 1000 rpm in a sealed Air-free flask at 75 °C for 72 h. The reaction mixture was then cooled to room temperature and poured into acetone and centrifuged. The liquid was decanted and the red solid precipitate was partially dissolved in chloroform and then precipitated in methanol. The red solid obtained after second precipitation was dried in vacuo to afford 20 mg (40%) of polymer **P5,** M_n 12 kDa, PDI 1.7. ^{1}H NMR ($CDCl_3$) δ 10.43 (s, 1H), 8.19 (s, 1H), 7.98-7.81 (m, 3H), 7.45-7.28 (m, 2H), 4.32-4.0 (m, 4H), 3.98-3.78 (m, 8H), 3.60-3.49 (m, 4H), 3.39 (s, 6H).

Conversion of Aldehyde Polymer (P5) to (P4). Aldehyde polymer **P5** (8mg) was suspended in 15 ml of n-butanol and chloroform mixture (1:1) and 10 mg (0.032 mmol, 20 eqv) of **18** was added and the resulting mixture was refluxed for 24 h. The reaction mixture was allowed to cool down to room temperature and concentrated in vacuo to afford dark brown red solid which was partially dissolved in chloroform. The colloidal solution was precipitated in methanol and dried. The solid obtained was mixture of starting aldehyde polymer and unidentified insoluble degradation product.

Co-Aldehyde Polymer (P5). A mixture of 40.0 mg (0.15 mmol) of **19**, 206.0 mg (0.33 mmol) of **15**, 122.0 mg (0.15 mmol) of **13**, 200.0 mg (1.5 mmol) of K_2CO_3, 400.0 mg (1.5 mmol) of SDS, 20.0 mg (0.015 mmol) of $Pd(PPh_3)_4$ in 32 ml of Toluene: H_2O: EtOH (1:2:5) mixture was stirred in a sealed Air-free flask and heated at 75°C for 48 h. The reaction mixture was then allowed to

cool to room temperature, poured into acetone and centrifuged. The liquid was decanted and the red solid precipitate was washed with water and then centrifuged. The solid obtained was then dissolved in chloroform and then twice precipitated in methanol. The red solid obtained was dried in vacuo to afford 80 mg (50%) of polymer **P5** as red solid, M_n 10 kDa, PDI 1.6. ^{1}H NMR ($CDCl_3$) δ 10.43 (1H, s), 8.19 (s, 1H), 7.98-7.81 (m, 3H), 7.45-7.28 (m, 2H), 4.30 (s, 4H), 3.98-3.78 (m, 12H), 3.60-3.49 (m, 8H), 3.39 (s, 6H).

Attempted Conversion of Aldehyde Polymer P5 to MC-Polymer (P4). Co-Aldehyde polymer **P5** 50 mg (0.01 mmol) was dissolved in 10 ml of n-butanol and chloroform mixture (1:1) and 35 mg (0.1mmol, 10 eqv) of **18** was added and the resulting mixture was refluxed for 24 h. The reaction mixture was cooled down to room temperature and concentrated in vacuo to afford a red solid which was washed with methanol and dried. The solid obtained was the starting aldehyde polymer. The conversion of aldehyde polymer to MC-polymer was tried again with different bases such as piperidine, NaOH, TEA, Diisopropylethylamine, still the conversion was not successful. The reaction mixture was monitored every six hours for 36 h, and even after 36 h in some cases aldehyde polymer was obtained whereas in NaOH degraded polymer was obtained.

Polymer (P6). A mixture of 100.0 mg (0.162 mmol) of **6**, 39.5 mg (0.070 mmol) of **15**, 4.0 mg (0.0035 mmol) of $Pd(PPh_3)_4$, 134.0 mg (0.97 mmol) of K_2CO_3, and 200.0 mg (0.69 mmol) of sodium dodecylsulfate (SDS) in 30 ml of a mixture of water – toluene – ethanol (15:8:2) was stirred at 1000 rpm in a sealed Air-free flask at 75 °C for 72 h. After cooling down to room temperature, the reaction mixture was poured into methanol, centrifuged, and supernatant solution was discarded. The solid residue was dissolved in chloroform and precipitated into methanol. The process was repeated two times to afford dark red solid polymer. Finally, the

product was dried in vacuo to afford 40 mg (50%) of the polymer **P1**, as a red solid, M_n 6 kDa, PDI 1.8. ^{1}H NMR ($CDCl_3$) δ 13.80 (broad s, 1H), 10.82 (broad s, 1H), 8.30-8.28 (m, 2H), 7.87-7.59 (m, 6H), 7.12-7.11 (m, 2H), 4.33 (broad s, 4H), 4.01-3.63 (m, 12H), 3.42 (s, 6H).

Polymer (P7). Polymer **P6** (10 mg) was dissolved in 10 ml of n-butanol and chloroform mixture (1:1) and 20 mg (0.05 mmol, 20eqv) of **18** was added and the resulting mixture was refluxed for 24 h. The reaction mixture was cooled down to room temperature and concentrated in vacuo to afford a dark green solid. The solid was then washed with water and then dried in high vacuum to afford 5mg (~ 25%) of dark green crude polymer **P1**. ^{1}H NMR (DMSO-d_6) δ 8.6 (s, 1H), 8.51-8.19 (m, 3H), 8.15-7.12 (m, 10H), 6.74-6.70 (m, 3H), 5.97 (s, 2H), 4.30 (m, 4H) 3.97-3.71 (m, 20H), 1.9 (4H, m).

Polymer (P8). A mixture of 20 mg (0.041 mmol) of **21**, 20 mg (0.043 mmol) of **14**, 5 mg of $Pd(PPh_3)_4$, and 1 mg of CuI in 12 ml of toluene – *i*-Pr_2NH (7:3) mixture was stirred in a sealed Air-free flask at 70 °C for 18 h. After allowing to cool to room temperature, the crude product was poured into acetone and centrifuged. The liquid was decanted and the red solid precipitate was partially dissolved in chloroform and then precipitated in methanol. The yellow- green solid obtained after second precipitation was dried in vacuo to afford 15 mg (25%) of the polymer **P8.** ^{1}H NMR (DMSO-d_6) δ 8.16-8.10 (m, 1H), 7.62-7.54 (m, 3H), 7.29 (s, 1H), 6.52 (s, 1H), 5.74 (s, 2H), 4.20 (s, 4H) 3.76 (s, 6H), 3.63 (s, 6H), 3.50 (s, 9H), 3.17 (s, 6H).

(4-Iodophenyl)hydrazine (**22**) was prepared following a general literature procedure.[9] A solution of 2.0 g (9.1 mmol) of 4-iodoaniline in 40 ml of conc. HCl was prepared upon heating, and cooled down to 0 °C. An aqueous solution of 0.7 g (10.0 mmol) of $NaNO_2$ was added dropwise, and the reaction mixture was stirred at 0 °C for 1 h. Then a solution of 12.3 g (54.4

mmol) of $SnCl_2 \times 2H_2O$ in 10 ml of HCl was added dropwise over 15 min that resulted in immediate formation of a beige precipitate. The resulting mixture was stirred for 3 h at 0 ^oC, and quenched with 50% NaOH aqueous solution until pH 14. The organic product was extracted with ethyl acetate, washed with water and dried over Na_2SO_4.Concentration in vacuo resulted in 1.14 g (53%) of a crude product as a bright-beige solid, which was used for the next step without further purification. ^1H NMR (250 MHz, $CDCl_3$) δ 7.49 (d, *J* = 8.8 Hz, 2H), 6.62 (d, *J* = 8.8 Hz, 2H), 5.25 (br. s, 1H), 3.65 (br. s, 2H).

5-Iodo-1,2,3,3-tetramethylindolium iodide (**23**) was prepared following a literature procedure.[10] A mixture of 1.08 g (4.6 mmol) of **22**, 5 ml of acetic acid, and 0.42 g (0.52 ml, 4.9 mmol) of isopropylmethyl ketone was refluxed for 3 h. The resulting solution was then diluted with water and $NaHCO_3$ was added until pH 7. The crude indole compound was extracted with ethyl acetate, and the extract was concentrated in vacuo to yield a brown oil which was dissolved in 10 ml of methanol. Iodomethane (1.31 g, 9.2 mmol) was added and the resulting mixture was heated in a sealed tube at 110 °C for 24 h. The product precipitate was filtered, washed with chloroform and recrystallized from a mixture of DMSO and chloroform to afford 0.73 g (31%) of **23** as a red solid. ^1H NMR (250 MHz, DMSO-d_6) δ 8.28 (d, *J* = 1.6 Hz, 1H), 8.00 (dd, J_1 = 8.4, J_2 = 1.6 Hz, 1H), 7.70 (d, *J* = 8.4Hz, 1H), 3.91 (s, 3H), 2.71 (s, 3H), 1.50 (s, 6H).

2-[5-(1,3-Dihydro-5-iodo-1,3,3-trimethyl-2H-indol-2-ylidene)-1,3-pentadienyl]-5-iodo-1,3,3-trimethyl-3H-indolium iodide (**24**) was prepared following the published general procedure.[11] A mixture of 0.20 g (0.47 mmol) of **23**, 0.054 g (0.24 mmol) of 3-anilinoacrolein anil and 0.23 g (2.35 mmol) of potassium acetate in 5 ml of acetic anhydride was refluxed for 30 min. The resulting green precipitate was collected by filtration, washed with cold ethanol, and

recrystallized from methanol to afford 0.10 g (60%) of **24** as green crystalline material, mp 273-274 °C. ^{1}H NMR (250 MHz, DMSO-d_6) δ 8.32 (t, *J* = 13.0 Hz, 2H), 8.04 (s, 2H), 7.73 (d, *J* = 8.4 Hz, 2H), 7.21 (d, *J* = 8.4 Hz, 2H), 6.54 (t, *J* = 13.0 Hz, 1H), 6.25 (d, *J* = 13.0 Hz, 2H), 3.56 (s, 6H), 1.67 (s, 12H). HRMS *m/e* 635.0419 ([M+H]+) (calcd for $C_{27}H_{29}I_2N_2$ 635.0415).

Cyanine polymer (P9). A mixture of 0.080 g (0.10 mmol) of **24**, 8.8 mg (10 µl, 0.08 mmol) of 1,5- cyclooctadiene (COD), 23.4 mg (0.15 mmol) of 2,2′-bipyridyl and 41.2 mg (0.15 mmol) of $Ni(COD)_2$ in 12 ml of anhydrous DMF was stirred in a sealed Air-free flask at 65 °C for 24 h. After allowing to cool to room temp, most of DMF was removed in vacuo, and the product was precipitated into the mixture of methanol – hexane (1:9) to yield crude polymer as a dark-purple solid. The crude product was placed into a Soxhlet extractor, and extracted successively with chloroform, acetone and methanol. The methanol fraction yielded 40 mg (~60%) of **cyanine polymer P9** as a dark-purple solid material.

4,4'-Dihydrazinyl-1,1'-biphenyl (26). A heterogeneous mixture of 2 g (7.78 mmol) of **25** in 10 ml of concentrated HCl was dissolved after adding 75 ml of boiling water, cooled down and a solution of 1.3 g (17.1 mmol) of $NaNO_2$ in 10 ml of water was added dropwise at 0 ^oC and stirred for an hour. A solution of 17.6 g (9.33 mmol) of $SnCl_2$ in 20 ml of concentrated HCl was added to the reaction mixture and stirred for another 3 h at room temp. The reaction mixture was then neutralized to pH 12 -13 and filtered to afford 4 g of compound **26** as a yellow sticky solid (crude product) which was used in the next step without further purification. ^{1}H NMR (DMSO- d_6, 250 MHz) δ 7.29 (d, *J* = 8.2 Hz, 4H), 6.77 (d, *J* = 8.4 Hz, 4H), 6.62 (s, 2H), 3.90 (s, 4H).

1,1', 2,2',3,3,3',3'-Octametamethyl-3H,3'H-5,5'-biindole-1,1'-diium iodide (28). A solution of 4 g (18.6 mmol) of **26**, 2.4 g (3 ml, 28 mmol) of isopropyl methyl ketone in 20 ml of acetic

acid was refluxed at 120 ^{o}C for 12 h. The reaction mixture was allowed to cool down to room temp and neutralized with NaOH to pH 12. The crude product was then extracted with ethyl acetate, washed with water, brine and dried over Na_2SO_4 and concentrated in vacuo to afford 1.6 g (27%) of **27** as brown sticky oil. The oil was dissolved in 10 ml of methanol and 5.3 g (38 mmol) of methyl iodide was added, purged with argon and heated at 110 ^{o}C in a sealed tube for 24 h. The reaction mixture was allowed to cool and the solid was separated by filtration and recrystallized using methanol to afford 0.35g (16%) of **28** as an off –white powder, mp 285-289^{o}C. ^{1}H NMR (DMSO- d_6) δ 8.27 (s, 4H), 8.03 (s, 4H), 4.00 (s, 6H), 1.59 (s, 12H).

1,3,3-Trimethyl-2-((1E,3E)-4-(N-phenylacetamido)buta-1,3-dien-1-yl)-3H-indol-1-ium iodide (29). A suspension of 0.25 g (0.83 mmol) of 1,2,3,3-tetramethyl-3H-indolium iodide and 0.3 g (1.35 mmol) of malonaldehyde bis(phenylimine) monohydrochloride in 2 ml of acetic acid-acetic anhydride mixture (1:1) was heated for 0.5 h from room temp to 120 ^{o}C. The reaction mixture was allowed to cool down to room temperature and precipitated twice in ether. The dark solid precipitate was dissolved in dichloromethane and centrifuged, the solid particles were removed and the liquid was concentrated in vacuo to afford 0.28 g (86%) of **29** as a dark brown solid, mp 200-205^{o}C . ^{1}H NMR (DMSO-d_6) δ 8.86 (d, J =11 Hz, 2H), 8.46 (m, 1H), 7.74-7.42 (m, 7H), 6.80 (d, J =13 Hz, 1H), 5.45-5.42 (m, 1H), 3.75 (s, 3H), 1.87 (s, 3H), 1.64 (s, 6H).

Compounds **30-34** were prepared by following a modified literature procedure.[12]

1,3,3-Trimethyl-2-((1E,3E,5E)-5-(1,3,3-trimethylindolin-2-ylidene)penta-1,3-dien-1-yl)-3H-indol-1-ium iodide (monomer 30). A mixture of 50 mg (0.12 mmol) of **29** and 80 mg (0.12 mmol) of 1,2,3,3-tetramethyl-3H-indolium iodide in 2 ml of acetic acid- acetic anhydride mixture (1:1) was heated for 2 h at 140 ^{o}C, allowed to cool down to room temp and precipitated twice in

ether. The dark blue solid was dried in vacuo and was further dissolved in methanol and mixed with 2 ml of concentrated Bu_4NI solution in acetone. The solution was precipitated in water to afford a dark blue powder which was dried in high vacuo to afford 40 mg (65%) of blue-green shiny crystals of **30**, mp 171-172 ^oC. ^1H NMR (DMSO- d_6) δ 8.32 (t, *J* =13.1 Hz, 1H), 7.62 (d, *J* = 11.7 Hz, 2H), 7.38-7.24 (m, 4H), 7.26-7.23 (m, 2H), 6.54 (t, *J* =12.4 Hz, 1H), 6.27 (d, *J* =13.6 Hz, 2H), 3.59 (6H, s), 1.68 (s, 12H).

Cyanine Dimer (31). A mixture of 50 mg (0.12 mmol) of **29** and 20 mg (0.06 mmol) of **28** in 2 ml of acetic acid - acetic anhydride mixture (1:1) was heated for 2 h at 140 ^oC. The reaction mixture was allowed to cool down to room temperature, precipitated in ether twice to afford blue solid which was dried in vacuo. The solid was further dissolved in methanol and mixed with 2 ml concentrated Bu_4NI in acetone and precipitated in water. The precipitate was dried in high vacuum to give 20 mg (33%) of **31** as a dark blue powder, mp 242-245^oC. ^1H NMR (DMSO- d_6) δ 8.31 (t, *J* =12 Hz, 2H), 7.97 (s, 1H), 7.76 (d, *J* = 9.6 Hz, 1H), 7.58-7.48 (m, 1H), 7.43-7.37 (m, 3H), 7.24-7.20 (m, 1H), 6.52 (t, *J* = 12.5 Hz, 1H), 6.28-6.23 (m, 2H), 3.61-3.58 (m, 6H), 1.73 (s, 6H), 1.65 (s, 6H).

Intermediate (32). A mixture of 14 mg (0.033 mmol) of **29** and 20 mg (0.055 mmol) of **28** in 2 ml acetic acid - acetic anhydride mixture (1:1) was heated for 2 h at 140 ^oC. The reaction mixture was allowed to cool down to room temperature and precipitated in ether twice to afford blue solid. The precipitate was dried in high vacuum to give 24 mg of **32** (100%) as a blue amorphous powder.^1H NMR (DMSO) δ 8.32-8.20 (m, 3H), 8.02-7.96 (m, 3H), 7.83-7.73 (m, 1H), 7.52-7.40 (m, 3H), 7.29-7.25 (m, 1H), 6.55-6.50 (m, 1H), 6.36-6.22 (m, 2H), 3.99 (s, 3H), 3.62 (s, 6H), 2.76 (s, 3H), 1.75-1.58 (m, 18H).

Intermediate (33). A mixture of 22 mg (0.06 mmol) of **28** and 15 mg (0.12 mmol) of malonaldehyde bis(phenylimine) monohydrochloride in 2 ml of acetic acid- acetic anhydride mixture (1:1) was heated for 2 h at 140 ^{o}C and then precipitated in ether twice and dried in vacuo to afford 26 mg (81%) of **33** as a dark blue solid. ^{1}H NMR (DMSO-d_6) δ 8.86 (s, 1H), 8.50 (m, 1H), 8.21 (s,1H), 7.96-7.79 (m, 1H), 7.77-7.60 (m, 1H), 7.59-7.42 (m, 5H), 6.80 (m, 1H), 5.48 (m, 1H), 3.78 (s, 3H), 1.87 (s, 3H), 1.73 (s, 6H).

Cyanine Tetramer (34).A mixture of 24 mg (0.036 mmol) of **32** and 14 mg (0.018 mmol) of **33** in 2 ml of acetic acid - acetic anhydride mixture (1:1) was heated for 2 h at 140 ^{o}C. The reaction mixture was allowed to cool down to room temperature, precipitated in ether twice and dried in vacuo. The solid was further dissolved in methanol and mixed with 2 ml of concentrated Bu_4NI solution in acetone and precipitated in water. The precipitate was dried in high vacuo to give 13 mg (40%) of **34** as a dark blue powder, mp > 380^{o}C. ^{1}H NMR (DMSO-d_6) δ 8.31 (t, J = 12.9 Hz, 4H), 7.97 (s, 3H), 7.76 (d, J = 9.6 Hz, 3H), 7.58 (d, J = 8.8 Hz, 3H), 7.45-7.36 (m, 7H), 7.22-7.20 (m, 2H), 6.57-6.49 (m, 1H), 6.27-6.23 (m, 4H), 3.65-3.55 (m, 12H), 1.73 (s, 18H), 1.65 (s, 9H).

Cyanine (polymer) (P9). A mixture of 50 mg (0.083 mmol) of **29**, 19 mg (0.083 mmol) of malonaldehyde bis(phenylimine) monohydrochloride, 41 mg (0.41 mmol) of potassium acetate in 6 ml of acetic anhydride was refluxed at 140 ^{o}C for 1 h. The dark-blue mixture was then precipitated twice in ether, dried in vacuo. The crude solid was dissolved in methanol and mixed with 2 ml of concentrated Bu_4NI solution in acetone. The mixture was precipitated in water and dried in high vacuo to give 46 mg of polymer **P9** as a dark blue powder. ^{1}H NMR (DMSO- d_6. , *100°C*) δ 8.28-8.24 (m, 2H), 7.97(broad s, 2H), 7.78 (broad s, 4H), 7.46-7.41 (m, 4H), 6.65-6.61 (m, 1H), 6.33-6.25 (m, 2H), 3.69 (s, 6H), 1.80 (s, 12H).

5.3. References

[1] Liang, Y.-H.; He, Q.-Q.; Zeng, Z.-S.; Liu, Z.-Q.; Feng, X.-Q.; Chen. F.-E.; Balzarini, J.; Pannecouque, C.; De Clercq, E. Synthesis and anti-HIV activity of 2-naphthyl substituted DAPY analogues as non-nucleoside reverse transcriptase inhibitors. *Bioorg. Med. Chem.* **2010,** *18*, 4601-4605.

[2] Feng, L.; Wang, Y.; Liang, F.; Xu, M.; Wang, X. Highly selective recognition of monosaccharide based on two-component system in aqueous solution *Tetrahedron* **2011,** *67*, 3175-3180.

[3] Giesa, R.; Schulz, R. C. Soluble poly (1,4-phenyleneethynylene)s. *Makromol. Chem.* **1990,** *191*, 857-867.

[4] Wu, X.-H.; Liang, J. H.; Xia, J.-L.; Jin, S.; Yu, G.-A.; Liu, S. H. Bimetallic Ruthenium Complexes: Synthesis, Characterization, and the Effect of Appending Long Carbon Chains to Their Bridges *Organometallics* **2010,** *29*, 1150-1156.

[5] Pereira, S.; Srebnik, M. Hydroboration of Alkynes with Pinacolborane Catalyzed by HZrCpzCl. *Organometallics* **1995,** *14*, 3127-3128.

[6] Hickmann, V.; Kondoh, A.; Gabor, B.; Alcarazo, M.; Fürstner, A. Catalysis-Based and Protecting-Group-Free Total Syntheses of the Marine Oxylipins Hybridalactone and the Ecklonialactones A, B, and C. *J. Am. Chem. Soc.* **2011,** *133*, 13471-13480.

[7] Li, J.; Kendig, C. E.; Nesterov, E. E. Chemosensory Performance of Molecularly Imprinted Fluorescent Conjugated Polymer Materials. *J. Am. Chem. Soc.* **2007,** *129*, 15911-15918.

[8] Shi, Z.; Peng, P.;DaStrohecker, D.; Liao, Y. Long-Lived Photoacid Based upon a Photochromic Reaction. *J. Am. Chem. Soc.* **2011,** *133*, 14699-14703.

[9] Murphy, S.; Yang, X.; Schuster, G. B. Cyanine Borate Salts that Form Penetrated Ion Pairs in Benzene Solution: Synthesis, Properties, and Structure. *J. Org. Chem.* **1995,** *60*, 2411-2422.

[10] Klotz, E. J. F.; Claridge, T. D. W.; Anderson. H. L. Homo- and Hetero-[3] Rotaxanes with Two π-Systems Clasped in a Single Macrocycle. *J. Am. Chem. Soc.* **2006,** *128*, 15374-15375.

[11] Hamer, F. M. The Cyanine Dyes and Related Compounds, Interscience Publishers, NewYork, **1964**.

[12] Mason S. J.; Hake, J. L.; Nairne J.; Cummins W. J.; Balasubramania, S. Solid-Phase Methods for the synthesis of Cyanine Dyes. *J. Org. Chem.* **2005,** *70*, 2939-2949.

Appendix A : NMR of the Selected Compounds

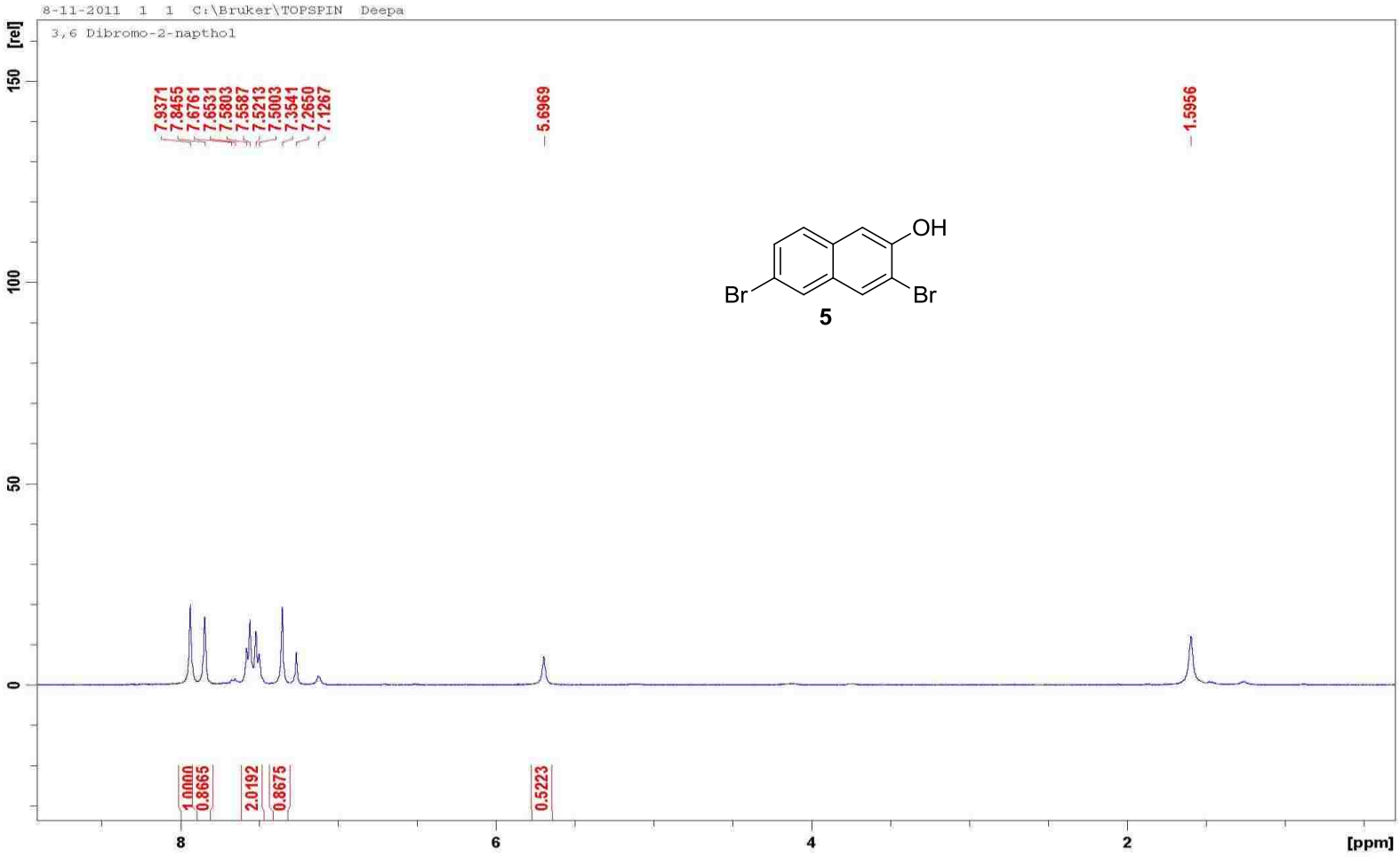

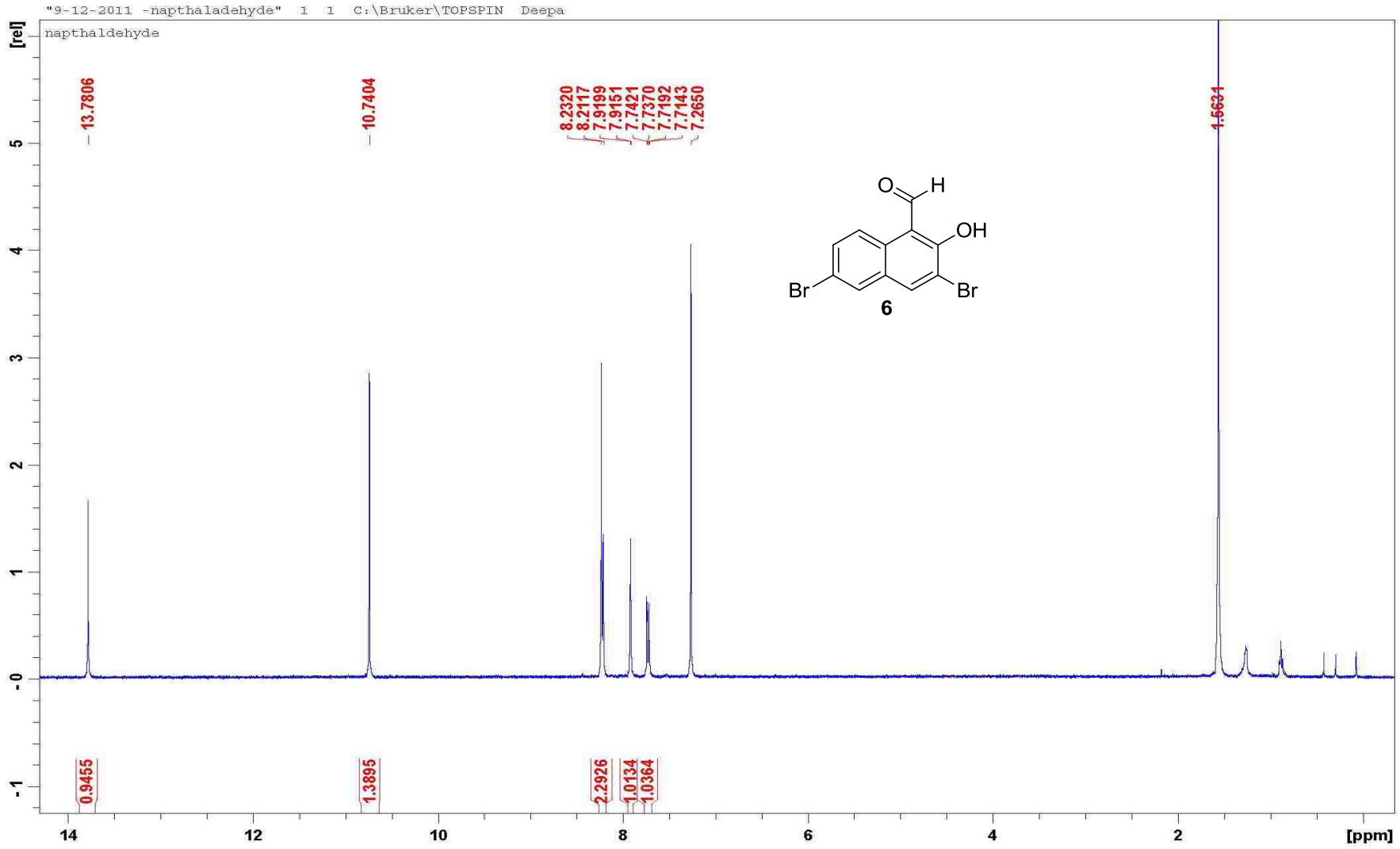
"9-12-2011 -napthaladehyde" 1 1 C:\Bruker\TOPSPIN Deepa
napthaldehyde
[rel]
13.7806
10.7404
8.2320
8.2117
7.9199
7.9151
7.7421
7.7370
7.7192
7.7143
7.2650
1.5631
0.9455
1.3895
2.2926
1.0134
1.0364
O
H
OH
Br
Br
6
14
12
10
8
6
4
2
[ppm]

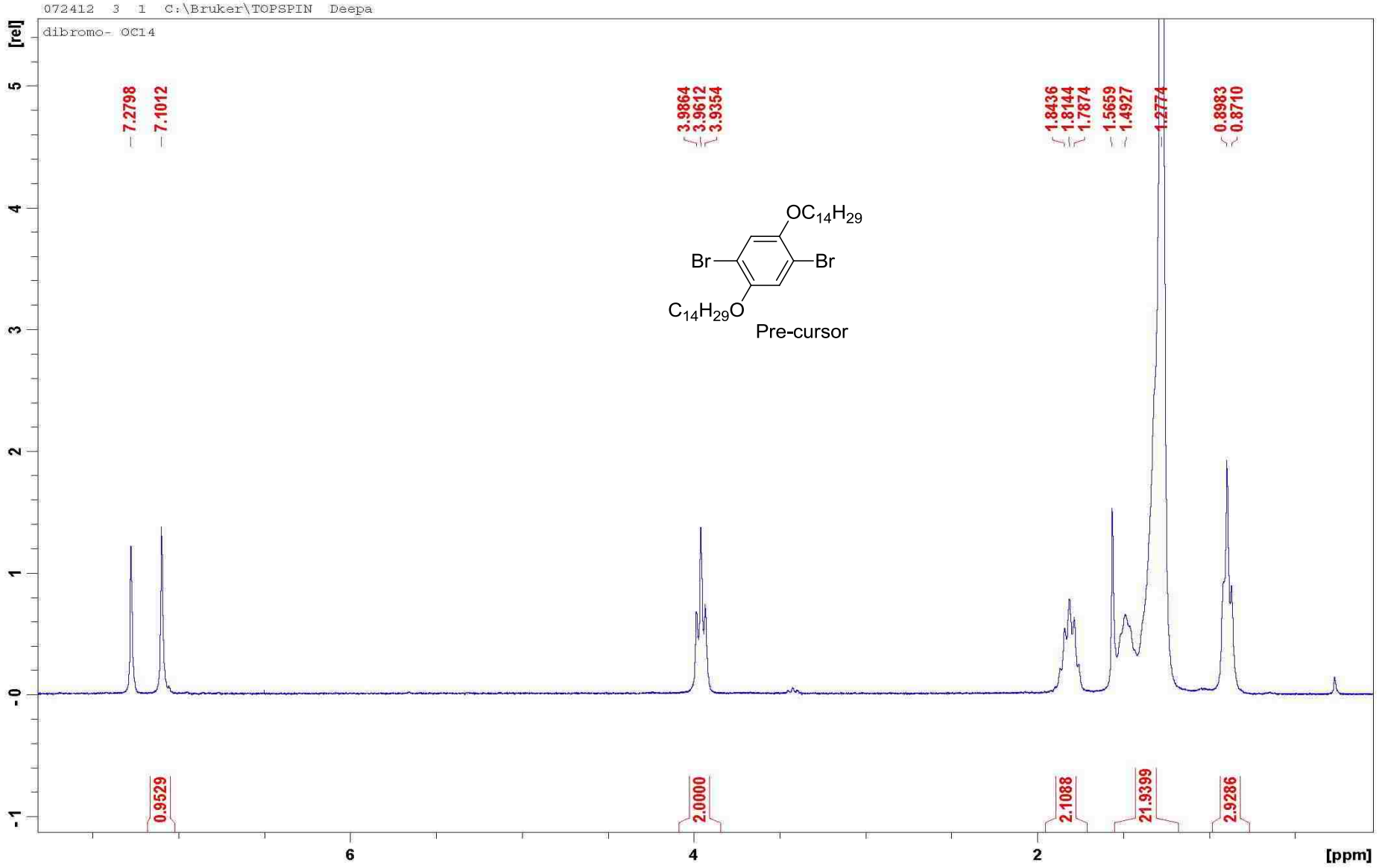
072412 3 1 C:\Bruker\TOPSPIN Deepa
dibromo- OC14
[rel]
7.2798
7.1012
3.9864
3.9612
3.9354
1.8436
1.8144
1.7874
1.5659
1.4927
1.2774
0.8983
0.8710
OC14H29
Br
Br
C14H29O
Pre-cursor
0.9529
2.0000
2.1088
21.9399
2.9286
[ppm]

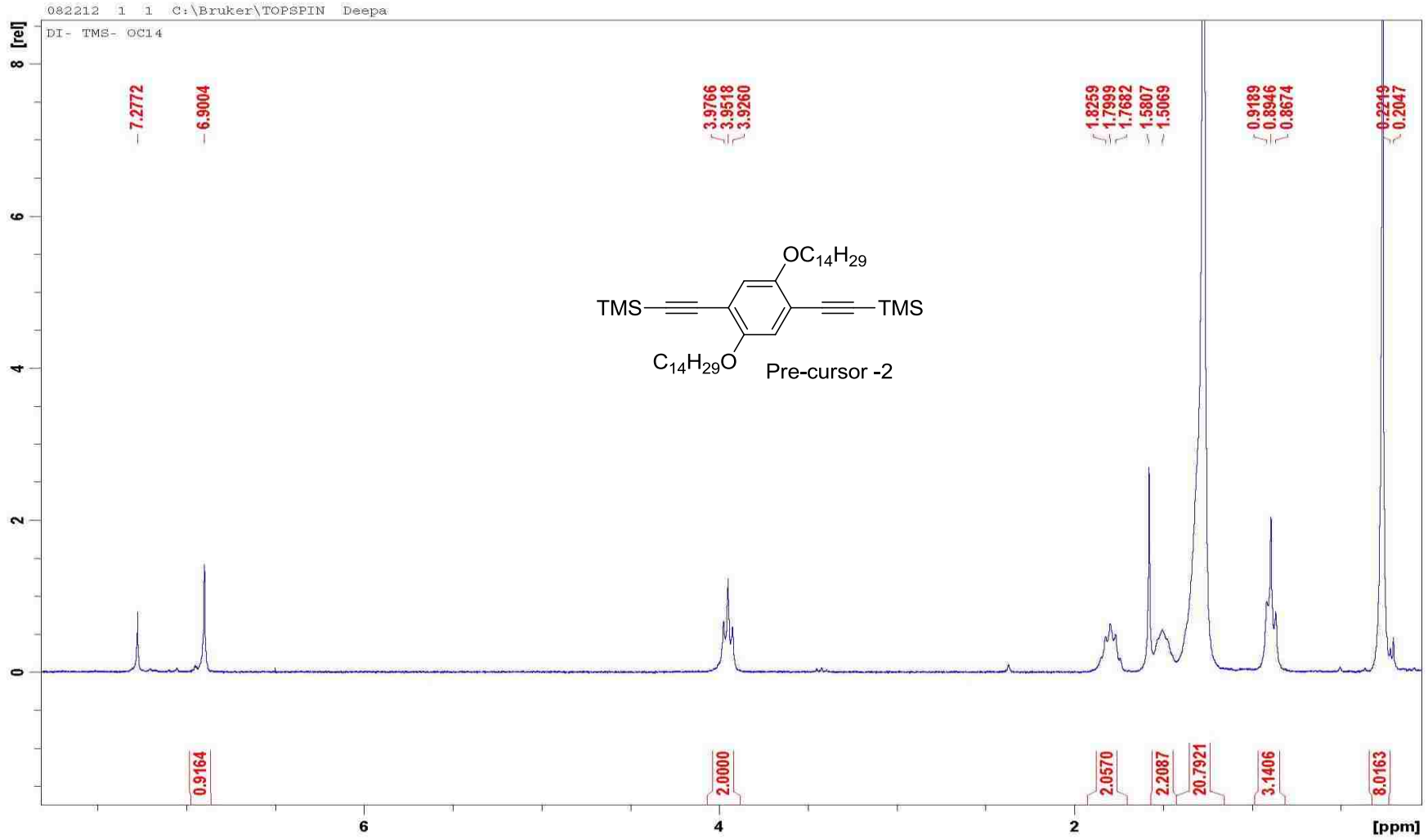
082212 1 1 C:\Bruker\TOPSPIN Deepa
DI- TMS- OC14
8 [rel]
6
4
2
0
7.2772
6.9004
3.9766
3.9518
3.9260
1.8259
1.7999
1.7682
1.5807
1.5069
0.9189
0.8946
0.8674
0.2249
0.2047
OC14H29
TMS
TMS
C14H29O
Pre-cursor -2
0.9164
2.0000
2.0570
2.2087
20.7921
3.1406
8.0163
6
4
2
[ppm]

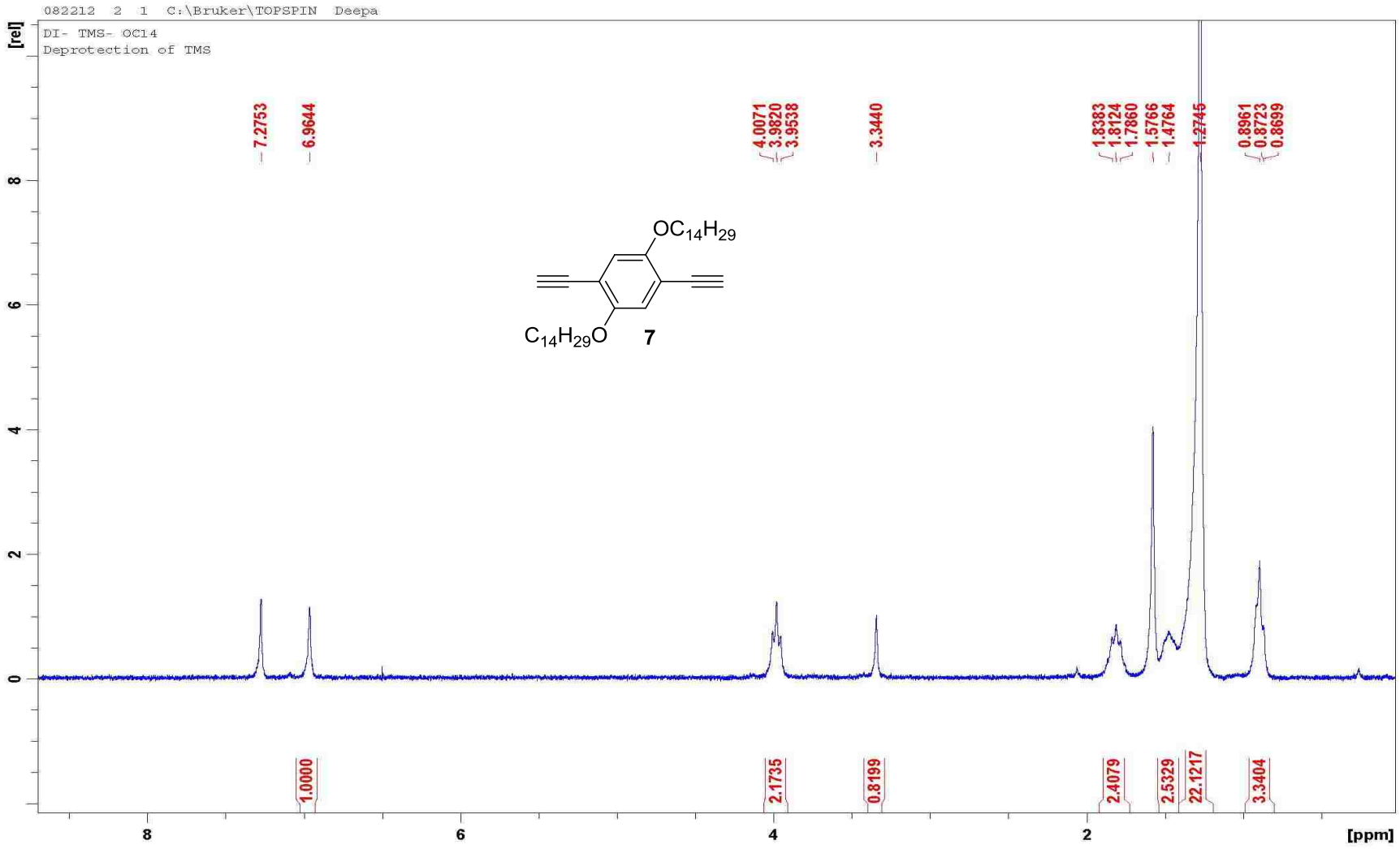
082212 2 1 C:\Bruker\TOPSPIN Deepa
DI- TMS- OC14
Deprotection of TMS
[rel]
7.2753
6.9644
4.0071
3.9820
3.9538
3.3440
1.8383
1.8124
1.7860
1.5766
1.4764
1.2745
0.8961
0.8723
0.8699
OC14H29
C14H29O
7
1.0000
2.1735
0.8199
2.4079
2.5329
22.1217
3.3404
[ppm]

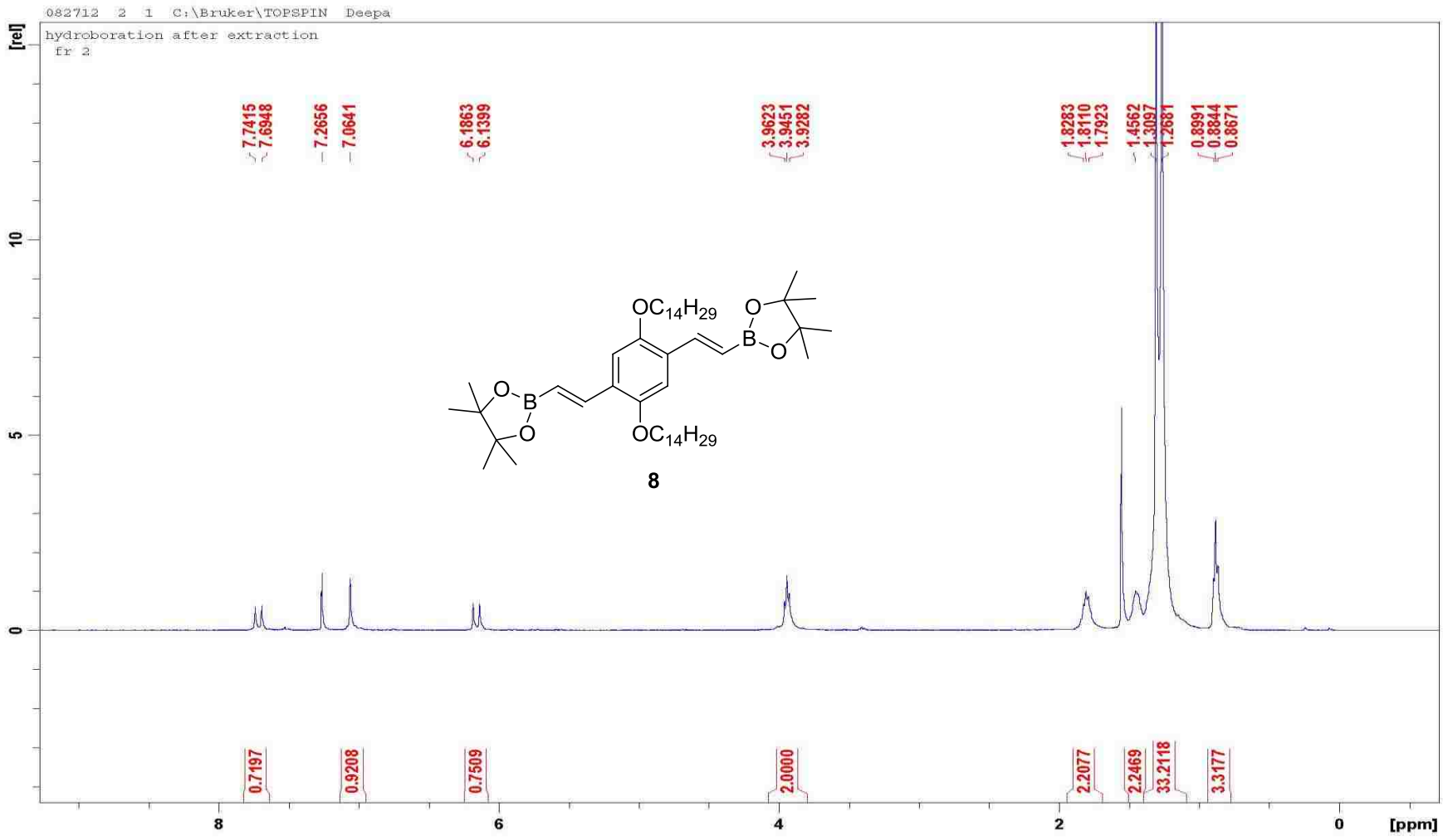
082712 2 1 C:\Bruker\TOPSPIN Deepa
hydroboration after extraction
fr 2
[rel]
7.7415
7.6948
7.2656
7.0641
6.1863
6.1399
3.9623
3.9451
3.9282
1.8283
1.8110
1.7923
1.4562
1.3097
1.2681
0.8991
0.8844
0.8671
0.7197
0.9208
0.7509
2.0000
2.2077
2.2469
33.2118
3.3177
[ppm]
OC14H29
OC14H29
B
O
8

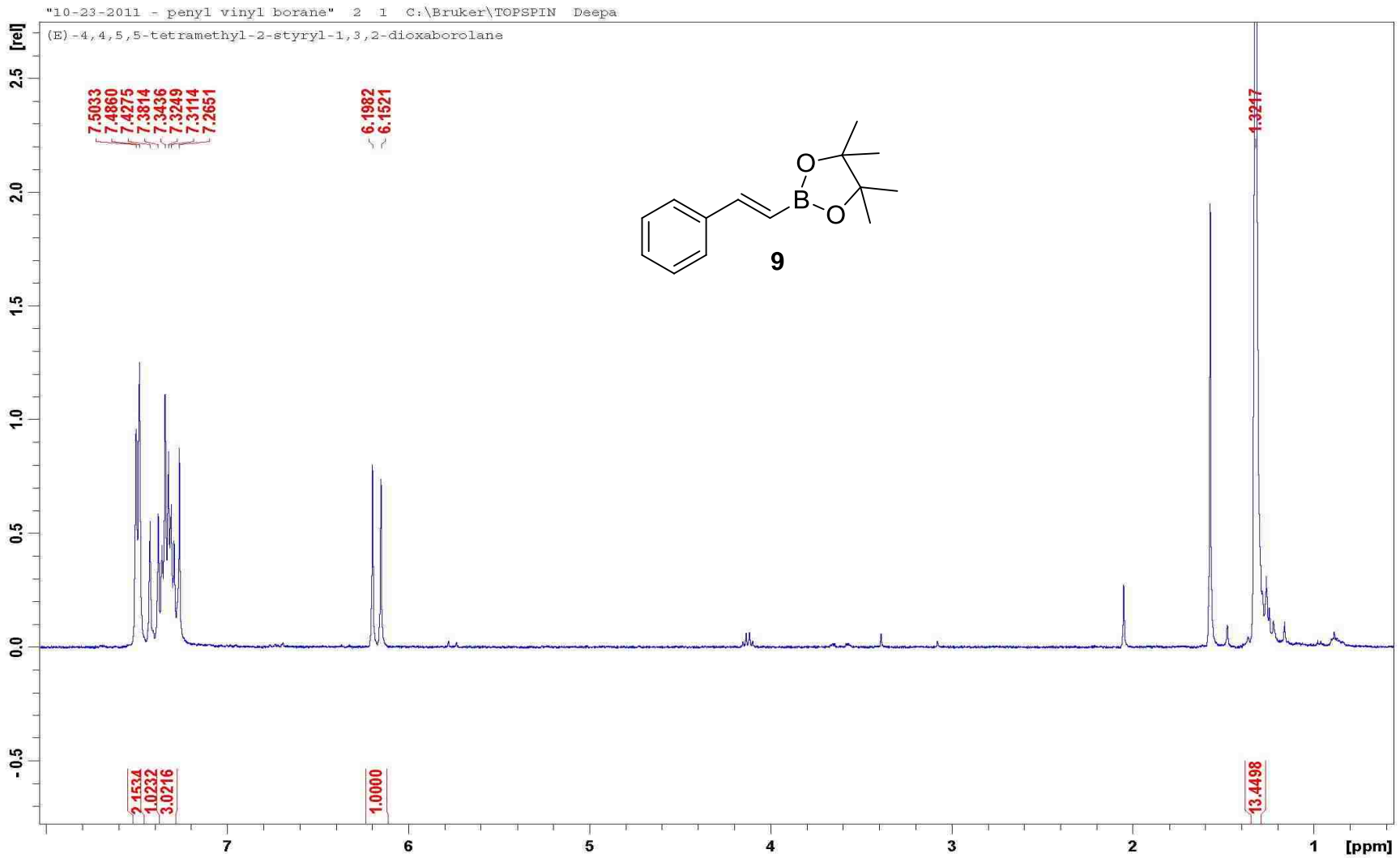
"10-23-2011 - penyl vinyl borane" 2 1 C:\Bruker\TOPSPIN Deepa
(E)-4,4,5,5-tetramethyl-2-styryl-1,3,2-dioxaborolane
7.5033
7.4860
7.4275
7.3814
7.3436
7.3249
7.3114
7.2651
6.1982
6.1521
1.3217
9
2.1534
1.0232
3.0216
1.0000
13.4498
[rel]
[ppm]

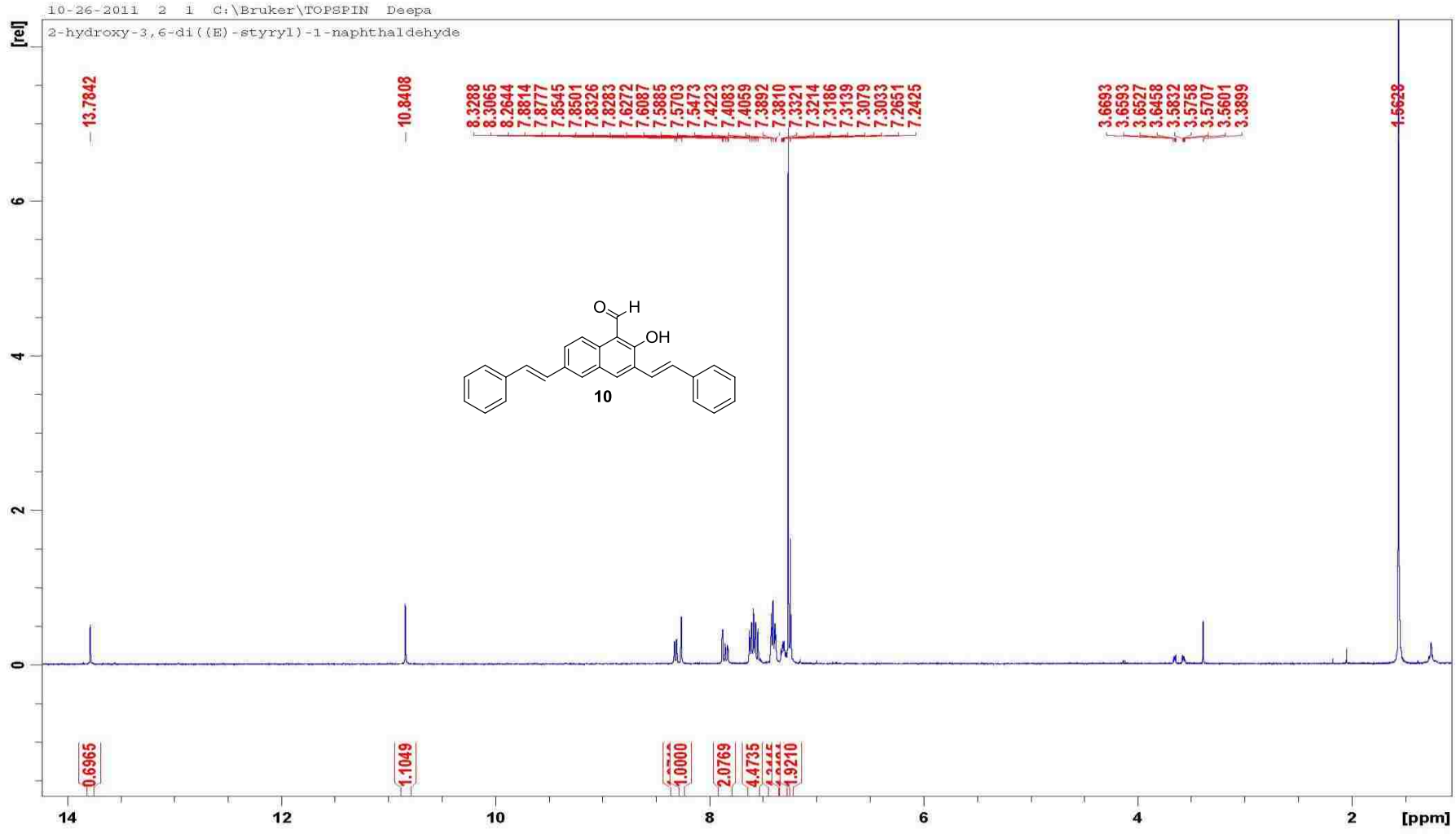
10-26-2011 2 1 C:\Bruker\TOPSPIN Deepa
2-hydroxy-3,6-di((E)-styryl)-1-naphthaldehyde
[rel]
13.7842
10.8408
8.3288
8.3065
8.2644
7.8814
7.8777
7.8545
7.8501
7.8326
7.8283
7.6272
7.6087
7.5885
7.5703
7.5473
7.4223
7.4083
7.4059
7.3892
7.3810
7.3321
7.3214
7.3186
7.3139
7.3079
7.3033
7.2651
7.2425
3.6693
3.6593
3.6527
3.6458
3.5832
3.5758
3.5707
3.5601
3.3899
1.5628
O
H
OH
10
0.6965
1.1049
1.0000
2.0769
4.4735
1.9210
14
12
10
8
6
4
2
[ppm]

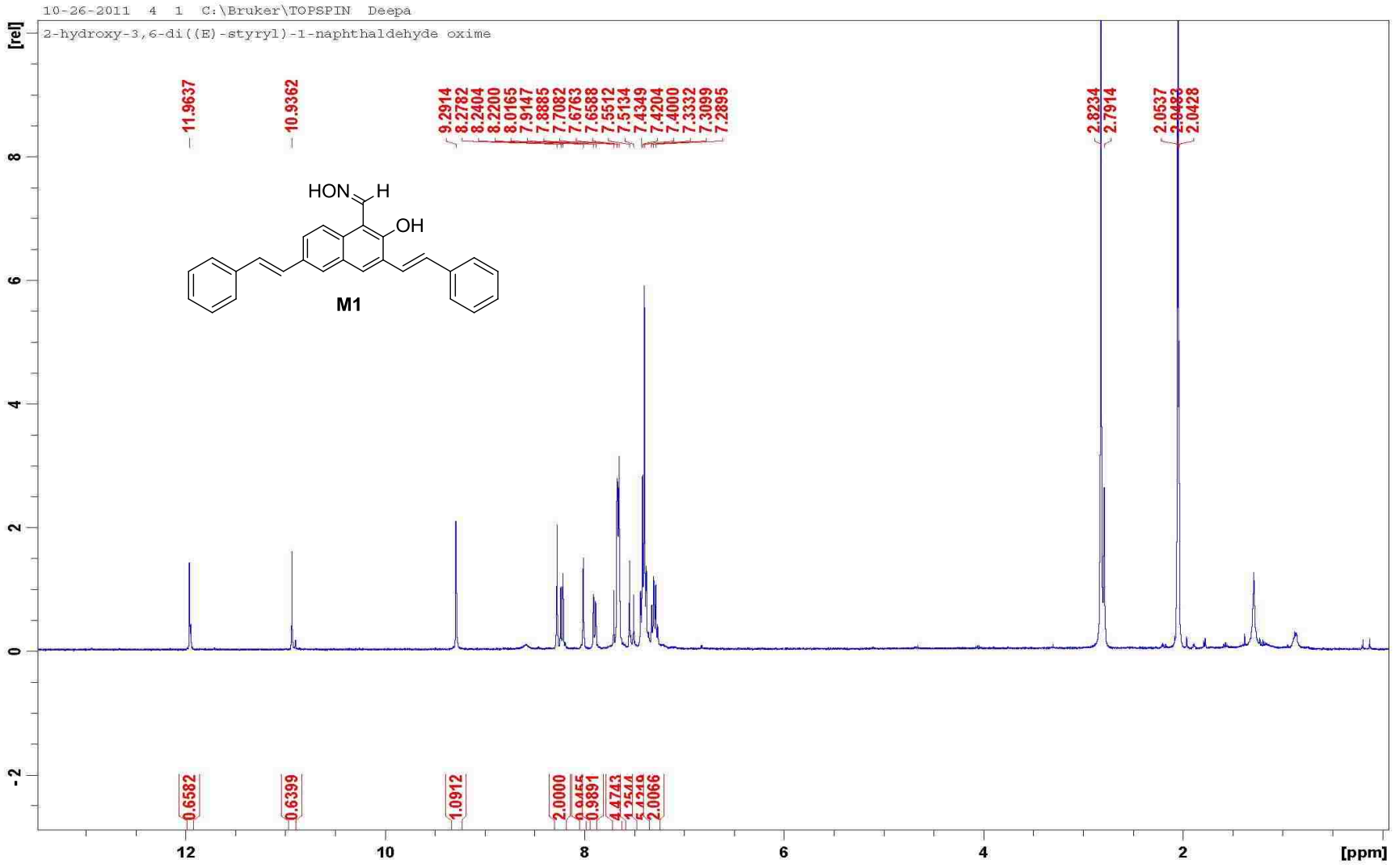
10-26-2011 4 1 C:\Bruker\TOPSPIN Deepa
2-hydroxy-3,6-di((E)-styryl)-1-naphthaldehyde oxime
11.9637
10.9362
9.2914
8.2782
8.2404
8.2200
8.0165
7.9147
7.8885
7.7082
7.6763
7.6588
7.5512
7.5134
7.4349
7.4204
7.4000
7.3332
7.3099
7.2895
2.8234
2.7914
2.0537
2.0428
HON
H
OH
M1
0.6582
0.6399
1.0912
2.0000
0.9891
4.4743
2.0066
[rel]
[ppm]

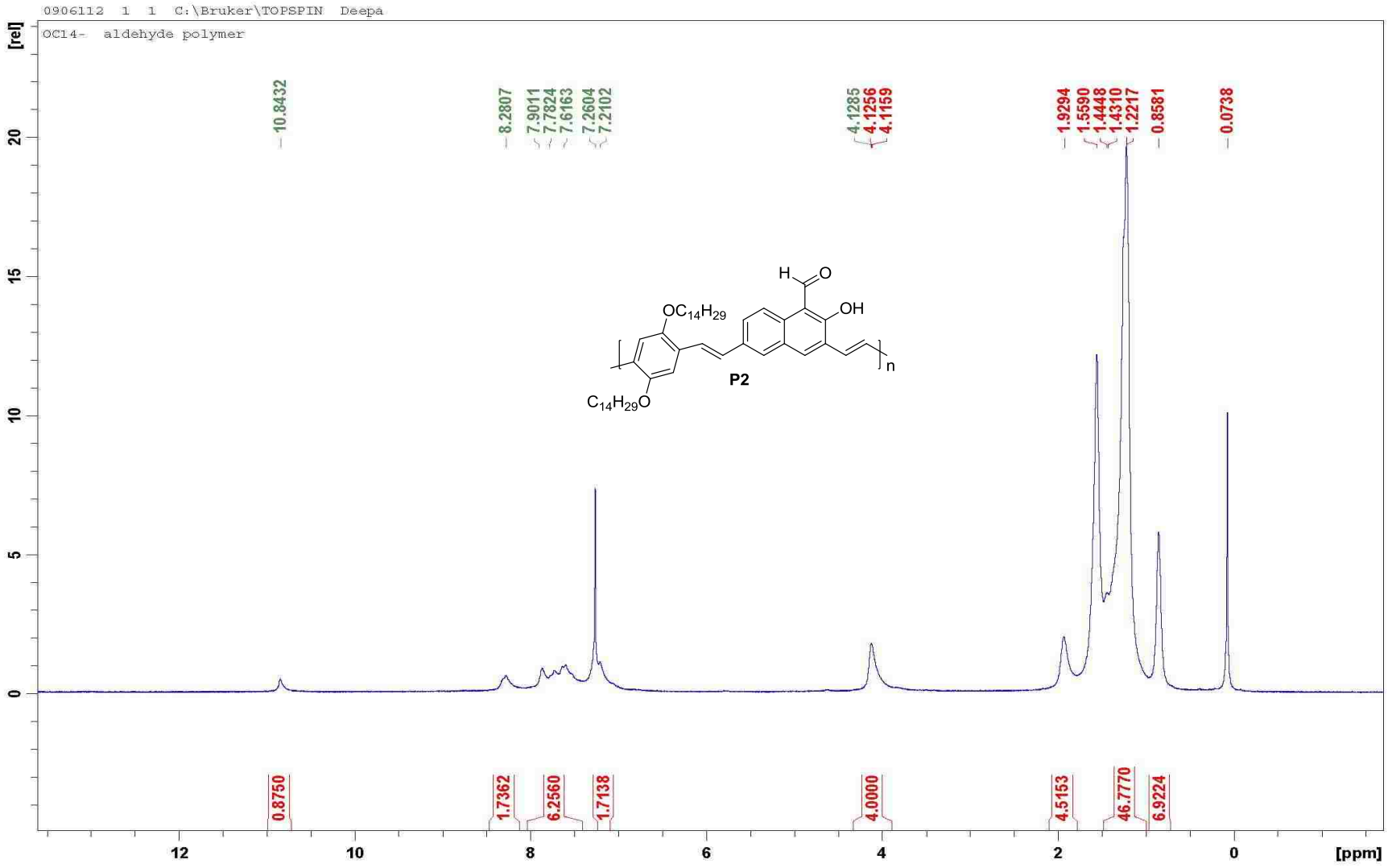
0906112 1 1 C:\Bruker\TOPSPIN Deepa
OC14- aldehyde polymer
[rel]
10.8432
8.2807
7.9011
7.7824
7.6163
7.2604
7.2102
4.1285
4.1256
4.1159
1.9294
1.5590
1.4448
1.4310
1.2217
0.8581
0.0738
H
O
OC14H29
OH
n
P2
C14H29O
0.8750
1.7362
6.2560
1.7138
4.0000
4.5153
46.7770
6.9224
[ppm]

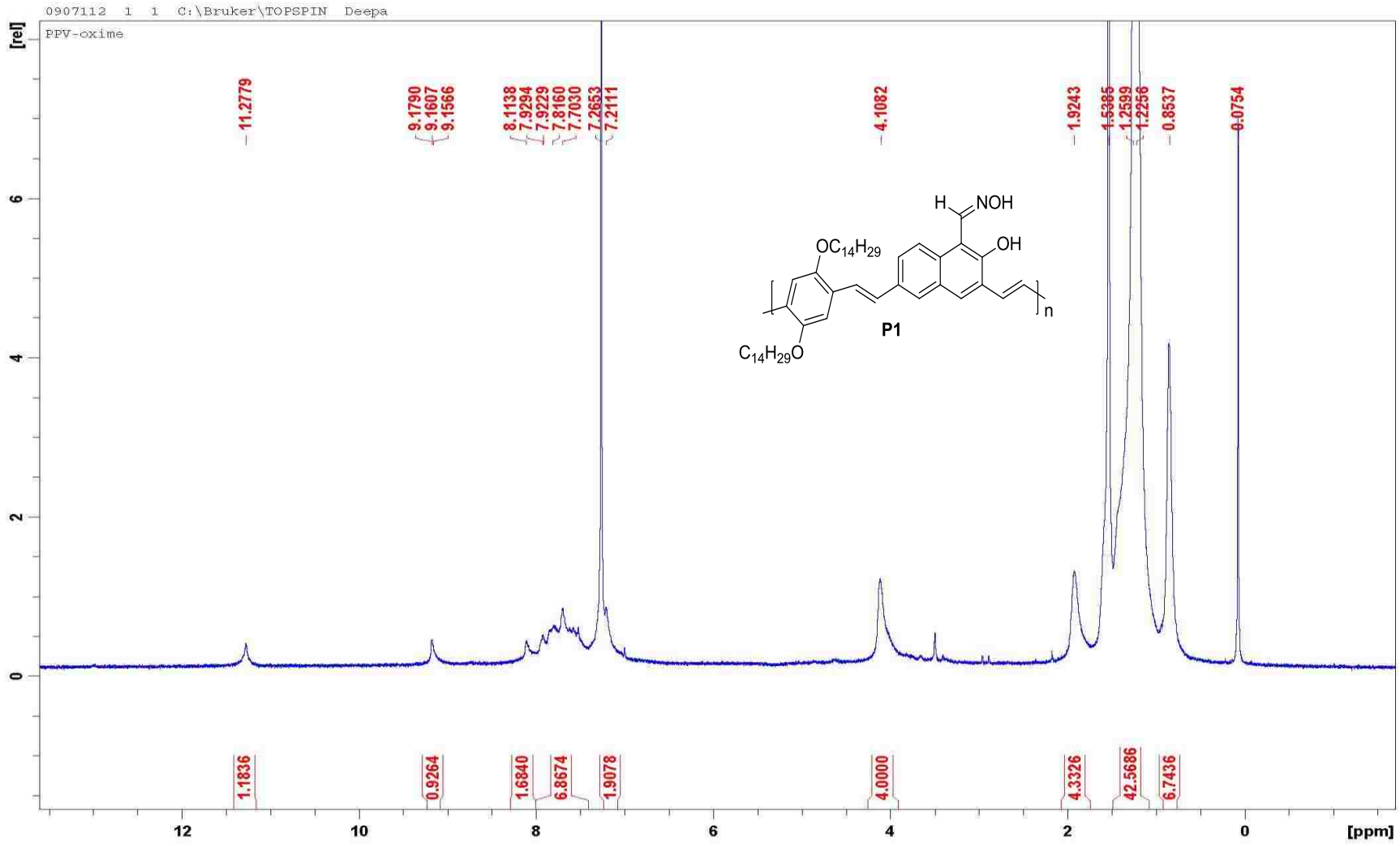
0907112 1 1 C:\Bruker\TOPSPIN Deepa
PPV-oxime
[rel]
11.2779
9.1790
9.1607
9.1566
8.1138
7.9294
7.9229
7.8160
7.7030
7.2653
7.2111
4.1082
1.9243
1.5385
1.2599
1.2256
0.8537
0.0754
H
NOH
OH
OC14H29
C14H29O
n
P1
1.1836
0.9264
1.6840
6.8674
1.9078
4.0000
4.3326
42.5686
6.7436
12
10
8
6
4
2
0
[ppm]

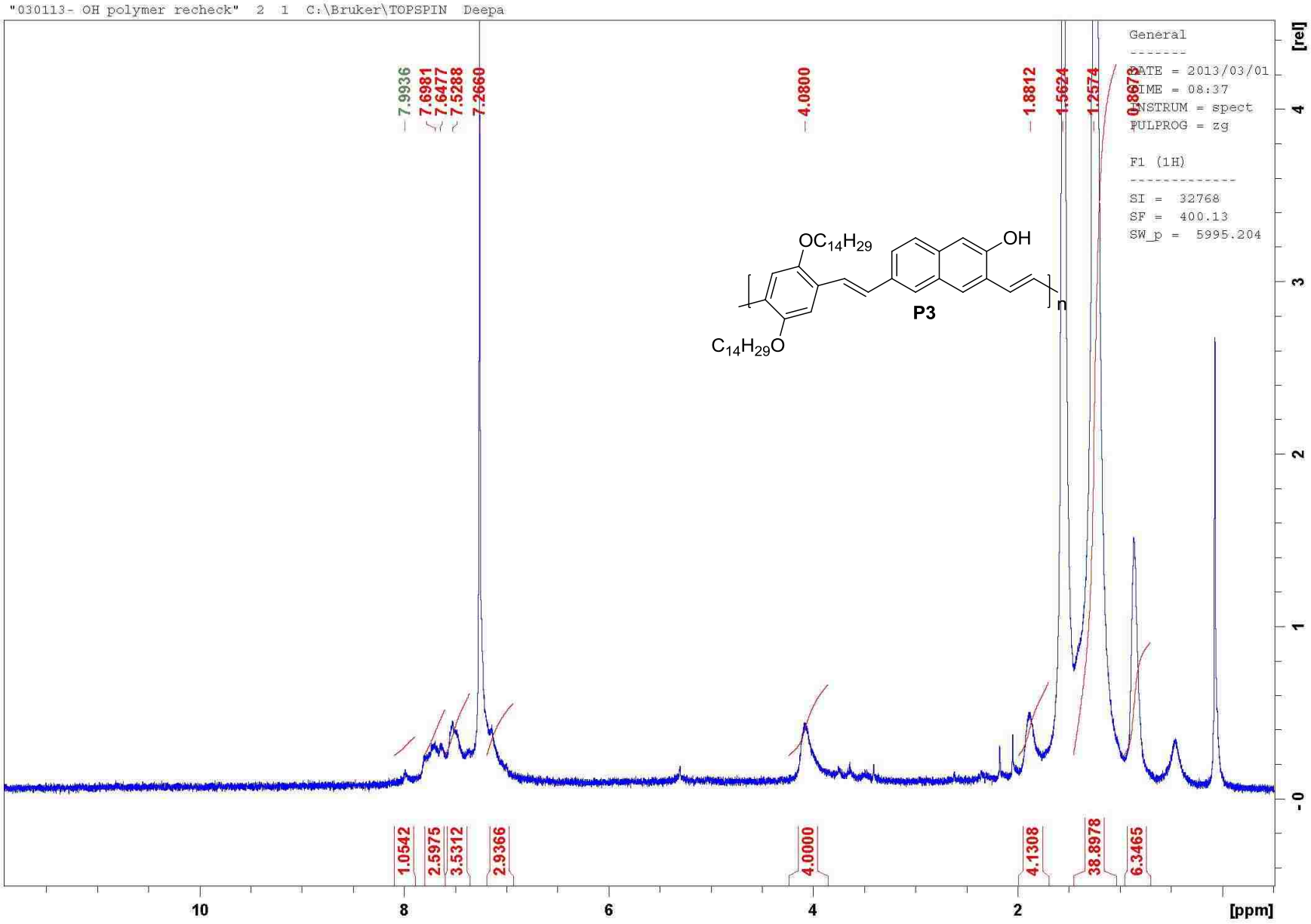
"030113- OH polymer recheck" 2 1 C:\Bruker\TOPSPIN Deepa
General
DATE = 2013/03/01
TIME = 08:37
INSTRUM = spect
PULPROG = zg
F1 (1H)
SI = 32768
SF = 400.13
SW_p = 5995.204
7.9936
7.6981
7.6477
7.5288
7.2660
4.0800
1.8812
1.5624
1.2574
0.8673
OC14H29
OH
C14H29O
n
P3
1.0542
2.5975
3.5312
2.9366
4.0000
4.1308
38.8978
6.3465
10
8
6
4
2
[ppm]
[rel]

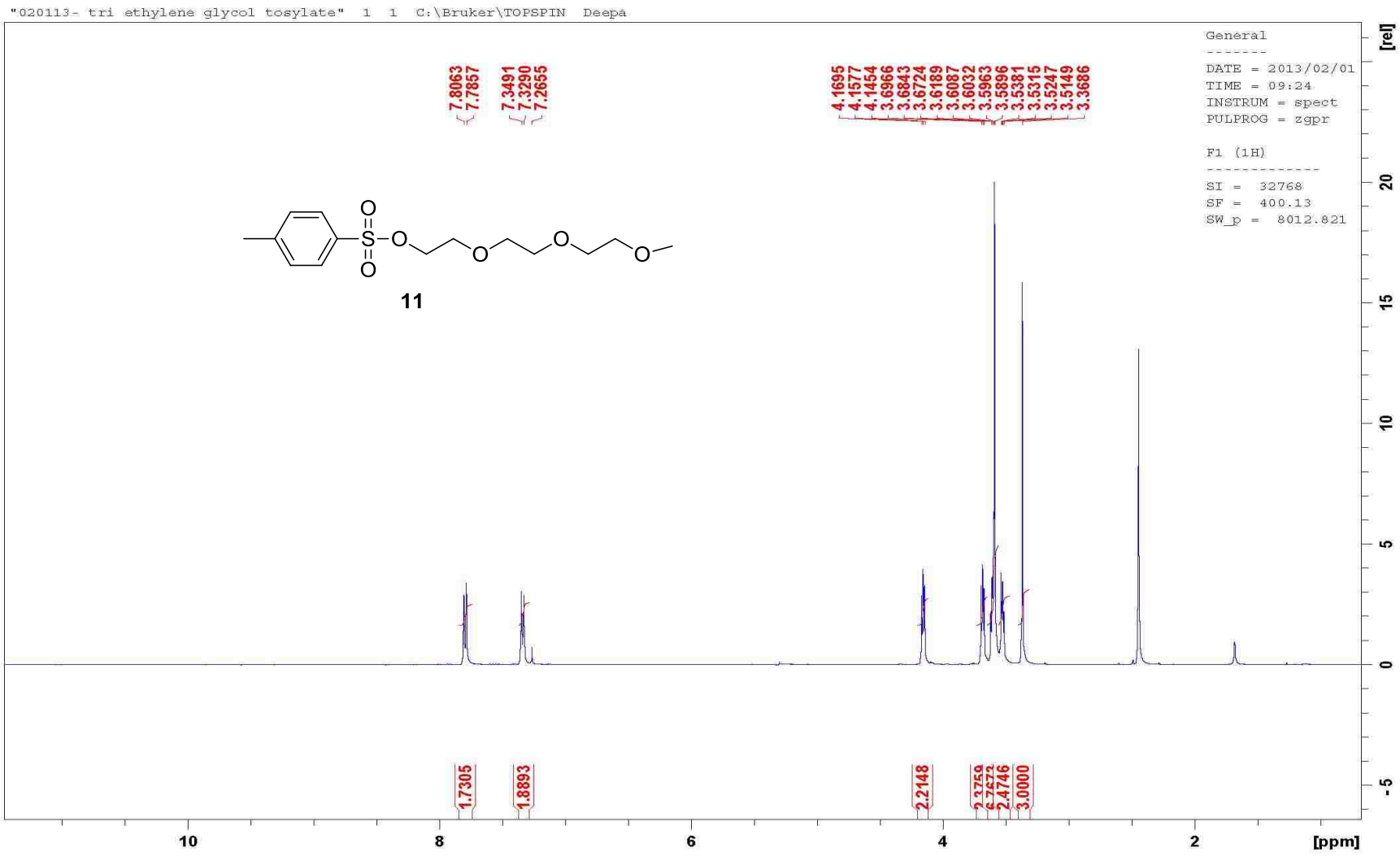
"020113- tri ethylene glycol tosylate" 1 1 C:\Bruker\TOPSPIN Deepa
General
DATE = 2013/02/01
TIME = 09:24
INSTRUM = spect
PULPROG = zgpr
F1 (1H)
SI = 32768
SF = 400.13
SW_p = 8012.821
7.8063
7.7857
7.3491
7.3290
7.2655
4.1695
4.1577
4.1454
3.6966
3.6843
3.6724
3.6189
3.6087
3.6032
3.5963
3.5896
3.5381
3.5315
3.5247
3.5149
3.3686
11
1.7305
1.8893
2.2148
2.3759
2.3672
2.4746
3.0000
[rel]
[ppm]

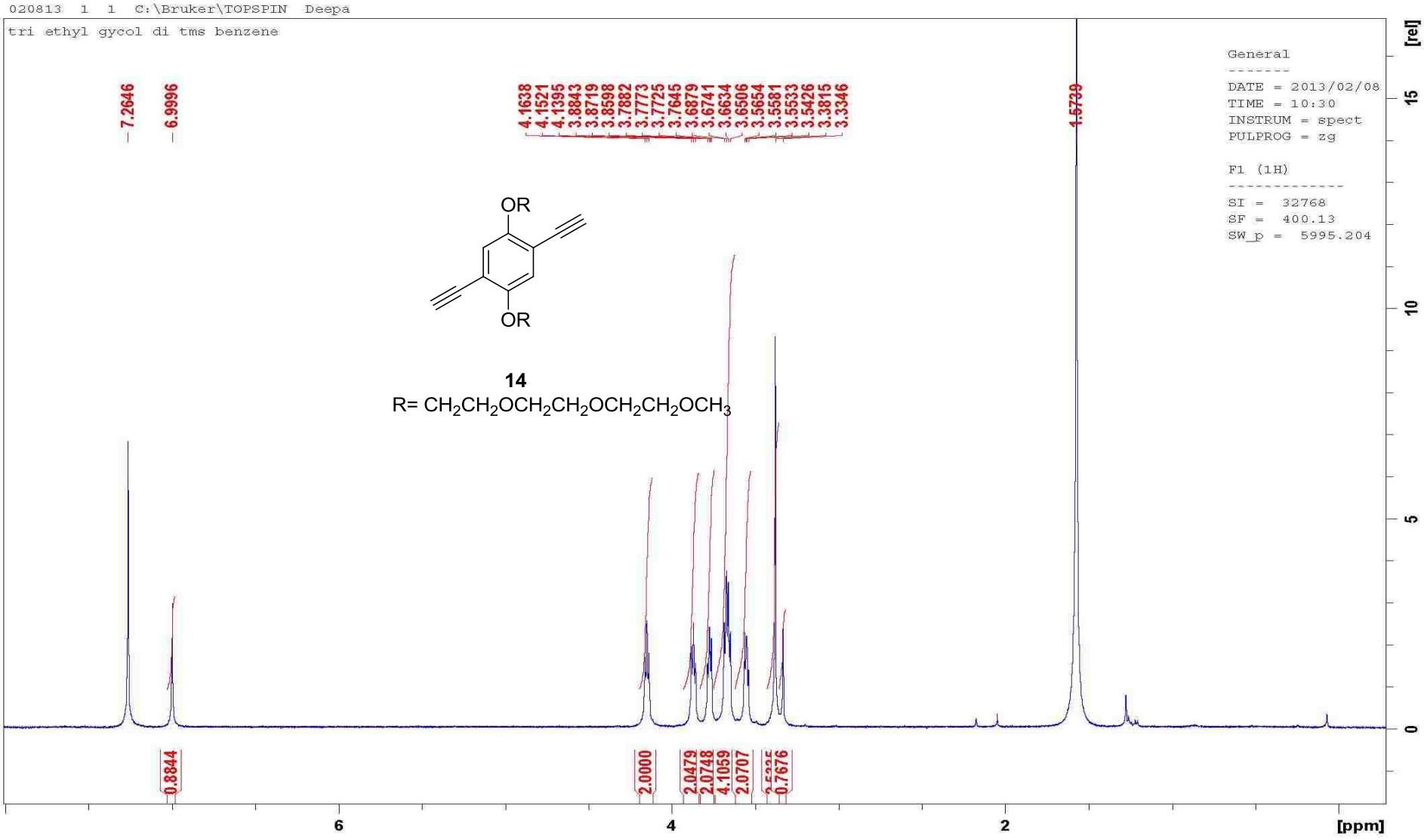
020813 1 1 C:\Bruker\TOPSPIN Deepa
tri ethyl gycol di tms benzene
7.2646
6.9996
4.1638
4.1521
4.1395
3.8843
3.8719
3.8598
3.7882
3.7773
3.7725
3.7645
3.6879
3.6741
3.6634
3.6506
3.5654
3.5581
3.5533
3.5426
3.3815
3.3346
1.5739
General
DATE = 2013/02/08
TIME = 10:30
INSTRUM = spect
PULPROG = zg
F1 (1H)
SI = 32768
SF = 400.13
SW_p = 5995.204
OR
OR
14
R= CH2CH2OCH2CH2OCH2CH2OCH3
0.8844
2.0000
2.0479
2.0748
4.1059
2.0707
0.7676
6
4
2
[ppm]
[rel]
15
10
5
0

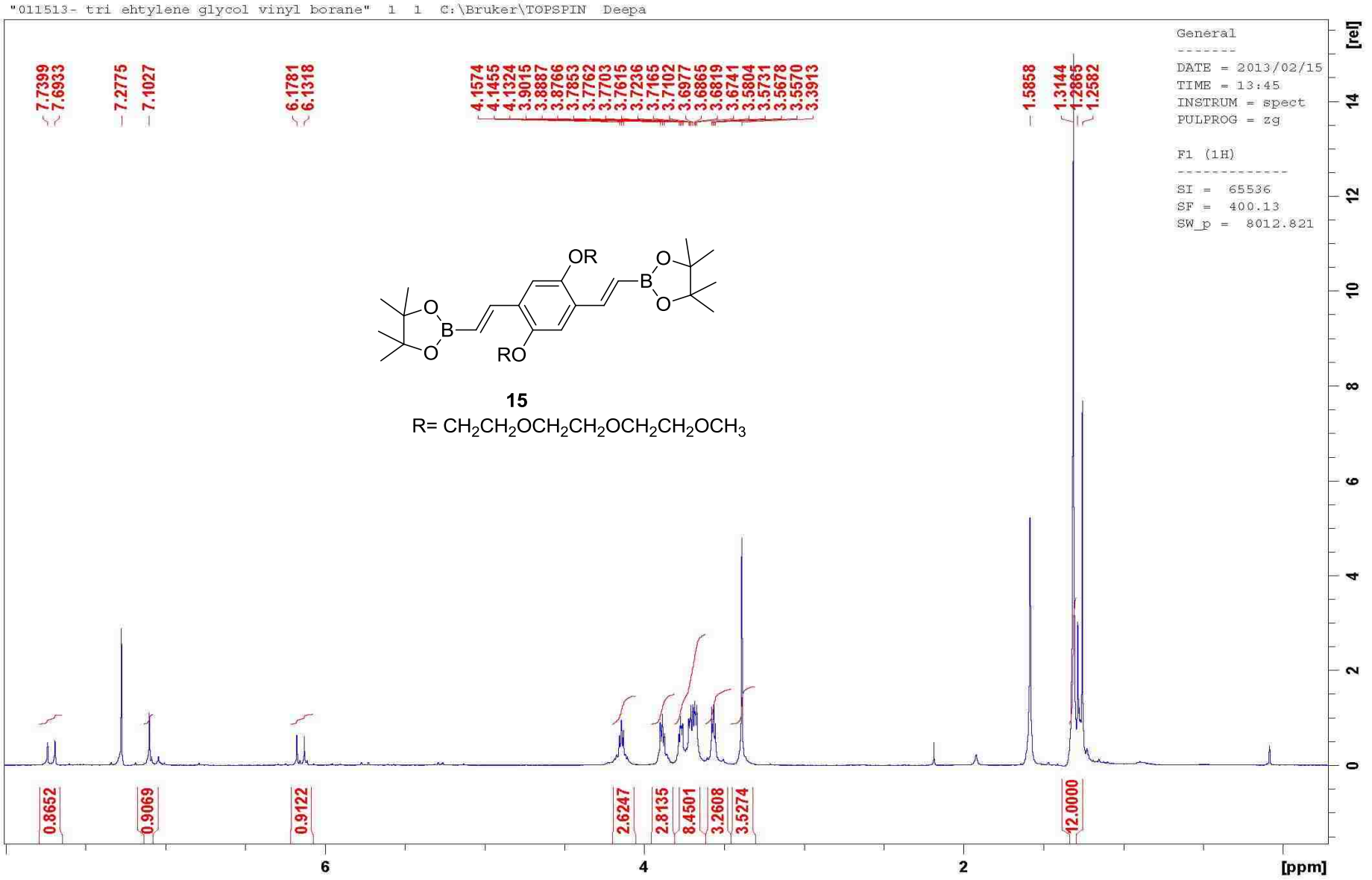

15

R= $CH_2CH_2OCH_2CH_2OCH_2CH_2OCH_3$

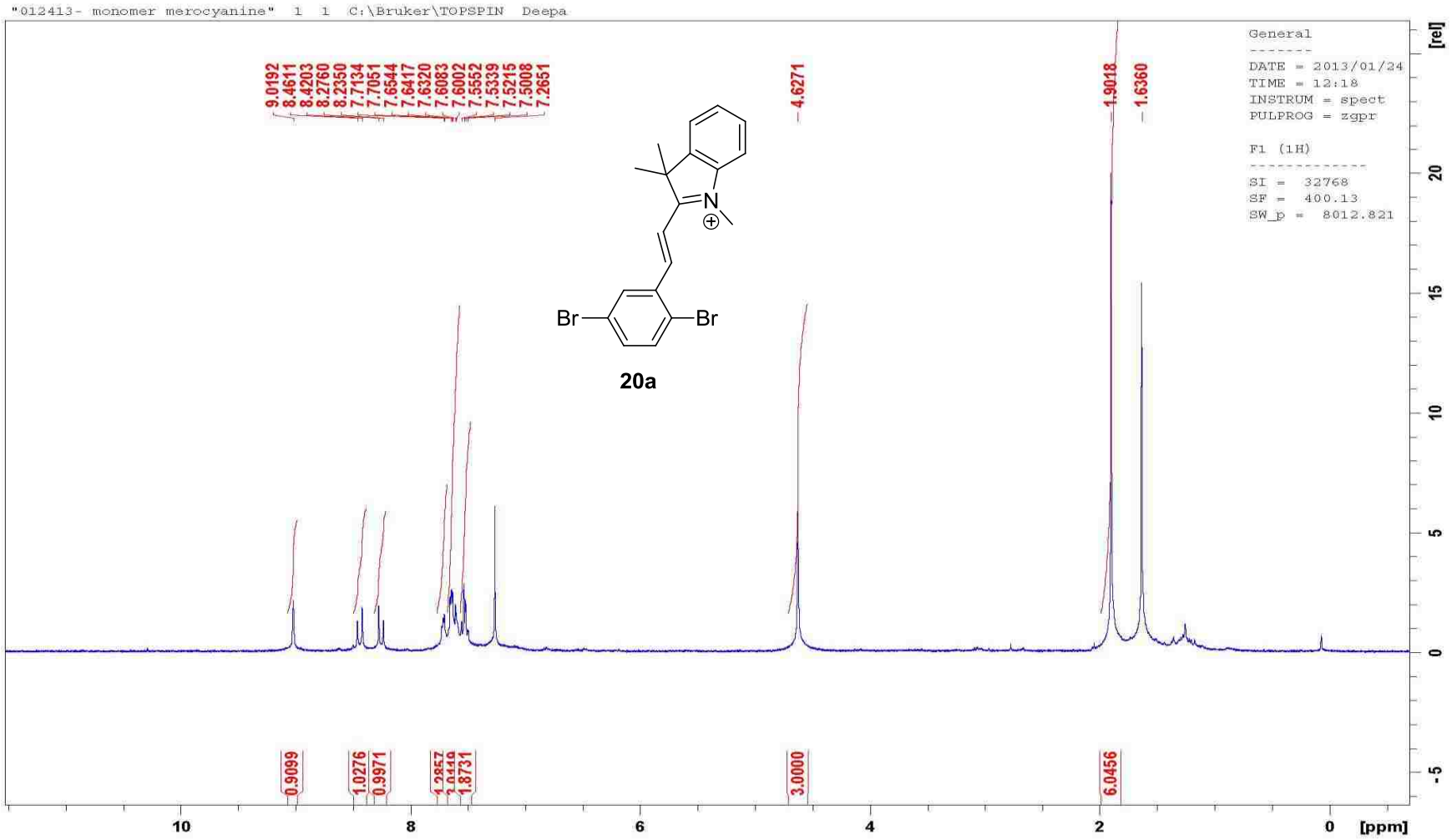
"012413- monomer merocyanine" 1 1 C:\Bruker\TOPSPIN Deepa
9.0192
8.4611
8.4203
8.2760
8.2350
7.7134
7.7051
7.6544
7.6417
7.6320
7.6083
7.6002
7.5552
7.5339
7.5215
7.5008
7.2651
4.6271
1.9018
1.6360
General
DATE = 2013/01/24
TIME = 12:18
INSTRUM = spect
PULPROG = zgpr
F1 (1H)
SI = 32768
SF = 400.13
SW_p = 8012.821
Br
Br
N
20a
0.9099
1.0276
0.9971
1.2857
2.0440
1.8731
3.0000
6.0456
10
8
6
4
2
0
[ppm]
[rel]
20
15
10
5
0
-5

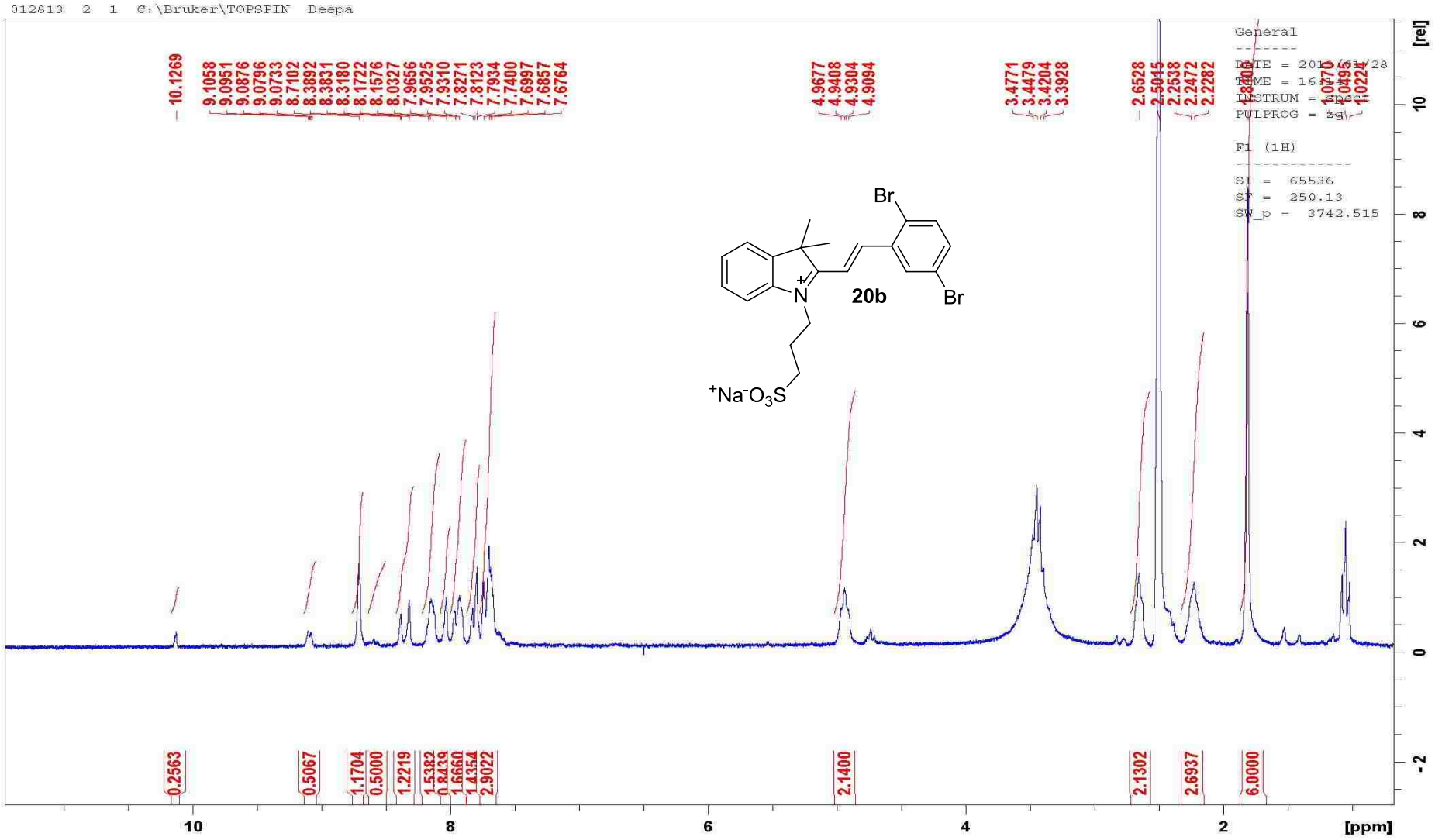
012813 2 1 C:\Bruker\TOPSPIN Deepa
General
F1 (1H)
SI = 65536
SF = 250.13
SW_p = 3742.515
Br
Br
20b
+Na-O3S
[ppm]
[rel]

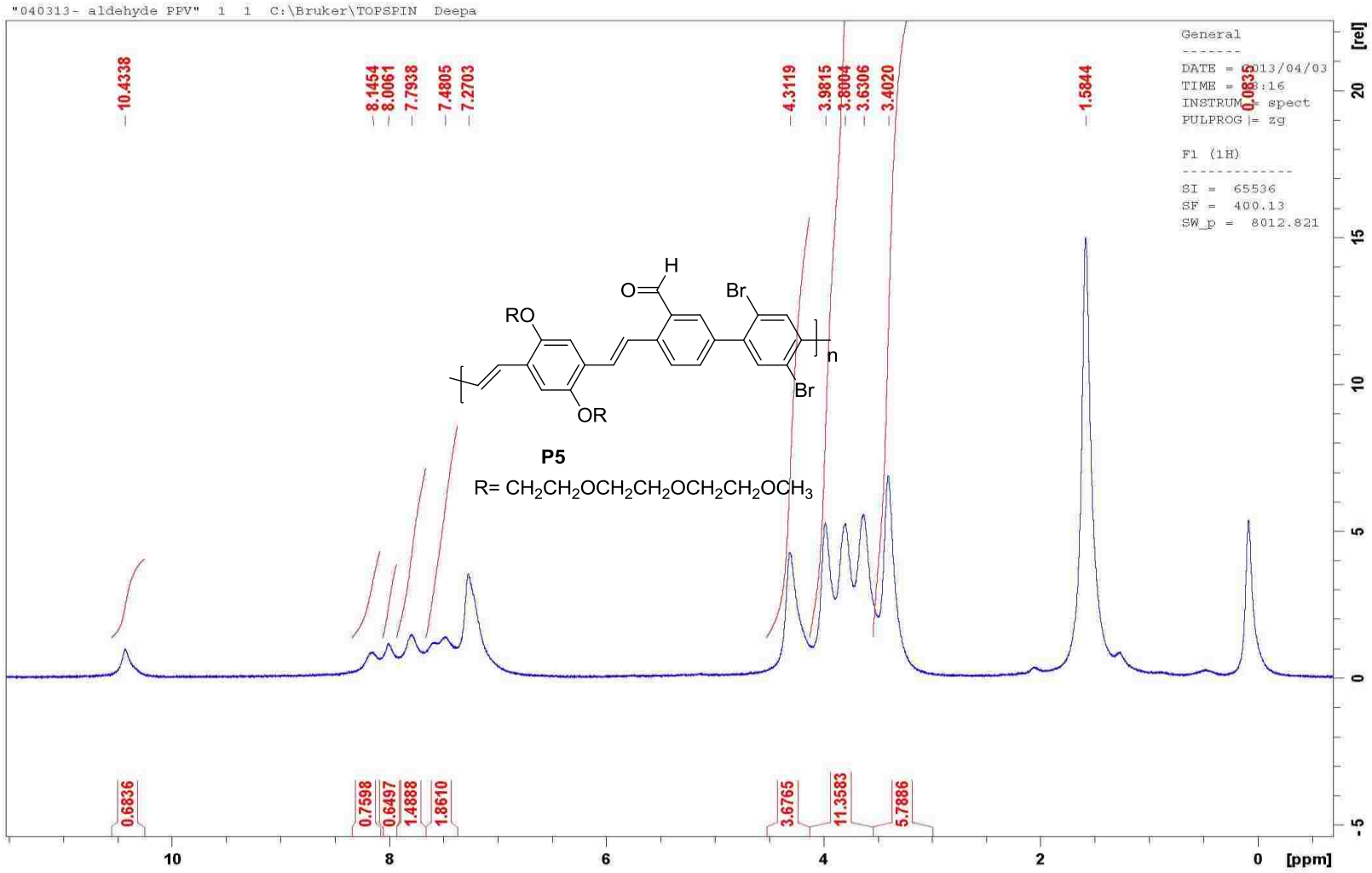
"040313- aldehyde PPV" 1 1 C:\Bruker\TOPSPIN Deepa
10.4338
8.1454
8.0061
7.7938
7.4805
7.2703
4.3119
3.9815
3.8004
3.6306
3.4020
1.5844
1.0836
General
DATE = 2013/04/03
TIME = 16:16
INSTRUM = spect
PULPROG = zg
F1 (1H)
SI = 65536
SF = 400.13
SW_p = 8012.821
H
O
Br
RO
n
Br
OR
P5
R= CH2CH2OCH2CH2OCH2CH2OCH3
0.6836
0.7598
0.6497
1.4888
1.8610
3.6765
11.3583
5.7886
10
8
6
4
2
0
[ppm]
[rel]
20
15
10
5
0
-5

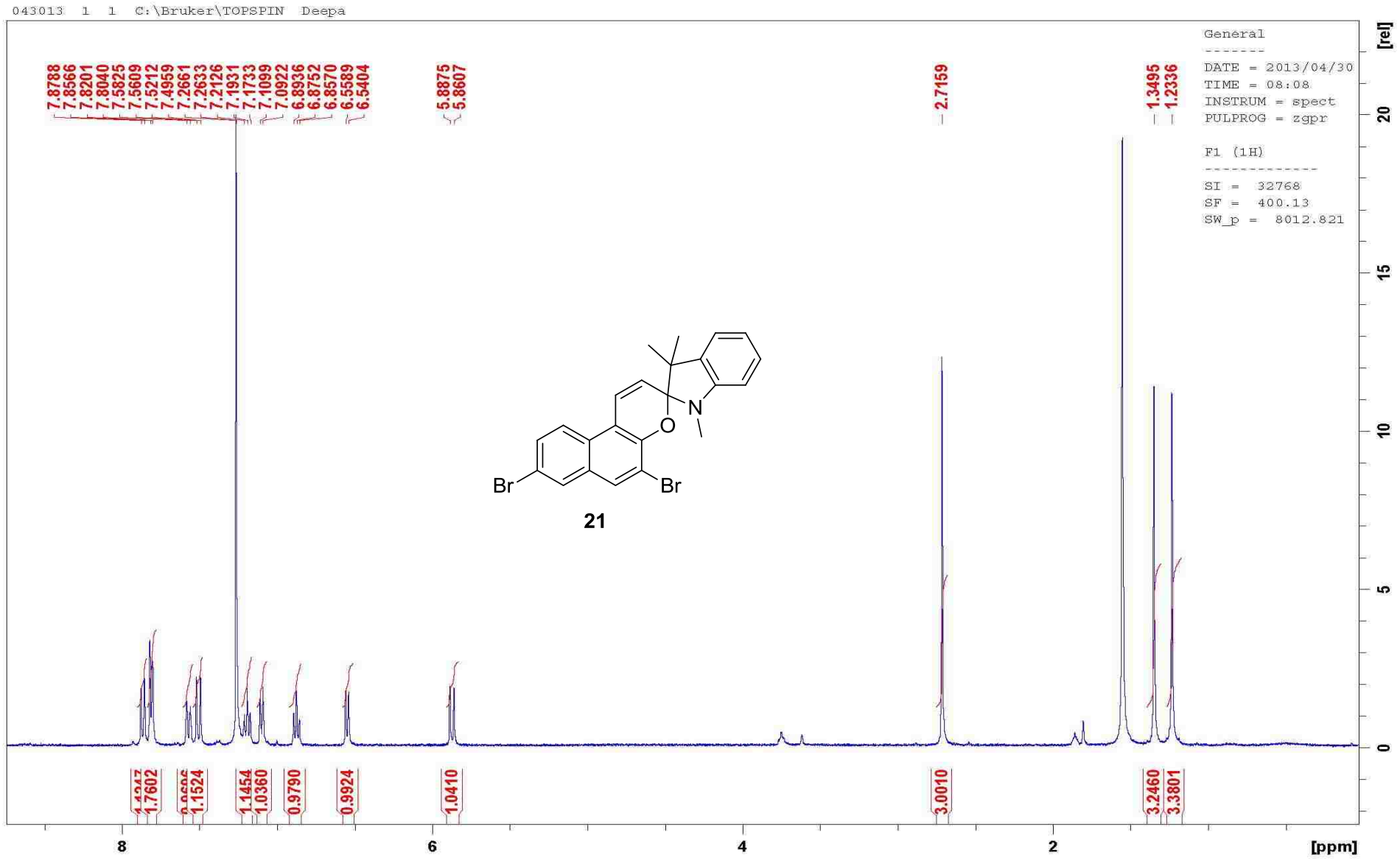
043013 1 1 C:\Bruker\TOPSPIN Deepa
7.8788
7.8566
7.8201
7.8040
7.5825
7.5609
7.5212
7.4959
7.2661
7.2633
7.2126
7.1931
7.1733
7.1099
7.0922
6.8936
6.8752
6.8570
6.5589
6.5404
5.8875
5.8607
2.7159
1.3495
1.2336
General
DATE = 2013/04/30
TIME = 08:08
INSTRUM = spect
PULPROG = zgpr
F1 (1H)
SI = 32768
SF = 400.13
SW_p = 8012.821
Br
Br
O
N
21
1.7602
1.1524
1.1454
1.0360
0.9790
0.9924
1.0410
3.0010
3.2460
3.3801
8
6
4
2
[ppm]
[rel]

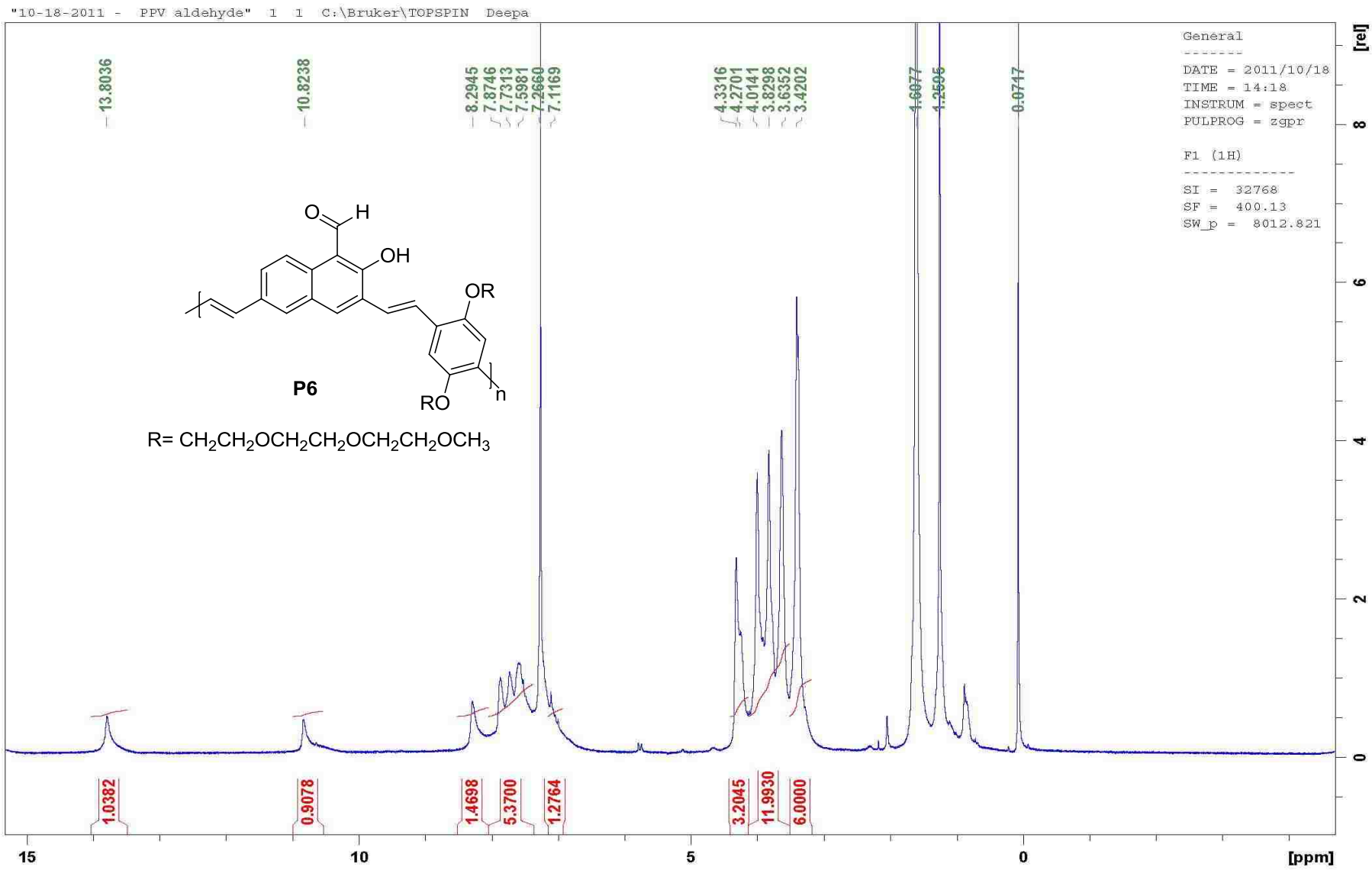
"10-18-2011 - PPV aldehyde" 1 1 C:\Bruker\TOPSPIN Deepa
13.8036
10.8238
8.2945
7.8746
7.7313
7.5981
7.2660
7.1169
4.3316
4.2701
4.0141
3.8298
3.6352
3.4202
1.6077
1.2595
0.0747
General
DATE = 2011/10/18
TIME = 14:18
INSTRUM = spect
PULPROG = zgpr
F1 (1H)
SI = 32768
SF = 400.13
SW_p = 8012.821
O
H
OH
OR
RO
n
P6
R= CH2CH2OCH2CH2OCH2CH2OCH3
1.0382
0.9078
1.4698
5.3700
1.2764
3.2045
11.9930
6.0000
15
10
5
0
[ppm]
[rel]

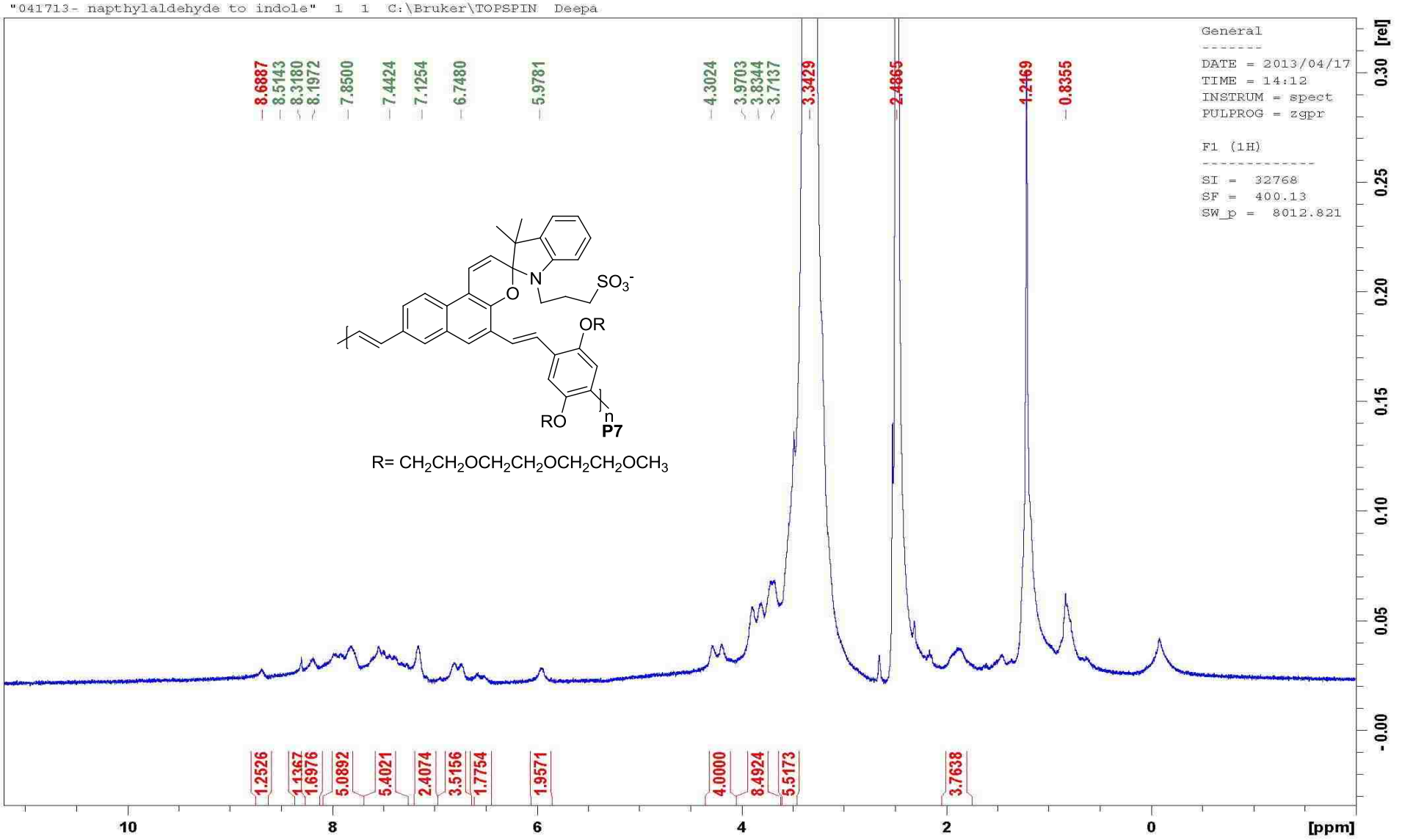
"041713- napthylaldehyde to indole" 1 1 C:\Bruker\TOPSPIN Deepa
General
DATE = 2013/04/17
TIME = 14:12
INSTRUM = spect
PULPROG = zgpr
F1 (1H)
SI = 32768
SF = 400.13
SW_p = 8012.821
8.6887
8.5143
8.3180
8.1972
7.8500
7.4424
7.1254
6.7480
5.9781
4.3024
3.9703
3.8344
3.7137
3.3429
2.4865
1.2469
0.8355
1.2526
1.1367
1.6976
5.0892
5.4021
2.4074
3.5156
1.7754
1.9571
4.0000
8.4924
5.5173
3.7638
10
8
6
4
2
0
[ppm]
0.30
0.25
0.20
0.15
0.10
0.05
-0.00
[rel]
N
O
SO3-
OR
RO
n
P7
R= CH2CH2OCH2CH2OCH2CH2OCH3

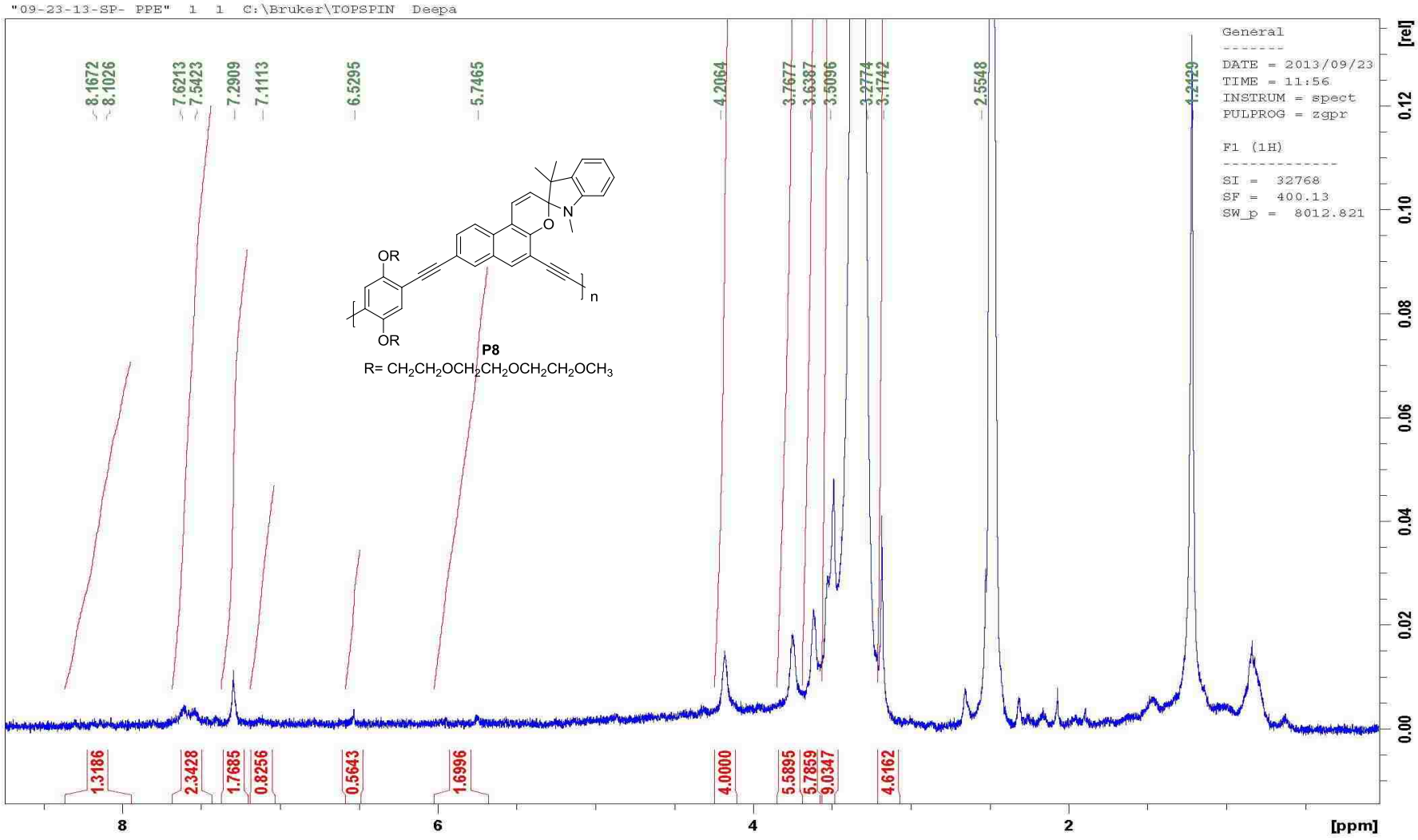
"09-23-13-SP- PPE" 1 1 C:\Bruker\TOPSPIN Deepa
8.1672
8.1026
7.6213
7.5423
7.2909
7.1113
6.5295
5.7465
4.2064
3.7677
3.6387
3.5096
3.2774
3.1742
2.5548
1.2429
General
DATE = 2013/09/23
TIME = 11:56
INSTRUM = spect
PULPROG = zgpr
F1 (1H)
SI = 32768
SF = 400.13
SW_p = 8012.821
OR
OR
n
P8
R= CH2CH2OCH2CH2OCH2CH2OCH3
1.3186
2.3428
1.7685
0.8256
0.5643
1.6996
4.0000
5.5895
5.7859
9.0347
4.6162
8
6
4
2
[ppm]
[rel]
0.00
0.02
0.04
0.06
0.08
0.10
0.12

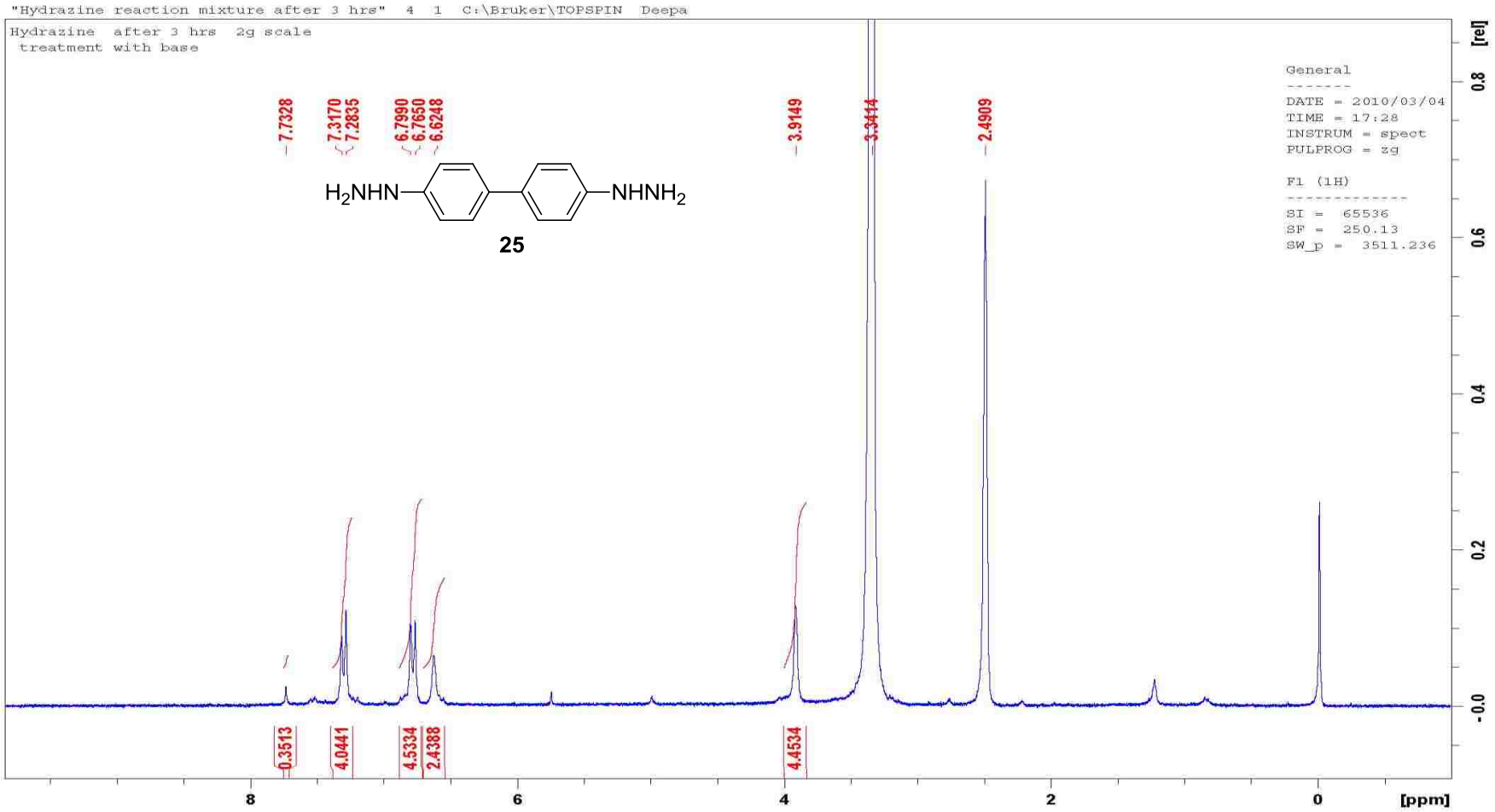
"Hydrazine reaction mixture after 3 hrs" 4 1 C:\Bruker\TOPSPIN Deepa
Hydrazine after 3 hrs 2g scale
treatment with base
7.7328
7.3170
7.2835
6.7990
6.7650
6.6248
3.9149
3.3414
2.4909
H2NHN
NHNH2
25
General
DATE = 2010/03/04
TIME = 17:28
INSTRUM = spect
PULPROG = zg
F1 (1H)
SI = 65536
SF = 250.13
SW_p = 3511.236
0.3513
4.0441
4.5334
2.4388
4.4534
8
6
4
2
0
[ppm]
0.8
0.6
0.4
0.2
-0.0
[rel]

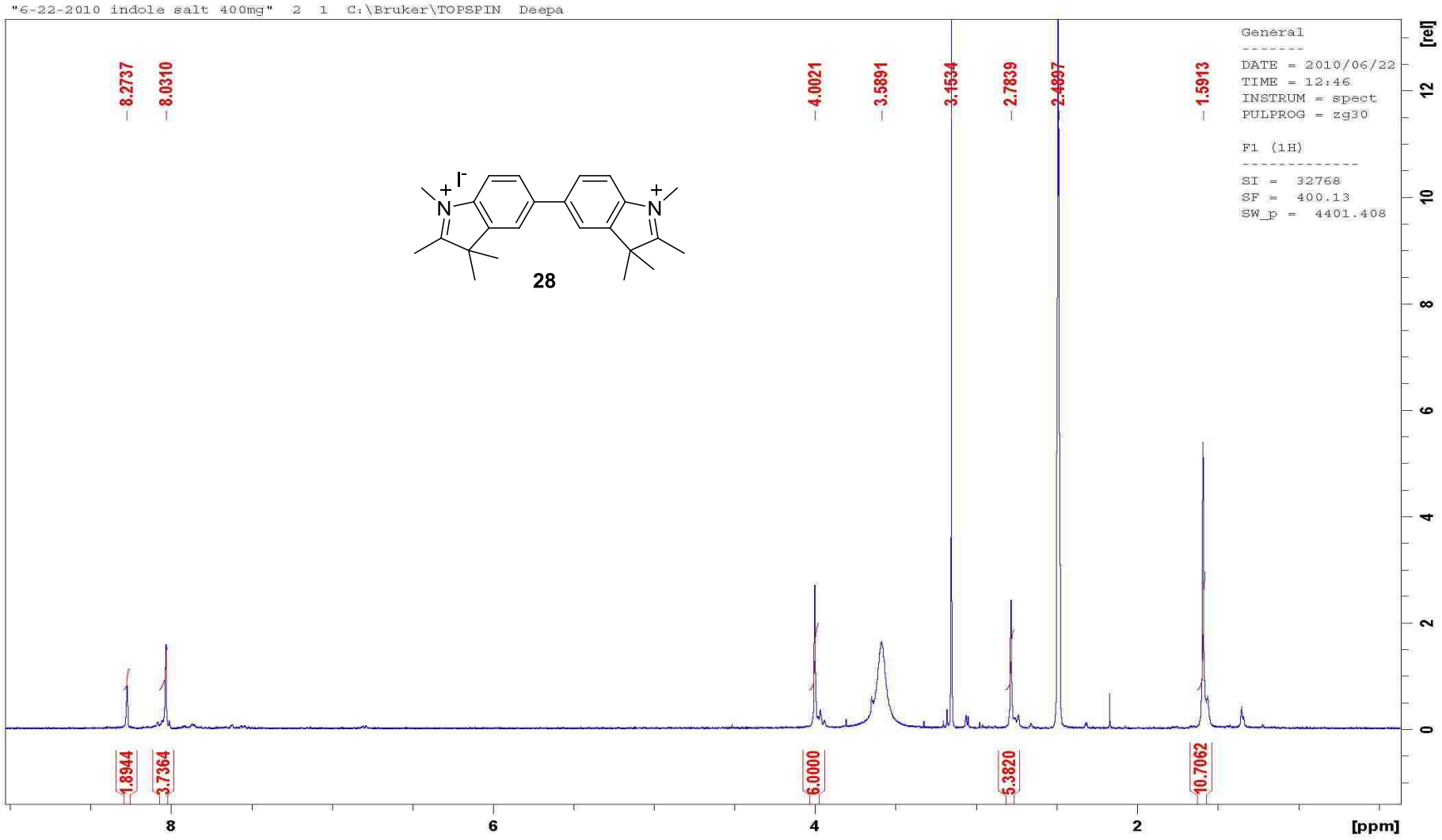
"6-22-2010 indole salt 400mg" 2 1 C:\Bruker\TOPSPIN Deepa
8.2737
8.0310
4.0021
3.5891
3.4534
2.7839
2.4807
1.5913
General
DATE = 2010/06/22
TIME = 12:46
INSTRUM = spect
PULPROG = zg30
F1 (1H)
SI = 32768
SF = 400.13
SW_p = 4401.408
28
1.8944
3.7364
6.0000
5.3820
10.7062
[ppm]
[rel]

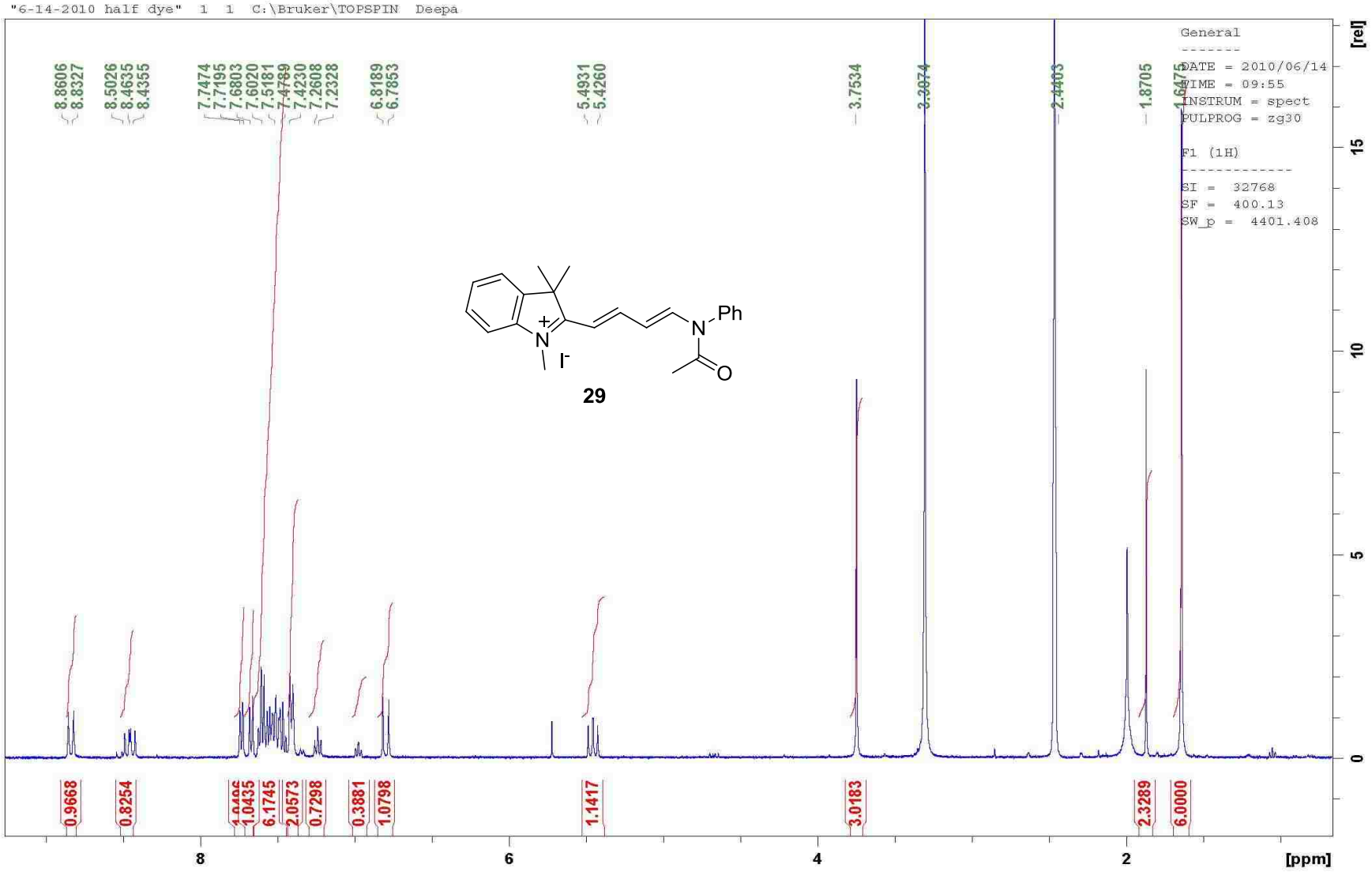
"6-14-2010 half dye" 1 1 C:\Bruker\TOPSPIN Deepa
General
DATE = 2010/06/14
TIME = 09:55
INSTRUM = spect
PULPROG = zg30
F1 (1H)
SI = 32768
SF = 400.13
SW_p = 4401.408
8.8606
8.8327
8.5026
8.4635
8.4355
7.7474
7.7195
7.6803
7.6020
7.5181
7.4789
7.4230
7.2608
7.2328
6.8189
6.7853
5.4931
5.4260
3.7534
3.3074
2.4403
1.8705
1.6475
0.9668
0.8254
1.0435
6.1745
2.0573
0.7298
0.3881
1.0798
1.1417
3.0183
2.3289
6.0000
[rel]
[ppm]
Ph
N
O
I-

29

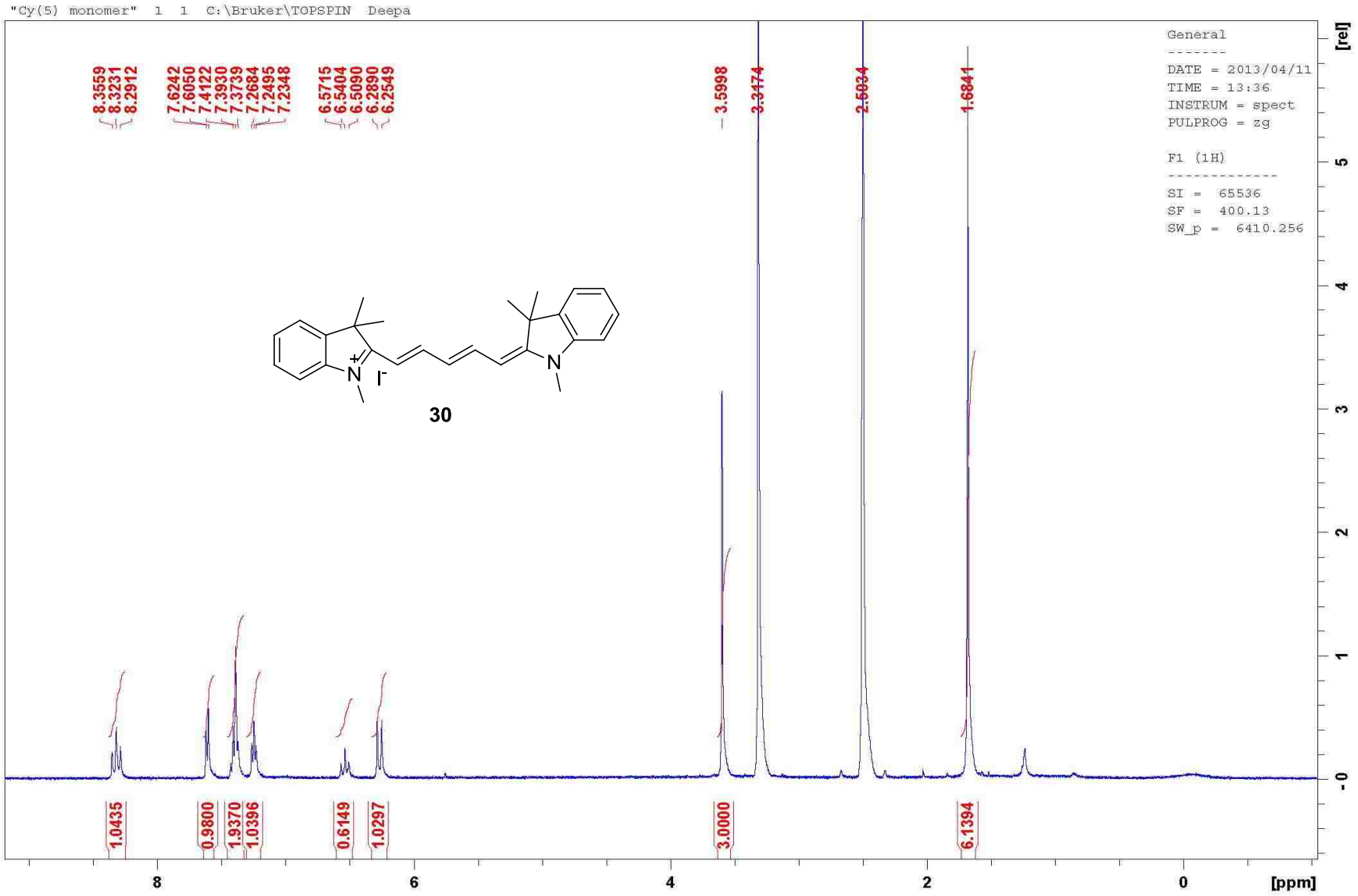
"Cy(5) monomer" 1 1 C:\Bruker\TOPSPIN Deepa
8.3559
8.3231
8.2912
7.6242
7.6050
7.4122
7.3930
7.3739
7.2684
7.2495
7.2348
6.5715
6.5404
6.5090
6.2890
6.2549
3.5998
3.3474
2.5034
1.6841
General
DATE = 2013/04/11
TIME = 13:36
INSTRUM = spect
PULPROG = zg
F1 (1H)
SI = 65536
SF = 400.13
SW_p = 6410.256
[rel]
1.0435
0.9800
1.9370
1.0396
0.6149
1.0297
3.0000
6.1394
8
6
4
2
0
[ppm]

30

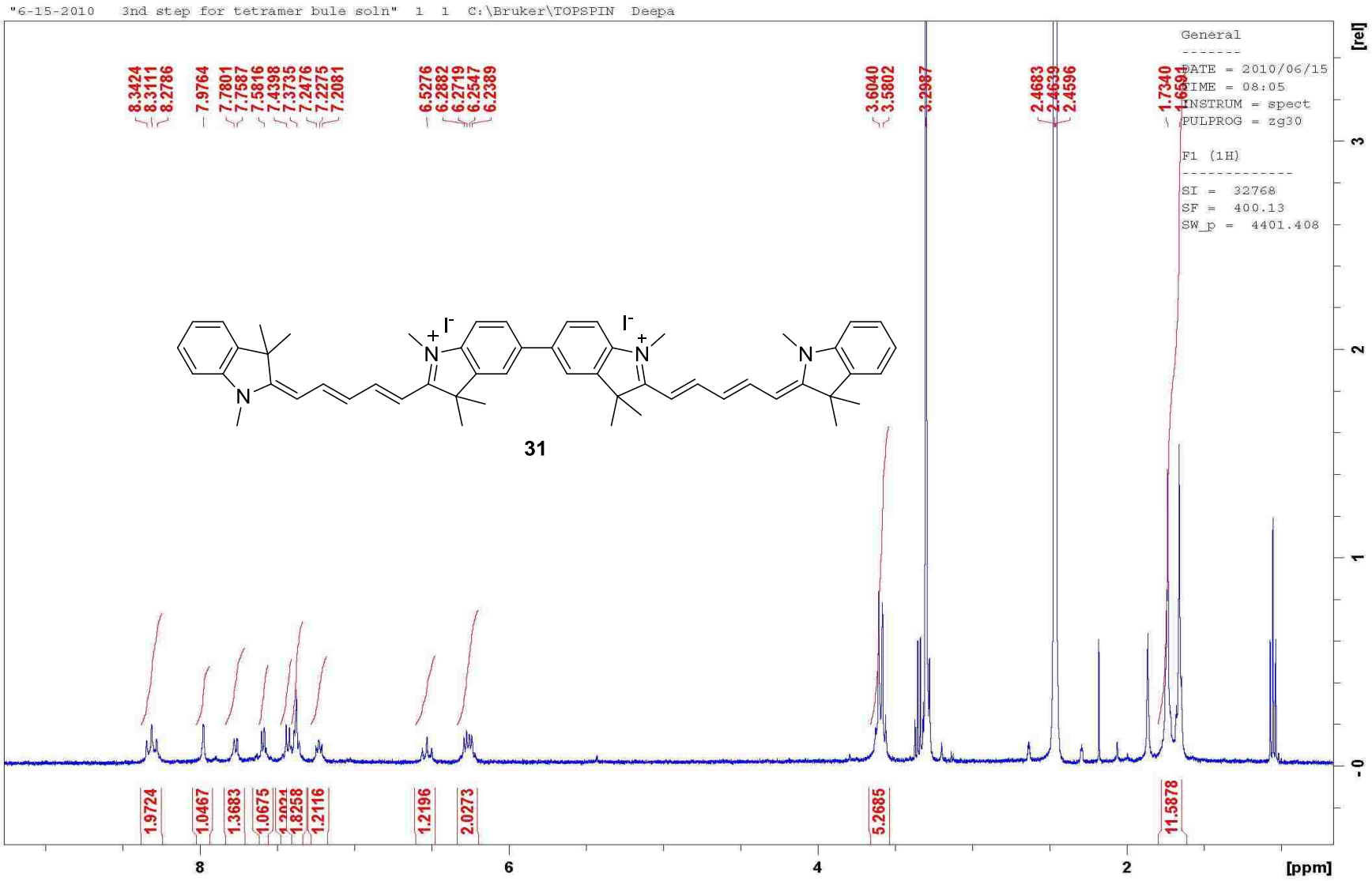
"6-15-2010 3nd step for tetramer bule soln" 1 1 C:\Bruker\TOPSPIN Deepa
General
DATE = 2010/06/15
TIME = 08:05
INSTRUM = spect
PULPROG = zg30
F1 (1H)
SI = 32768
SF = 400.13
SW_p = 4401.408
8.3424
8.3111
8.2786
7.9764
7.7801
7.7587
7.5816
7.4398
7.3735
7.2476
7.2275
7.2081
6.5276
6.2882
6.2719
6.2547
6.2389
3.6040
3.5802
3.2987
2.4683
2.4639
2.4596
1.7340
1.6594
1.9724
1.0467
1.3683
1.0675
1.2021
1.8258
1.2116
1.2196
2.0273
5.2685
11.5878
[rel]
[ppm]
31

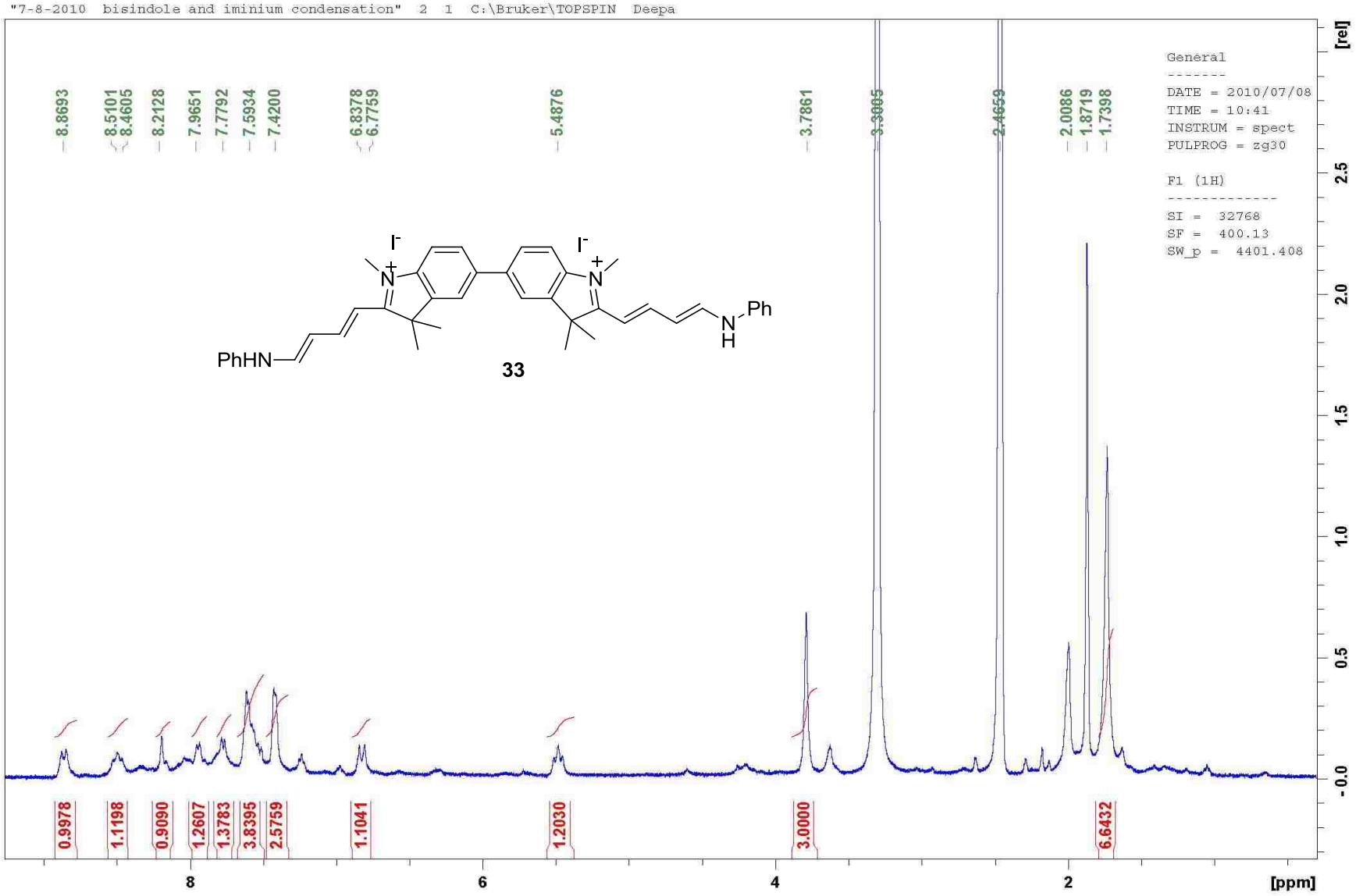
"7-8-2010 bisindole and iminium condensation" 2 1 C:\Bruker\TOPSPIN Deepa
8.8693
8.5101
8.4605
8.2128
7.9651
7.7792
7.5934
7.4200
6.8378
6.7759
5.4876
3.7861
3.3005
2.4659
2.0086
1.8719
1.7398
General
DATE = 2010/07/08
TIME = 10:41
INSTRUM = spect
PULPROG = zg30
F1 (1H)
SI = 32768
SF = 400.13
SW_p = 4401.408
PhHN
Ph
N
H
33
0.9978
1.1198
0.9090
1.2607
1.3783
3.8395
2.5759
1.1041
1.2030
3.0000
6.6432
8
6
4
2
[ppm]
[rel]
2.5
2.0
1.5
1.0
0.5
-0.0

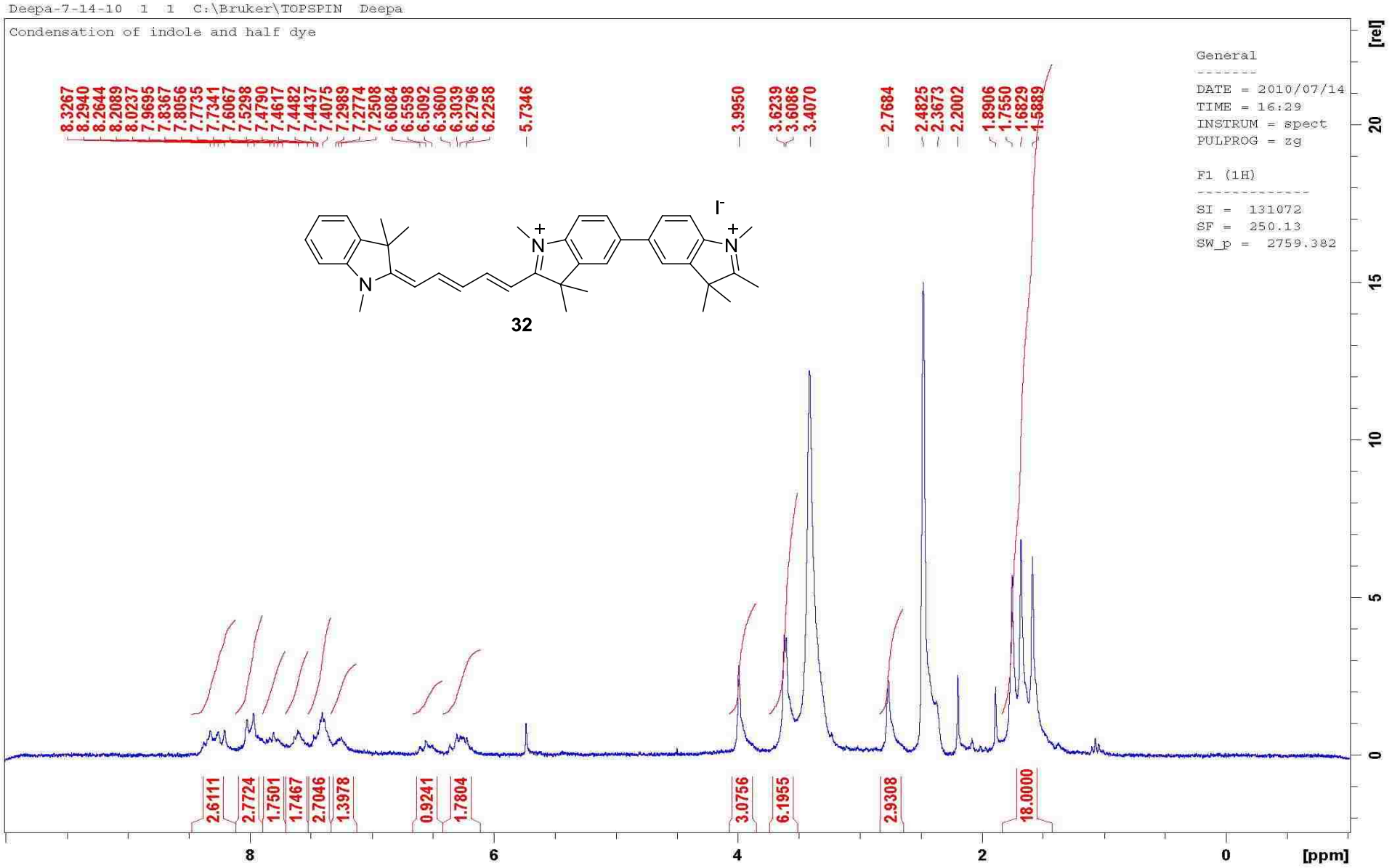
Deepa-7-14-10 1 1 C:\Bruker\TOPSPIN Deepa
Condensation of indole and half dye
8.3267
8.2940
8.2644
8.2089
8.0237
7.9695
7.8367
7.8056
7.7735
7.7341
7.6067
7.5298
7.4790
7.4617
7.4482
7.4437
7.4075
7.2989
7.2774
7.2508
6.6084
6.5598
6.5092
6.3600
6.3039
6.2796
6.2258
5.7346
3.9950
3.6239
3.6086
3.4070
2.7684
2.4825
2.3673
2.2002
1.8906
1.7550
1.6829
1.5889
General
DATE = 2010/07/14
TIME = 16:29
INSTRUM = spect
PULPROG = zg
F1 (1H)
SI = 131072
SF = 250.13
SW_p = 2759.382
I-
N+
N
32
2.6111
2.7724
1.7501
1.7467
2.7046
1.3978
0.9241
1.7804
3.0756
6.1955
2.9308
18.0000
8
6
4
2
0
[ppm]
[rel]
20
15
10
5
0

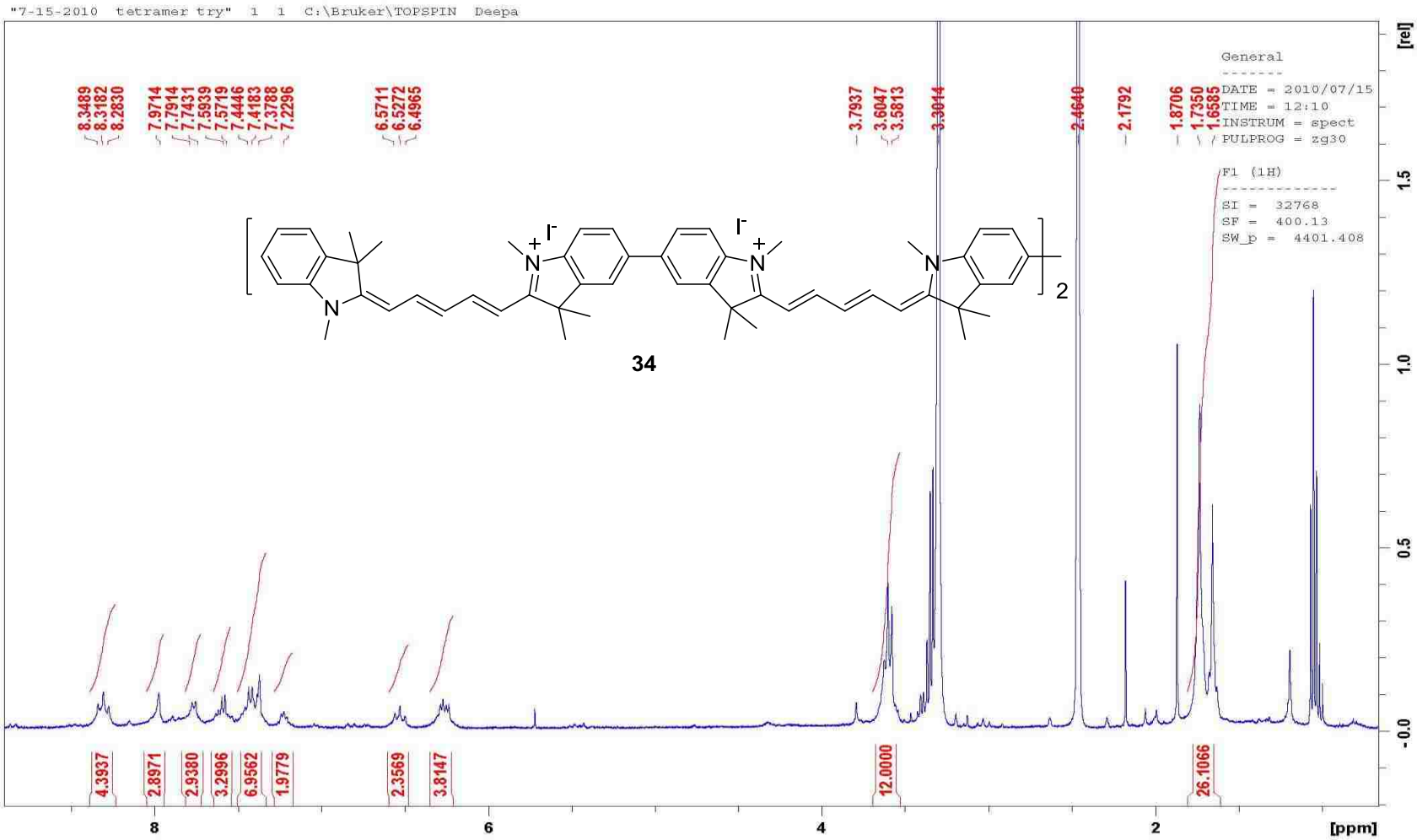
"7-15-2010 tetramer try" 1 1 C:\Bruker\TOPSPIN Deepa
8.3489
8.3182
8.2830
7.9714
7.7914
7.7431
7.5939
7.5719
7.4446
7.4183
7.3788
7.2296
6.5711
6.5272
6.4965
3.7937
3.6047
3.5813
3.3014
2.4640
2.1792
1.8706
1.7350
1.6585
General
DATE = 2010/07/15
TIME = 12:10
INSTRUM = spect
PULPROG = zg30
F1 (1H)
SI = 32768
SF = 400.13
SW_p = 4401.408
I-
I-
2
34
4.3937
2.8971
2.9380
3.2996
6.9562
1.9779
2.3569
3.8147
12.0000
26.1066
8
6
4
2
[ppm]
[rel]
1.5
1.0
0.5
-0.0

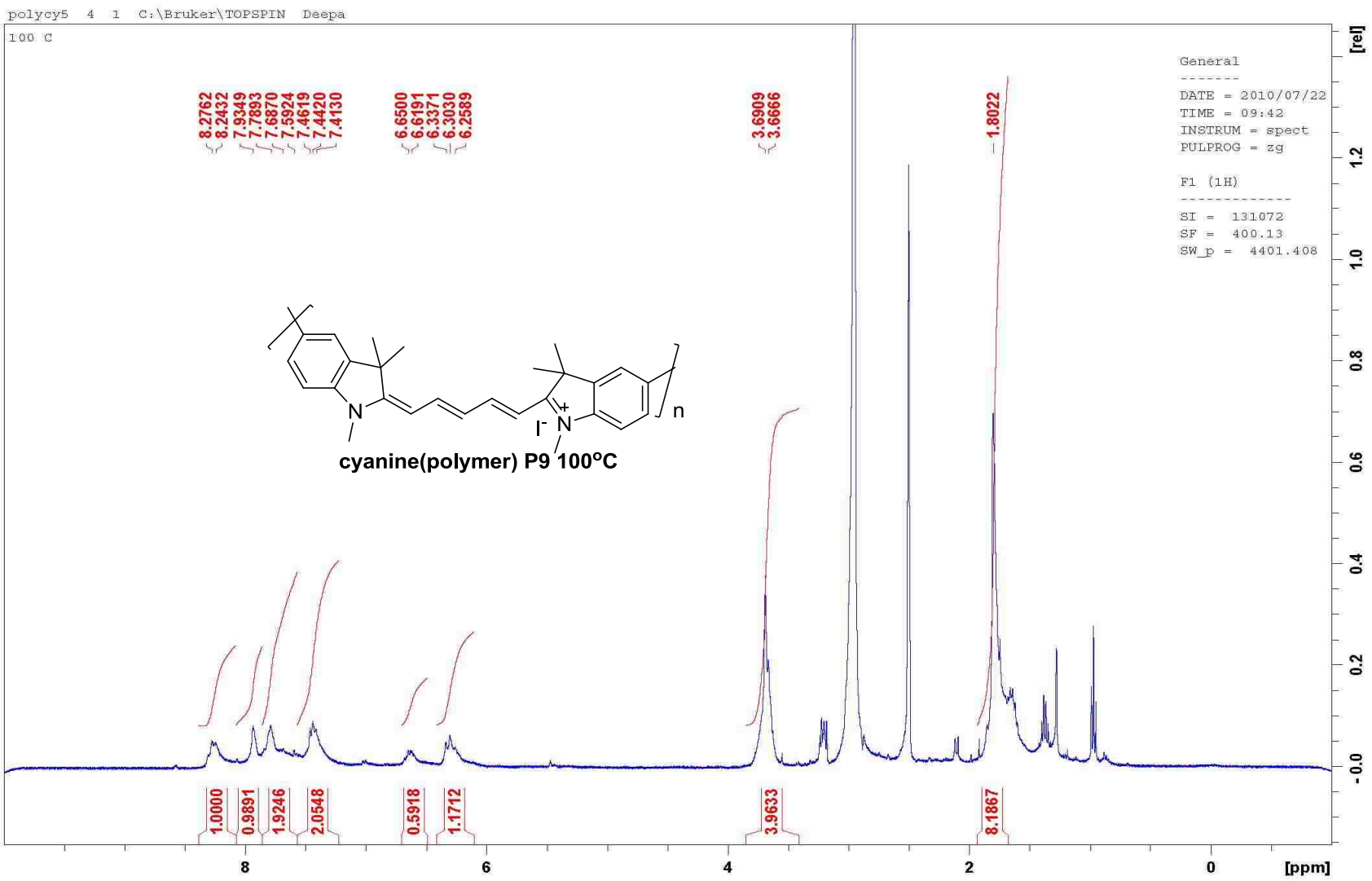
polycy5 4 1 C:\Bruker\TOPSPIN Deepa
100 C
8.2762
8.2432
7.9349
7.7893
7.6870
7.5924
7.4619
7.4420
7.4130
6.6500
6.6191
6.3371
6.3030
6.2589
3.6909
3.6666
1.8022
General
DATE = 2010/07/22
TIME = 09:42
INSTRUM = spect
PULPROG = zg
F1 (1H)
SI = 131072
SF = 400.13
SW_p = 4401.408
cyanine(polymer) P9 100°C
1.0000
0.9891
1.9246
2.0548
0.5918
1.1712
3.9633
8.1867
[rel]
[ppm]

Appendix B: Permission to Reuse Contents from Publications

RightsLink®

Home | Account Info | Help

Title: Fluorescent Chemosensors Based on Energy Migration in Conjugated Polymers: The Molecular Wire Approach to Increased Sensitivity

Author: Qin Zhou and Timothy M. Swager

Publication: Journal of the American Chemical Society

Publisher: American Chemical Society

Date: Dec 1, 1995

Logged in as:
Deepa Pangeni
Account #: 3000674554

LOGOUT

PERMISSION/LICENSE IS GRANTED FOR YOUR ORDER AT NO CHARGE

This type of permission/license, instead of the standard Terms & Conditions, is sent to you because no fee is being charged for your order. Please note the following:

- Permission is granted for your request in both print and electronic formats, and translations.
- If figures and/or tables were requested, they may be adapted or used in part.
- Please print this page for your records and send a copy of it to your publisher/graduate school.
- Appropriate credit for the requested material should be given as follows: "Reprinted (adapted) with permission from (COMPLETE REFERENCE CITATION). Copyright (YEAR) American Chemical Society." Insert appropriate information in place of the capitalized words.
- One-time permission is granted only for the use specified in your request. No additional uses are granted (such as derivative works or other editions). For any other uses, please submit a new request.

If credit is given to another source for the material you requested, permission must be obtained

from that source.

BACK CLOSE WINDOW

Copyright Clearance Center RightsLink® Home Account Info Help

ACS Publications High quality. High impact.

Title: Method for enhancing the sensitivity of fluorescent chemosensors: energy migration in conjugated polymers

Author: Qin Zhou and Timothy M. Swager

Publication: Journal of the American Chemical Society

Publisher: American Chemical Society

Date: Jul 1, 1995

Logged in as:
Deepa Pangeni
Account #:
3000674554
LOGOUT

PERMISSION/LICENSE IS GRANTED FOR YOUR ORDER AT NO CHARGE

This type of permission/license, instead of the standard Terms & Conditions, is sent to you because no fee is being charged for your order. Please note the following:

- Permission is granted for your request in both print and electronic formats, and translations.
- If figures and/or tables were requested, they may be adapted or used in part.
- Please print this page for your records and send a copy of it to your publisher/graduate school.
- Appropriate credit for the requested material should be given as follows: "Reprinted (adapted) with permission from (COMPLETE REFERENCE CITATION). Copyright

(YEAR) American Chemical Society." Insert appropriate information in place of the capitalized words.

- One-time permission is granted only for the use specified in your request. No additional uses are granted (such as derivative works or other editions). For any other uses, please submit a new request.

If credit is given to another source for the material you requested, permission must be obtained from that source.

BACK CLOSE WINDOW

Copyright Clearance Center RightsLink® Home Account Info Help

ACS Publications High quality. High impact.

Logged in as:
Deepa Pangeni
Account #: 3000674554
LOGOUT

Title: Fluorescent Porous Polymer Films as TNT Chemosensors: Electronic and Structural Effects

Author: Jye-Shane Yang and and Timothy M. Swager*

Publication: Journal of the American Chemical Society

Publisher: American Chemical Society

Date: Nov 1, 1998

PERMISSION/LICENSE IS GRANTED FOR YOUR ORDER AT NO CHARGE

This type of permission/license, instead of the standard Terms & Conditions, is sent to you because no fee is being charged for your order. Please note the following:

- Permission is granted for your request in both print and electronic formats, and translations.
- If figures and/or tables were requested, they may be adapted or used in part.
- Please print this page for your records and send a copy of it to your publisher/graduate school.
- Appropriate credit for the requested material should be given as follows: "Reprinted (adapted) with permission from (COMPLETE REFERENCE CITATION). Copyright (YEAR) American Chemical Society." Insert appropriate information in place of the capitalized words.
- One-time permission is granted only for the use specified in your request. No additional uses are granted (such as derivative works or other editions). For any other uses, please submit a new request.

If credit is given to another source for the material you requested, permission must be obtained from that source.

BACK CLOSE WINDOW

Chemical Society

Publisher: American Chemical Society

Date: Jul 1, 1995

PERMISSION/LICENSE IS GRANTED FOR YOUR ORDER AT NO CHARGE

This type of permission/license, instead of the standard Terms & Conditions, is sent to you because no fee is being charged for your order. Please note the following:

- Permission is granted for your request in both print and electronic formats, and translations.
- If figures and/or tables were requested, they may be adapted or used in part.
- Please print this page for your records and send a copy of it to your publisher/graduate school.
- Appropriate credit for the requested material should be given as follows: "Reprinted (adapted) with permission from (COMPLETE REFERENCE CITATION). Copyright (YEAR) American Chemical Society." Insert appropriate information in place of the capitalized words.
- One-time permission is granted only for the use specified in your request. No additional uses are granted (such as derivative works or other editions). For any other uses, please submit a new request.

If credit is given to another source for the material you requested, permission must be obtained from that source.

BACK CLOSE WINDOW

Title: Method for enhancing the sensitivity of fluorescent chemosensors: energy migration in conjugated polymers

Author: Qin Zhou and Timothy M. Swager

Publication: Journal of the American Chemical Society

Publisher: American Chemical Society

Date: Jul 1, 1995

PERMISSION/LICENSE IS GRANTED FOR YOUR ORDER AT NO CHARGE

This type of permission/license, instead of the standard Terms & Conditions, is sent to you because no fee is being charged for your order. Please note the following:

- Permission is granted for your request in both print and electronic formats, and translations.
- If figures and/or tables were requested, they may be adapted or used in part.
- Please print this page for your records and send a copy of it to your publisher/graduate school.
- Appropriate credit for the requested material should be given as follows: "Reprinted (adapted) with permission from (COMPLETE REFERENCE CITATION). Copyright (YEAR) American Chemical Society." Insert appropriate information in place of the capitalized words.
- One-time permission is granted only for the use specified in your request. No additional uses are granted (such as derivative works or other editions). For any other uses, please submit a new request.

If credit is given to another source for the material you requested, permission must be obtained from that source.

JOHN WILEY AND SONS LICENSE TERMS AND CONDITIONS

Oct 10, 2013

This is a License Agreement between Deepa Pangeni ("You") and John Wiley and Sons ("John Wiley and Sons") provided by Copyright Clearance Center ("CCC"). The license consists of your order details, the terms and conditions provided by John Wiley and Sons, and the payment terms and conditions.

All payments must be made in full to CCC. For payment instructions, please see information listed at the bottom of this form.

License Number	3245471177408
License date	Oct 10, 2013
Licensed content publisher	John Wiley and Sons
Licensed content publication	Angewandte Chemie
Licensed content title	Ion-Specific Aggregation in Conjugated Polymers: Highly Sensitive and Selective Fluorescent Ion Chemosensors
Licensed copyright line	© 2000 WILEY-VCH Verlag GmbH, Weinheim, Fed. Rep. of Germany
Licensed content author	Jinsang Kim,D. Tyler McQuade,Sean K. McHugh,Timothy M. Swager
Licensed content date	Oct 27, 2000

Start page	4026
End page	4030
Type of use	Dissertation/Thesis
Requestor type	University/Academic
Format	Print and electronic
Portion	Figure/table
Number of figures/tables	2
Original Wiley figure/table number(s)	SCHEME 1 FIGURE 2
Will you be translating?	No
Total	0.00 USD

JOHN WILEY AND SONS LICENSE TERMS AND CONDITIONS

Oct 10, 2013

This is a License Agreement between Deepa Pangeni ("You") and John Wiley and Sons ("John Wiley and Sons") provided by Copyright Clearance Center ("CCC"). The license consists of your order details, the terms and conditions provided by John Wiley and Sons, and the payment terms and conditions.

All payments must be made in full to CCC. For payment instructions, please see information listed at the bottom of this form.

License Number	3245480033179
License date	Oct 10, 2013
Licensed content publisher	John Wiley and Sons
Licensed content publication	Macromolecular Rapid Communications
Licensed content title	A Reversible and Highly Selective Fluorescent Sensor for Mercury(II) Using Poly(thiophene)s that Contain Thymine Moieties
Licensed copyright line	Copyright © 2006 WILEY-VCH Verlag GmbH & Co. KGaA, Weinheim
Licensed content author	Yanli Tang,Fang He,Minghui Yu,Fude Feng,Lingling An,Huan Sun,Shu Wang,Yuliang Li,Daoben Zhu
Licensed content date	Mar 2, 2006
Start page	389
End page	392
Type of use	Dissertation/Thesis
Requestor type	University/Academic
Format	Print and electronic
Portion	Figure/table
Number of figures/tables	1
Original Wiley figure/table number(s)	FIG 1
Will you be translating?	No
Total	0.00 USD

JOHN WILEY AND SONS LICENSE TERMS AND CONDITIONS

Oct 10, 2013

This is a License Agreement between Deepa Pangeni ("You") and John Wiley and Sons ("John Wiley and Sons") provided by Copyright Clearance Center ("CCC"). The license consists of your order details, the terms and conditions provided by John Wiley and Sons, and the payment terms and conditions.

All payments must be made in full to CCC. For payment instructions, please see information listed at the bottom of this form.

License Number	3245480125006
License date	Oct 10, 2013
Licensed content publisher	John Wiley and Sons
Licensed content publication	Chemistry - A European Journal
Licensed content title	Sugar–Poly(para-phenylene ethynylene) Conjugates as Sensory Materials: Efficient Quenching by Hg2 and Pb2 Ions
Licensed copyright line	Copyright © 2004 WILEY-VCH Verlag GmbH & Co. KGaA, Weinheim
Licensed content author	Ik-Bum Kim,Belma Erdogan,James N. Wilson,Uwe H. F. Bunz
Licensed content date	Nov 3, 2004
Start page	6247
End page	6254
Type of use	Dissertation/Thesis
Requestor type	University/Academic
Format	Print and electronic

Portion	Figure/table
Number of figures/tables	1
Original Wiley figure/table number(s)	FIG 2
Will you be translating?	No
Total	0.00 USD

Home | Account Info | Help

Title: Fluorescein Provides a Resonance Gate for FRET from Conjugated Polymers to DNA Intercalated Dyes

Author: Shu Wang,Brent S. Gaylord, and, and Guillermo C. Bazan*

Publication: Journal of the American Chemical Society

Publisher: American Chemical Society

Date: May 1, 2004

Logged in as:
Deepa Pangeni
Account #:
3000674554

LOGOUT

PERMISSION/LICENSE IS GRANTED FOR YOUR ORDER AT NO CHARGE

This type of permission/license, instead of the standard Terms & Conditions, is sent to you because no fee is being charged for your order. Please note the following:

- Permission is granted for your request in both print and electronic formats, and translations.

- If figures and/or tables were requested, they may be adapted or used in part.
- Please print this page for your records and send a copy of it to your publisher/graduate school.
- Appropriate credit for the requested material should be given as follows: "Reprinted (adapted) with permission from (COMPLETE REFERENCE CITATION). Copyright (YEAR) American Chemical Society." Insert appropriate information in place of the capitalized words.
- One-time permission is granted only for the use specified in your request. No additional uses are granted (such as derivative works or other editions). For any other uses, please submit a new request.

If credit is given to another source for the material you requested, permission must be obtained from that source.

BACK CLOSE WINDOW

OHN WILEY AND SONS LICENSE TERMS AND CONDITIONS

Oct 10, 2013

This is a License Agreement between Deepa Pangeni ("You") and John Wiley and Sons ("John Wiley and Sons") provided by Copyright Clearance Center ("CCC"). The license consists of your order details, the terms and conditions provided by John Wiley and Sons, and the payment terms and conditions.

All payments must be made in full to CCC. For payment instructions, please see information listed at the bottom of this form.

License Number	3245480033179
License date	Oct 10, 2013
Licensed content publisher	John Wiley and Sons
Licensed content publication	Macromolecular Rapid Communications
Licensed content title	A Reversible and Highly Selective Fluorescent Sensor for Mercury(II) Using Poly(thiophene)s that Contain Thymine Moieties
Licensed copyright line	Copyright © 2006 WILEY-VCH Verlag GmbH & Co. KGaA, Weinheim
Licensed content author	Yanli Tang,Fang He,Minghui Yu,Fude Feng,Lingling An,Huan Sun,Shu Wang,Yuliang Li,Daoben Zhu
Licensed content date	Mar 2, 2006
Start page	389
End page	392
Type of use	Dissertation/Thesis
Requestor type	University/Academic
Format	Print and electronic
Portion	Figure/table
Number of figures/tables	1
Original Wiley figure/table number(s)	FIG 1
Will you be translating?	No
Total	0.00 USD

JOHN WILEY AND SONS LICENSE TERMS AND CONDITIONS

Oct 10, 2013

This is a License Agreement between Deepa Pangeni ("You") and John Wiley and Sons ("John Wiley and Sons") provided by Copyright Clearance Center ("CCC"). The license consists of your order details, the terms and conditions provided by John Wiley and Sons, and the payment terms and conditions.

All payments must be made in full to CCC. For payment instructions, please see information listed at the bottom of this form.

License Number	3245471177408
License date	Oct 10, 2013
Licensed content publisher	John Wiley and Sons
Licensed content publication	Angewandte Chemie
Licensed content title	Ion-Specific Aggregation in Conjugated Polymers: Highly Sensitive and Selective Fluorescent Ion Chemosensors
Licensed copyright line	© 2000 WILEY-VCH Verlag GmbH, Weinheim, Fed. Rep. of Germany
Licensed content author	Jinsang Kim,D. Tyler McQuade,Sean K. McHugh,Timothy M. Swager
Licensed content date	Oct 27, 2000
Start page	4026
End page	4030
Type of use	Dissertation/Thesis
Requestor type	University/Academic
Format	Print and electronic

Portion	Figure/table
Number of figures/tables	2
Original Wiley figure/table number(s)	SCHEME 1 FIGURE 2
Will you be translating?	No
Total	0.00 USD

RightsLink®

Home | Account Info | Help

Title: Fluorescein Provides a Resonance Gate for FRET from Conjugated Polymers to DNA Intercalated Dyes

Author: Shu Wang,Brent S. Gaylord, and, and Guillermo C. Bazan*

Publication: Journal of the American Chemical Society

Publisher: American Chemical Society

Date: May 1, 2004

Logged in as:
Deepa Pangeni
Account #:
3000674554

LOGOUT

PERMISSION/LICENSE IS GRANTED FOR YOUR ORDER AT NO CHARGE

This type of permission/license, instead of the standard Terms & Conditions, is sent to you because no fee is being charged for your order. Please note the following:

- Permission is granted for your request in both print and electronic formats, and translations.
- If figures and/or tables were requested, they may be adapted or used in part.

- Please print this page for your records and send a copy of it to your publisher/graduate school.
- Appropriate credit for the requested material should be given as follows: "Reprinted (adapted) with permission from (COMPLETE REFERENCE CITATION). Copyright (YEAR) American Chemical Society." Insert appropriate information in place of the capitalized words.
- One-time permission is granted only for the use specified in your request. No additional uses are granted (such as derivative works or other editions). For any other uses, please submit a new request.

If credit is given to another source for the material you requested, permission must be obtained from that source.

BACK CLOSE WINDOW

Copyright Clearance Center RightsLink®

Home Account Info Help

ACS Publications High quality. High impact.

Title: "Turn-On" Conjugated Polymer Fluorescent Chemosensor for Fluoride Ion

Author: Hui Tong,Lixiang Wang,*, Xiabin Jing, and, and Fosong Wang

Publication: Macromolecules

Publisher: American Chemical Society

Date: Apr 1, 2003

Logged in as:
Deepa Pangeni
Account #:
3000674554

LOGOUT

PERMISSION/LICENSE IS GRANTED FOR YOUR ORDER AT NO CHARGE

This type of permission/license, instead of the standard Terms & Conditions, is sent to you because no fee is being charged for your order. Please note the following:

- Permission is granted for your request in both print and electronic formats, and translations.
- If figures and/or tables were requested, they may be adapted or used in part.
- Please print this page for your records and send a copy of it to your publisher/graduate school.
- Appropriate credit for the requested material should be given as follows: "Reprinted (adapted) with permission from (COMPLETE REFERENCE CITATION). Copyright (YEAR) American Chemical Society." Insert appropriate information in place of the capitalized words.
- One-time permission is granted only for the use specified in your request. No additional uses are granted (such as derivative works or other editions). For any other uses, please submit a new request.

If credit is given to another source for the material you requested, permission must be obtained from that source.

BACK CLOSE WINDOW

This is a License Agreement between Deepa Pangeni ("You") and John Wiley and Sons ("John Wiley and Sons") provided by Copyright Clearance Center ("CCC"). The license consists of your order details, the terms and conditions provided by John Wiley and Sons, and the payment terms and conditions.

All payments must be made in full to CCC. For payment instructions, please see

information listed at the bottom of this form.

License Number	3245480366263
License date	Oct 10, 2013
Licensed content publisher	John Wiley and Sons
Licensed content publication	Angewandte Chemie
Licensed content title	A Fluorescent Self-Amplifying Wavelength-Responsive Sensory Polymer for Fluoride Ions
Licensed copyright line	Copyright © 2003 WILEY-VCH Verlag GmbH & Co. KGaA, Weinheim
Licensed content author	Tae-Hyun Kim,Timothy M. Swager
Licensed content date	Sep 23, 2003
Start page	4951
End page	4954
Type of use	Dissertation/Thesis
Requestor type	University/Academic
Format	Print and electronic
Portion	Figure/table
Number of figures/tables	2
Original Wiley figure/table number(s)	FIG 1 AND 2
Will you be translating?	No
Total	0.00 USD

BACK CLOSE WINDOW

JOHN WILEY AND SONS LICENSE TERMS AND CONDITIONS

Oct 10, 2013

This is a License Agreement between Deepa Pangeni ("You") and John Wiley and Sons ("John Wiley and Sons") provided by Copyright Clearance Center ("CCC"). The license consists of your order details, the terms and conditions provided by John Wiley and Sons, and the payment terms and conditions.

All payments must be made in full to CCC. For payment instructions, please see information listed at the bottom of this form.

License Number	3245480531026
License date	Oct 10, 2013
Licensed content publisher	John Wiley and Sons
Licensed content publication	Angewandte Chemie International Edition
Licensed content title	A Ratiometric Fluorescent Probe for Rapid Detection of Hydrogen Sulfide in Mitochondria
Licensed copyright line	Copyright © 2013 WILEY-VCH Verlag GmbH & Co. KGaA,

	Weinheim
Licensed content author	Yuncong Chen,Chengcheng Zhu,Zhenghao Yang,Junjie Chen,Yafeng He,Yang Jiao,Weijiang He,Lin Qiu,Jiajie Cen,Zijian Guo
Licensed content date	Jan 3, 2013
Start page	1688
End page	1691
Type of use	Dissertation/Thesis
Requestor type	University/Academic
Format	Print and electronic
Portion	Figure/table
Number of figures/tables	1
Original Wiley figure/table number(s)	FIG 1
Will you be translating?	No
Total	0.00 USD

The Vita

Deepa Pangeni was born in 1985 in Waling, Nepal. She graduated from High School in 2002 and came to United States in 2003 to pursue Bachelor's Degree in Biology at Hanover College, IN. During her first semester, she preferred Chemistry and Mathematics over Biology and eventually finished her Bachelors with double degree in Mathematics and Chemistry in 2007. She decided to pursue her PhD in Chemistry and attended Louisiana State University, LA in 2007 and joined Dr. Evgueni E. Nesterov Lab in 2008 and started working in the field of synthesis and characterization of amplifying fluorescent conjugated polymers. Deepa is a candidate for the Doctor of Philosophy in Organic Chemistry which will be awarded in December 2013 with a dissertation entitled "Amplifying Fluorescent Conjugated Polymers."